



MANGROVE FORESTS CHANGES AND RESPONSES TO SEA LEVEL RISE
BASED ON REMOTE SENSING AND GIS IN PKWS, CAMBODIA

NAYELIN PHORN

A THESIS SUBMITTED IN PARTIAL FULFILLMENT OF
THE REQUIREMENTS FOR THE MASTER DEGREE OF SCIENCE
IN GEOINFORMATICS
FACULTY OF GEOINFORMATICS
BURAPHA UNIVERSITY

2021

COPYRIGHT OF BURAPHA UNIVERSITY

การศึกษาการเปลี่ยนแปลงของพื้นที่ป่าชายเลน ที่มีผลกระทบมาจากระดับน้ำทะเล ด้วยวิธีการรับรู้
ระยะไกลและเทคนิคทางภูมิสารสนเทศในพื้นที่เขตรักษาพันธุ์สัตว์ป่า PEAM KRASOP,
กัมพูชา



วิทยานิพนธ์นี้เป็นส่วนหนึ่งของการศึกษาตามหลักสูตรวิทยาศาสตรมหาบัณฑิต
สาขาวิชาภูมิสารสนเทศศาสตร์
คณะภูมิสารสนเทศศาสตร์ มหาวิทยาลัยบูรพา
2564
ลิขสิทธิ์เป็นของมหาวิทยาลัยบูรพา

MANGROVE FORESTS CHANGES AND RESPONSES TO SEA LEVEL RISE
BASED ON REMOTE SENSING AND GIS IN PKWS, CAMBODIA



NAYELIN PHORN

A THESIS SUBMITTED IN PARTIAL FULFILLMENT OF
THE REQUIREMENTS FOR THE MASTER DEGREE OF SCIENCE
IN GEOINFORMATICS
FACULTY OF GEOINFORMATICS
BURAPHA UNIVERSITY
2021
COPYRIGHT OF BURAPHA UNIVERSITY

The Thesis of Nayelin Phorn has been approved by the examining committee to be partial fulfillment of the requirements for the Master Degree of Science in Geoinformatics of Burapha University

Advisory Committee

Examining Committee

Principal advisor

(Jianzhong Lu)

----- Principal
examiner

(Xiaobin Cai)

Co-advisor

(Phattraporn Soyong)

----- Member

(Jianzhong Lu)

----- Member

(Phattraporn Soyong)

----- Member

(Zhenfeng Shao)

----- Member

(Timo Balz)

----- Dean of the Faculty of Geoinformatics

(Kitsanai Charoenjit)

This Thesis has been approved by Graduate School Burapha University to be partial fulfillment of the requirements for the Master Degree of Science in Geoinformatics of Burapha University

----- Dean of Graduate School

(Associate Professor Dr. Nujjaree Chaimongkol)

62910210: MAJOR: GEOINFORMATICS; M.Sc. (GEOINFORMATICS)

KEYWORDS: Mangrove forests, Sea Level Rise, Remote Sensing, GIS

NAYELIN PHORN : MANGROVE FORESTS CHANGES AND RESPONSES TO SEA LEVEL RISE BASED ON REMOTE SENSING AND GIS IN PKWS, CAMBODIA. ADVISORY COMMITTEE: JIANZHONG LU, , PHATTRAPORN SOYTONG 2021.

Cambodia is a country that can be found rich in mangrove forests area. Cambodia's mangrove forests are found along a coastline of 435 km that consists of Koh Kong province, Kampot, Sihanouk Ville, and Kep province. Mangrove forests in Cambodia are considered essential forests that provide food sources, shelters, and nurseries along the coastal zone. These mangrove ecosystems have decline and change to shrimp farming, salt farming, charcoal production, pollution, illegal logging, and threatened to climate change such Sea level rise (SLR). Sea level rise can be as a parameter to assess the vulnerability of coastal mangroves in Cambodia due to be Sea level rise can lead a significant impact on mangrove ecosystems.

This research reveals the mangrove forests extraction and change from 2015 to 2020. Then, the vulnerable area of mangrove forests due to three different SLR scenarios in Peam Krasop Wildlife Sanctuary (PKWS) in Cambodia. To extract the mangrove forests area in this study, Sentinel-2 multi-temporal data from 2015 to 2020 were used to classify and identify the mangrove forests and other classes using Random Forest classifier Machine Learning in the DZetsaka plugin in QGIS. For analyzed and produced the changes of mangrove forests map between 2015 to 2020 using MOLUSCE in QGIS. To predict the vulnerable area of mangrove forests by future SLR, a model of Geospatial Model based on SRTM DEM and IPCC's SLR scenarios will be used to delineate mangrove areas in 2020. Three different SLR scenarios have been adopted in this study such as SLR 40 cm, SLR 60 cm, SLR 1 m. For DEM data was SRTM that download from USGS, and this SRTM was created, manipulated, and processed in ArcMap.

The experimental results are satisfactory, mangrove forest areas were estimated at 7157.90 ha in 2015, 7495.21 ha in 2016, 7337.47 ha in 2017, 6436.26 ha in 2018, 6761.66 ha in 2019, and 7045.64 ha in 2020.

Furthermore, mangrove forests in PKWS in this study were changed from 7150.90 ha to 7495.21 ha (2015-2016), between this period, mangrove forests were significant increased by 337.31 ha. Mangrove forests in PKWS were changed from 7495.21 ha to 7337.47 ha (2016-2017), between this period, mangrove forests were extremely decreased by 157.74 ha. Similarly, mangrove forests have continued to decrease 901.21 ha from 7337.47 ha to 6436.26 ha (2017-2018). However, mangrove forests started to increase 325.40 ha in PKWS in 2019, mangrove forests were changed from 6436.26 ha to 6761.66 ha (2018-2019). Between 2019 and 2020, mangrove forests have increased by approximately 283.98 ha mangrove forests have changed from 6761.66 ha to 7045.64 ha (2019-2020). The total long-term change in mangrove forests areas in PKWS from 2015 to 2020, mangrove forests were decreased 112.26 ha from 7157.90 ha to 7045.64 ha.

Based on the result of the study finds that when sea level rise by 40 and 60 cm, the mangrove forests areas are projected to be inundated or impacted on areas about 40.44 ha at the end of the twenty-first century, and mangrove forests areas are predicted future inundated by 53.14 ha beside increasing 1 m for high Sea level rise scenarios respectively.

ACKNOWLEDGEMENTS

First, I would like to show my gratefulness to advisor Associated Prof. Jianzhong Lu of Wuhan University, and co-advisor Dr. Pakorn Petchprayoon of Burapha University, for accepted me as his student. For all their supports, guidance, patience, motivation, and immense knowledge, that help me to achieved in my Master thesis and research writing. I could not imagine no having a better advisor and co-visor for this M.Sc. study.

Besides my advisor and co-advisor, I have a desire thank to Dr. Tanita Suepa of GISTDA, and Dr. Haoran Zhang of GISTDA, for their encouragements, insightful comments, and they always pay attention and follow up on my thesis writing.

My sincere thanks also go to Geo-Informatics and Space Technology Development Agency (GISTDA), Burapha University (BUU), and Wuhan University, for offering me to have the opportunities in this SCGI Master program.

I also grateful to the staffs of Burapha University (BUU) and Geo-Informatics and Space Technology Development Agency (GISTDA), Minlada Rattnakul, Chonthicha Chitapaiboon, and Petjaraj Techakriangkai for their supports and follow up me at Thailand. Also, I thank to the staffs of State Key Laboratory for Information Engineering in Surveying, Mapping and Remote Sensing (LIESMARS), Guan Lin, Wei Min, and Shi Lite and the staff of the School of International Education at Wuhan University who without their supports, this dissertation would not have been possible.

I thank my classmates from Cambodia and Thailand, including Suwatcharapong Surasanpreedee, Anurak Chakpor, Arpakorn Wongsit, Nittaya Katekaew, Sopaphan Chinnabut, Lay Hong, and Mot Ly, for their helping, good advice, working together, and having fun together in the last two years.

Lastly, I would like to show my respect and love to my parents Nuon Kimseat and Phorn Say for giving birth to me, for their love and encouragement, and for supporting through my life.

Nayelin Phorn



TABLE OF CONTENTS

	Page
ABSTRACT.....	D
ACKNOWLEDGEMENTS.....	F
TABLE OF CONTENTS.....	H
LIST OF TABLES.....	K
LIST OF FIGURES	L
LIST OF LIST OF ACRONYMS AND ABBREVIATIONS.....	N
CHAPTER 1 INTRODUCTION.....	1
1.1 Mangroves in Cambodia.....	1
1.1 Sea Level Rise in Cambodia.....	2
1.2 Research Objective and Problems	2
1.3 Research Questions	3
1.4 The Significant	3
1.5 Limitation of This Study	4
CHAPTER 2 LITERATURE REVIEWS.....	5
2.1 Keywords.....	5
2.2 General Mangroves Remote Sensing (RS).....	5
2.3 Analysis Impact of Sea Level Rise using GIS Methods.....	6
2.4 Mangrove Forests and Sea Level Rise in Cambodia.....	8
2.4.1 Mangrove Forests Situation.....	8
2.4.2 Mangroves Issue.....	9
2.4.3 Relative Sea Level Rise.....	10
2.5 Classification Methods	11
2.5.1 Object-based Classification.....	12
2.5.2 Pixel-based Classification	12
2.5.3 Easy Random Forest in Dzetsaka Plugin	12

CHAPTER 3 METHODOLOGY	15
3.1 Study Area	15
3.2 Methodology Workflow	16
3.3 Data Acquisitions	18
3.3.1 Sentinel-2 Imagery	18
3.3.2 Digital Elevation Model (DEM)	19
3.3.3 Sea Level Rise (SLR) Scenarios	20
3.4 Data Processing	21
3.4.1 Mangrove Forests Extraction	21
3.4.2 Analysis Changes of Mangrove Forests	23
3.4.3 Analysis Potential Impacts of SLR on Mangrove Forests	24
3.5 Accuracy Assessments	24
CHAPTER 4 EXPERIMENT RESULT	25
4.1 Land Cover of Mangrove Forests Extraction from 2015 to 2020	25
4.1.1 Land Cover Classes Level I	25
4.1.2 Land Cover Classes Level II	27
4.1.3 Land Cover Level III	29
4.2 Mangrove Forests Change from 2015 to 2020 Using MOLUSCE	31
4.2.1 Mangrove Forests Change from 2015-2016	31
4.2.2 Mangrove Forests Change from 2016-2017	32
4.2.3 Mangrove Forests Change from 2017-2018	33
4.2.4 Mangrove Forests Change from 2018-2019	35
4.2.5 Mangrove Forests Change from 2019-2020	36
4.2.6 Mangrove Forests Change from 2015-2020	37
4.3 Potential Inundation of SLR on Mangrove Forests Area	39
CHAPTER 5 DISCUSSION, FUTURE WORK, AND CONCLUSION	42
5.1 Discussion	42
5.2 Future Work	44
5.3 Conclusion	44

REFERENCES	46
BIOGRAPHY	53
APPENDICES	54



LIST OF TABLES

	Page
Table 2. The studies of analysis SLR impacts using Remote Sensing and GIS	7
Table 3. The different estimates area of mangrove forests in Cambodia	8
Table 4. Description of spectral bands of Sentinel-2 (Hawryło & Wezyk, 2018).....	18
Table 5. Data Acquisition for Sentinel-2 imagery	19
Table 6. Summarized data acquisition	21
Table 7. Number of samples selected for training classification	22
Table 8. Mangrove forests classification levels	23
Table 9. The transition encoding of classes	24
Table 10. Land cover classes Level I of PKWS from 2015 to 2020	26
Table 11. Land cover classes Level II of PKWS from 2015 to 2020	29
Table 12. Land cover classes Level II of PKWS from 2015 to 2020	30
Table 13. Mangrove forests change (hectare) between 2015 to 2016	32
Table 14. Mangrove forests change (hectare) between 2016 to 2017	32
Table 15. Mangrove forests change (hectare) between 2017 to 2018	34
Table 16. Mangrove forests change (hectare) between 2018 to 2019	36
Table 17. Mangrove forests change (hectare) between 2019 to 2020	36
Table 18. Mangrove forests change (hectare) between 2015 to 2020	38
Table 19. The inundation of different SLR scenarios vulnerable to mangrove forests areas	40

LIST OF FIGURES

Page

Figure 1. The evolution of mangroves remote sensing from 1956 until 2018. Distribution mapping (yellow box), biophysical parameters inversion (pink box), and ecosystem process characterization (green box), (Wang et al., 2019).....	6
Figure 2. Before and after mangrove areas deforestation in Koh Kong province during from 1989 to 2017 (Bk & Quang, 2019).	9
Figure 3. Map of stations with sea-level data near Cambodia (BCC-PPCR, 2014). ..	10
Figure 4. Ensemble of Decision Trees (Random Forest).....	13
Figure 5. Map of Study area (Peam Krosop Wildlife Sanctuary).....	16
Figure 6. Potential inundation of SLR scenarios on mangroves forest areas by the end of this century workflow.	17
Figure 7. Land Cover Map level I of PWKS from 2015 to 2020. (a) Classify 2015, (b) Classify 2016, (c) Classify 2017, (d) Classify 2018, (e) Classify 2019, (f) Classify 2020.....	27
Figure 8. Land Cover Map Level II of PWKS from 2015 to 2020. (a) Classify 2015,	28
Figure 9. PWKS's mangrove forests from 2015 to 2020. (a) Classify 2015, (b) Classify 2016, (c) Classify 2017, (d) Classify 2018, (e) Classify 2019, (f) Classify 2020.....	30
Figure 10. PKWS's Mangrove forests change between 2015 and 2016.....	31
Figure 11. PKWS's Mangrove forests change between 2016 and 2017.....	33
Figure 12. PKWS's Mangrove forests change between 2017 and 2018.....	34
Figure 13. PKWS's Mangrove forests change between 2018 and 2019.....	35
Figure 14. PKWS's Mangrove forests change between 2019 and 2020.....	37
Figure 15. PKWS's Mangrove forests change between 2015 and 2020.....	38
Figure 16. Diagram of mangrove forests change during from 2015 to 2020.	39
Figure 17. Increased and Decreased of Mangrove forests area from 2015-2020.	39
Figure 18. Total mangrove forests area loss under three different SLR scenarios in Peam Krasop Wildlife Sanctuary by the end of the twenty-first century.	40

Figure 19. Analysis of the inundation of mangrove areas in Peam Krasop Wildlife Sanctuary due to three different SLR scenarios.....	41
---	----



LIST OF LIST OF ACRONYMS AND ABBREVIATIONS

AOGCMs	Atmosphere-ocean General Circulation models
CCMA	Climate Change Mitigation and Adaptation
CMIP5	Climate Research Programme Coupled Model Intercomparison Project Phase 5
DEM	Digital Elevation Model
DOFW	Department of Forestry and Wildlife
ESA	European Space Agency
FAO	Food and Agriculture Organization
GIS	Geographic Information System
GISTDA	Geo-Informatics and Space Technology Development Agency
IPCC	Intergovernmental Panel on Climate Change
IRD	Institute of Forest Wildlife Research and Education
IUCN	International Union for Conservation of Nature
MLUPC	Ministry of Land Management, Urban Planning and Construction
MoE	Ministry of Environment
MOLUSCE	Methods of Land Use Simulation Change Evaluation
MRC	Mekong River Commission
NASA	National Aeronautics and Space Administration
NCA	National Climate Assessment
NGA	National Geospatial-Intelligence Agency
NOAA	National Oceanic and Atmospheric Administration
ODC	Open Development Cambodia
PKWS	Peam Krasop Wildlife Sanctuary
RS	Remote Sensing
RF	Random Forest
SLR	Sea Level Rise
SRTM	The Shuttle Radar Topography Mission
UNDP	United Nations Development Programme
USGS	United State Geological Survey

CHAPTER 1 INTRODUCTION

Mangrove forests are the significant ecosystems found along the tropical and subtropical coastlines (Veettil, 2019). Mangrove forests are helped to protect the coastal area from the waves, storms, living habitat from the wave energy, and provide the critical coastal zone ecosystem (Brinkman RM, 1997; Dahdouh-Guebas et al., 2005; McIvor, 2012; Quartel, Kroon, Augustinus, Van Santen, & Tri, 2007). Despite, mangrove forests around 35% of the world have existed over the last two decades of the twenty century (Bosire et al., 2008; Valiela, Bowen, & York, 2001). Recent years, mangrove forests that found along coastlines of Cambodia have declined due to converting mangrove forests to aquacultures like shrimp farming, pollution, and threatened future climate change (Ward, Friess, Day, & Mackenzie, 2017).

In order, Remote Sensing (RS) has assisted as a supportable technique in mangrove forests studies (Blasco, Aizpuru, & Gers, 2001; T. Kumar, Panigrahy, Kumar, & Parihar, 2012; Vaiphasa, 2006), that mangroves remote sensing found since 1956. RS has evolved with the hot spot issues including biophysical parameters inversion, mangrove distribution mapping, and monitor the extent of change in mangroves (Wang, Jia, Yin, & Tian, 2019). To map and monitor the extent change in mangroves was verified as the most challenging depend on a combination of existing field maps and Remote Sensing data.

1.1 Mangroves in Cambodia

Mangrove forests could be found in the Southwestern part of Cambodia between 10°43' -11°85' N and 102°88'-104°44' E. Cambodia's mangrove forests consist of Koh Kong, Sihanouk Ville, Kampot, and Kep province (FAO, 2010). Mangrove habitat conditions were cleared by anthropogenic activities such as converting mangrove forest areas to charcoal production, illegal exports, salt fields, and shrimp farming. These anthropogenic activities were reflected as the main factors that caused the reduction, decline, and threat to mangrove forests in Koh Kong and Kampot coastal, Cambodia (Bann, 1997; MoE, 2009). As reported by The Royal Government of Cambodia, the coastal zone has identified as in center to adapt to existing and

future impacts of climate change in Cambodia's work. In recently, Koh Kong's coastal area is threatened to loss of mangrove forests due to the climate change such as seawater intrusion, Sea level rise, storm surges, storms, heavy rain, flooding, drought, and water stress.

1.1 Sea Level Rise in Cambodia

Sea level rise will have a significant impact on mangrove ecosystems and as an indicator system for assessment on vulnerable coastal mangroves in Cambodia that caused by climate change developing by Intergovernmental Panel on Climate Change (IPCC, 2013). In previously studied have indicated that Sea level rise 1 m would lead to loss of 4444 ha of coastline in Koh Kong and significantly raise the risk of severe flooding in Koh Kong City. The observed mean sea level rise in Cambodia, a 10 cm rising has been observed already in the last 40 years, and Sea level is continuing to rise. According to previous studies on climate change in Cambodia was estimated that sea-level will rise in Koh Kong province from 40 to 60 cm by the end of the century.

1.2 Research Objective and Problems

Cambodia's mangrove forests studies seem to lack data of mangrove forests change over time and how mangroves will face future Sea level rise. Over this problem, the purpose of this study is to apply the advanced technology by integrated Remote Sensing (RS) with Geographic Information System (GIS) tool to extract the mangrove forests at Peam Krasop Wildlife Sanctuary (PKWS) in Cambodia from 2015 to 2020 using multi-temporal derived from Sentinel-2 images with Random Forest Classification. To enhance mangrove forests changes in PKWS from 2015 to 2020 using MOLUSCE. Furthermore, to estimate the impacts of SLR on vulnerable areas of mangrove forests in PKWS, Cambodia by adopting the IPCC vulnerability assessment (IPCC, 2013) relied on the projection of Sea level rise by IPCC using a Geospatial model. In the aim of these problems, this study proposed an idea topic is "Mangrove Forests Changes and Responses to Sea Level Rise Based on Remote Sensing and GIS in PKWS, Cambodia". In this perspective, the study assists to achieve the research objectives:

- To extract mangrove forests in Peam Krasop Wildlife Sanctuary (PKWS), Cambodia, from 2015 to 2020 using multi-temporal derived from Sentinel-2 images with Random Forest Classification
- To analyze mangrove forests changes in PKWS from 2015 to 2020 using MOLUSCE
- To assess the vulnerable area of mangrove forests under different SLR scenarios using a Geospatial model based on IPCC's SLR projection

1.3 Research Questions

- What are the mangrove forest areas in Peam Krasop Wildlife Sanctuary in Cambodia between 2015 to 2020 using multi-temporal data of Sentinel-2 imageries with Random Forest classification?
- What are the mangrove forest changes taken place in Peam Krasop Wildlife Sanctuary in Cambodia between 2015 to 2020 using MOLUSCE in QGIS?
- What are the vulnerable area of mangrove forests under different Sea level rise scenarios using a Geospatial model?

1.4 The Significant

However, Mangrove RS has been studied since 1956, it still an interesting topic for researchers to do research on monitoring mangrove forests related to other sectors include natural resource, social-economic, and climate change.

Addiction, Cambodia has known as rich mangrove forests and a vulnerable country to climate change. Sea level rise (SLR) can lead a significant impact and threat to the coastal area, include mangrove forests. Peam Krasop Wildlife Sanctuary (PKWS) in Cambodia is a wildlife area that supports a significant mangrove ecosystem and threatened to climate change. This study will use a different method from others and can help to update the distribution and changing in mangrove forests in PKWS, and to enhance the most commonly vulnerable areas of mangrove forests due to the impact of future SLR. The first, classification method has been select Random Forest algorithm combine with training data 240 samples. After testing the classification of the training sample with the Random Forest algorithm, the result can

be reliable and higher than 90% of overall accuracy. For this sample data collection can be used to validate the data in reliability. Second, our study was developed the Geospatial model to analyze the vulnerable areas of mangrove forests due to impact of SLR in Peam Krasop Wildlife Sanctuary while no available tide gauge data or history Sea level rise (SLR) data. In this, build Geospatial model by a combination of SRTM DEM with SLR scenarios based on IPCC's SLR projection derived from IPCC's CMIP5 model. For SLR projection in Koh Kong province as this research study area, SLR is estimated to rise from 40 to 60 cm by the end of the twenty-first century. For this Geospatial model, DEM will process and combine with three different SLR scenarios include SLR 40 cm, SLR 60 m based on IPCC's CMIP5, and will develop one more SLR 1 m to see how mangrove forest faced to future Sa level rise (SLR) caused by climate change.

1.5 Limitation of This Study

For this study, Peam Krasop Wildlife Sanctuary (PKWS) is selected as the study area that a large area (25,897 ha) located in Koh Kong province, Cambodia, supporting a significant mangrove ecosystem. Due to lack of data and different data sources, to extract mangrove forests and analyze changes in mangrove forests from 2015 to 2020 were using multi-temporal Sentinel-2 images downloaded from ESA and USGS with Random forest machine learning in Dzetsaka plugin and analyze change using MOLUSCE in SCP plugin in QGIS. To assess the vulnerable area of mangrove forests under potential impact of Sea level rise, Digital Elevation Model is the main parameter to create the Geospatial modeling, and process the Sea level rise inundation based on SLR scenarios. The SRTM DEM data (30 meters' resolution) is available to download from USGS, SRTM will be used in this study. Also, no SLR observation station in Cambodia, for future SLR or SLR scenarios were adopted by IPCC's CMIP5 (2013). A geospatial model will be used to predict the future Sea level rise in Cambodia based on three different SLR scenarios such as SLR 40 cm, SLR 60 cm, SLR 1m. This Geospatial model was use to overlay with mangrove forests land cover in 2020 to assess the vulnerable area of mangrove forests under different SLR scenarios.

CHAPTER 2 LITERATURE REVIEWS

In the literature of this chapter, there is information about previous techniques studied. This chapter will give an overview of keywords, many techniques methods on mangroves Remote Sensing, and analysis the impact on land cover due to Sea level rise based on GIS methods.

2.1 Keywords

Before going deeply into the research topic “Mangrove forests changes and responses to Sea level rise based on Remote Sensing and GIS in PKWS, Cambodia”. This study will highlight some keywords such below:

- Mangrove forests are an ecosystem that grows between seawater and coastal areas (Hamilton & Snedaker, 1984).
- Sea Level Rise (SLR) is an increase in the level of the world’s oceans due to the effects of global warming derived from satellite observations and tide-gauge. The long-term average Sea level rise was called Relative Sea Level Rise derived from coastal tide gauges related to the local land level (Coastal Wiki, National Geographic).
- Geographic Information System (GIS) is a system designed to capture, manage, manipulate, analyze, store, and representing spatial or geographical data (GISTDA).
- Remote sensing (RS) is the processing of collecting Earth surfaces and phenomena information using sensors with no physical contact with the surface feature and phenomena (GISTDA).

2.2 General Mangroves Remote Sensing (RS)

Mangroves remote sensing has been studied since 1956. Over the last six decades, mangroves RS has evolved with hot spot topics such mangrove distribution mapping, ecosystem process characterization, biophysical parameters inversion, and monitoring the extent of changing of mangroves (Wang et al., 2019). Monitoring and

studying mangrove forest areas change over time are required cost-effective, convenient, accurate, and mapping techniques (Green, Clark, Mumby, Edwards, & Ellis, 1998). The providing of the historical evolution of mangroves remote sensing, the research topics, remote sensing techniques, and sensors from 1956 until 2018 (figure 1).

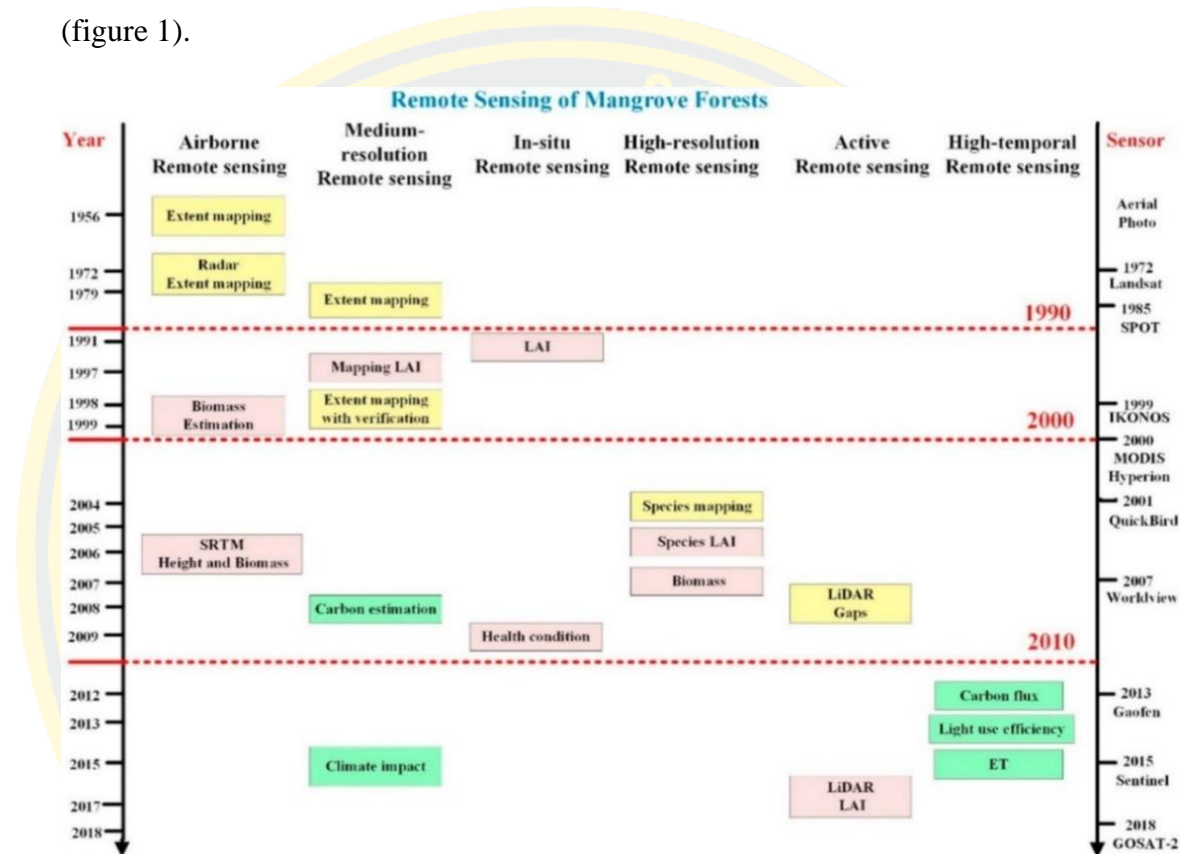


Figure 1. The evolution of mangroves remote sensing from 1956 until 2018. Distribution mapping (yellow box), biophysical parameters inversion (pink box), and ecosystem process characterization (green box), (Wang et al., 2019).

2.3 Analysis Impact of Sea Level Rise using GIS Methods

Geographic Information System (GIS) and Remote Sensing (RS) have been using as a powerful technique to study the relationship between Sea level rise and land use or coastal areas based on geospatial data and various data. Moreover, GIS is really important for simulating related to different Sea level rise scenarios. For analysis these scenarios are vital to measuring the vulnerability and risk from Sea level rise, to prevent the land cover and land use from Sea level rise risk. In recently, there are research studies about the effectiveness of land cover and coastal areas

associated due to Sea level rise. Particularly, these studies are crucial for developing and making the policy associated to the efficiency of Sea level rise and climate change. Alternatively, there are many research studies were conducted the analysis of Sea level rise impact on land cover at global scale, regional and local levels (Table 1).

Table 1. The studies of analysis SLR impacts using Remote Sensing and GIS

Previous Studies	References
To assess and visualize the global impacts of potential inundation by developed GIS methods based on global sea-level increase of 1 to 6 m	(X. Li et al., 2009)
To examined vulnerability implications of coastal inundation due to SLR for the coastal zone in Semarang city, Indonesia.	(Marfai & King, 2007)
Vulnerability assessment and adaptation to the impacts of sea level rise on the Kingdom of Bahrain	(Al-Jeneid S, 2008)
To developed a city based assessment of SLR for the Turkish Coastal Zone.	(Kuleli, 2010)
Analysis the potential impacts of SLR along Kanyakumari District's coastal zone in Tamilnadu, India.	(Natesan & Parthasarathy, 2010)
The assessment of the impact of SLR on mangrove dynamics using RS and GIS in Ganges Delta, India	(Pramanik, 2014)
Vulnerability assessment of the coastal mangrove ecosystems to SLR in Guangxi, China	(S. Li, Meng, Ge, & Zhang, 2014)
To assess the Bhitarkanika forest and adjacent eco-fragile area, Odisha, using Remote Sensing and GIS based SLR inundation	(M. Kumar, 2015)
Geospatial modeling of the impact of SLR on coastal communities: application of Richmond, British Columbia, Canada.	(Malik & Abdalla, 2016)
The assessment of SLR impacts on mangrove dynamics in the Indian Part of Sundarbans using Geospatial Techniques.	(Pramanik, 2016)
Geospatial modelling of the inundation levels in the Sundarbans mangrove forests due the impact of SLR and identify the effected species and regions.	(Ghosh, Kumar, & Kibet Langat, 2019)

Most studies used Remote Sensing data such Digital Elevation Model (DEM) to derive inundated areas, and DEM data has developed as the main approach. Even though, elevation data is a significant parameter to recognize the vulnerable coastal area and to define affecting area by Sea level rise along the coastal area and mangrove ecosystems.

2.4 Mangrove Forests and Sea Level Rise in Cambodia

2.4.1 Mangrove Forests Situation

Cambodia's mangrove forests are along the coastline with 435 km that consist of Koh Kong province, Sihanoukville, Kampot, and Kep province (Nop, 2017).

Table 2. The different estimates area of mangrove forests in Cambodia

Year	Area (ha)	Reference
1964	96,300	Report No.2 of Ministry of Water, Forests and Hunting in Ung (1991)
1973	94,600	UNDP, World Bank, FAO (1996)
1973	94,000	Ministry of Education (2009)
1975	94,600	MRC, UNDP, FAO
1980	91,200	The Food and Agriculture Organization (2005)
1989	88,413	(Veettil, 2019)
1990	82,400	The Food and Agriculture Organization (2005)
1992–93	37,000	Department of Fisheries
1992–93	85,100	MRC, UNDP, FAO
1993	77,669	DOFW, IRD
1993	62,416	Ministry of Education (2010)
1994	78,445	(Veettil, 2019)
1997	72,835	DOFW, IRD
1997	77,260	MRC, UNDP, FAO
1997	63,039	Ashwell (1997)
1997	57,482	Ministry of Education (2010)
2000	73,600	Ministry of Education (2005)
2002	56,241	Ministry of Education (2002)
2005	69,200	Ministry of Education (2005)
2006	33,087	MLMUPC, Cambodia
2009	58,934	(Veettil, 2019)
2010	78,405	Fishery Administration (FiA)
2015	43,000	Rizvi and Singer (2011)
2016-2017	51,603	(Veettil, 2019)

Mangrove forests in Cambodia are considered essential forests that provide food sources, shelters, and nurseries along the coastal zone. Mangrove forest ecosystems are crucial to the local communities in Cambodia. The coastal population of 70% is relying on mangrove resources and products. By the ways, mangrove forests have decreased by anthropogenic activities such as conversion mangrove forests area into shrimp farms, salt farms, charcoal production. These anthropogenic activities were affected the marine habitats and resistance to protect against the storms (Rizvi, 2011).

2.4.2 Mangroves Issue

While mangrove forests provide many benefits for the environment and social-economic, these mangrove forests are changed and destroyed from anthropogenic activities. The human activities such as illegal exports, shrimp farming, and charcoal production are examined as the foundation factors that led to the mangrove forests reduction and threatened mangrove areas in the coastal of Cambodia including Koh Kong and Kampot province (Bann, 1997; MoE, 2009). In recently, the results of analysis satellite imagery between 1989 and 2017 showed that mangrove forests have cleared along Cambodia's coastline was about 36,810 ha (42%). During 1989 and 2017, mangrove forests in coastal provinces of Koh Kong, Sihanoukville, Kampot, and Kep province, were lost about 26,437 ha, 1986 ha, 8127 ha, and 260 ha.

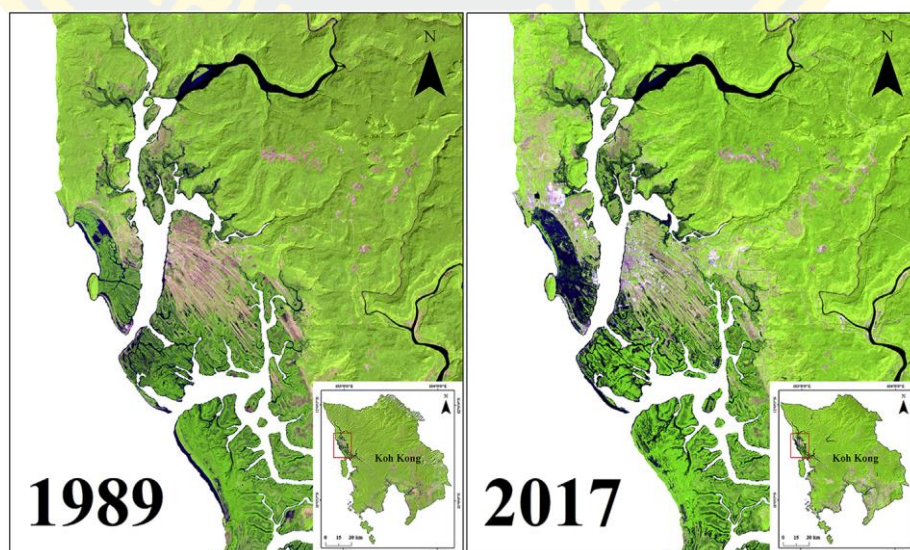


Figure 2. Before and after mangrove areas deforestation in Koh Kong province during from 1989 to 2017 (Bk & Quang, 2019).

Furthermore, the coastal zone has been identified as a central point to adapt to the existing and future impacts of climate change by The Royal Government of Cambodia. In that, Koh Kong province is the coastal area threatened to the impacts of seawater intrusion and Sea level rise, storms and storm surges, heavy rain and flooding, and drought and water stress. The possible threats of mangrove forests losing are from these factors such rising sea level, storm surges, tropical cyclones, coastal erosion, and saltwater intrusion into agricultural lands. Sea level rise will have a significant impact on mangrove ecosystems and also set as an indicator for assessment the coastal mangroves vulnerable that caused by climate change in Cambodia.

2.4.3 Relative Sea Level Rise

Although no direct observed sea-level data were available for Cambodia, many sea-level observing sites are available in nearby countries. So that made Cambodia no long-term quality-controlled dataset was available or can be obtained. Even though, Sea level rise data are examined from several nearby observing sites. The locations of the stations selected for this study shown in Figure 3 (obtained from <http://www.psmsl.org/data/obtaining/>).



Figure 3. Map of stations with sea-level data near Cambodia (BCC-PPCR, 2014).

There are variations in the annual cycle in sea-level at various locations due to the monsoonal influence. An increase in sea-level between 5 and 15 cm already been observed at several stations over the last several decades. The analysis includes data from these sites as well as from simulations of the twenty century and twenty-one century SLR predictions depended on the Atmosphere-Ocean General Circulation Models (AOGCMs) by the World Climate Research Programme from the Coupled Model Intercomparison Project Phase 5 (CMIP5) (Radić & Hock, 2011).

To determine changes in sea levels at a regional scale in Cambodia, the methods of Slangen et al. (2012) and Church et al. (2011) were used (Church & White, 2011); (Slangen, Katsman, van de Wal, Vermeersen, & Riva, 2011). These involved the combination of the dynamic ocean sea-level distribution through local change.

In Cambodia, results from other studies were used to derive conclusions for this region. The frequency of sea-levels extremely increases for example a result of the higher sea-levels in the 21st century. A one in 100-year flooding event could be occurring annually at many locations if Sea level rise 0.5 m by 2100, (Hunter, 2011). The observed mean sea level rise in Cambodia, a 10 cm rise already observed in the last 40 years, and estimated that Sea level rise from 40 to 60 cm will occur in Koh Kong province by the end of the century.

2.5 Classification Methods

There are two methods of Remote Sensing classification are object-based and pixel-based image classification (Aggarwal, Srivastava, & Dutta, 2016). The object-based classification method is an alternative when classify based on pixel values is not able to define spatial objects properly. The pixel-based classification method is Remote Sensing image classification method has been carried out according to the statistics difference ground spectrum information characteristics.

These methods are curious for identify and locate the land cover types such as forest and water bodies, agriculture, bare land, the built-up area known as a combination of experience and fieldwork. The analysis attempt to locate the specific

sites in Remote sensing and denote homogenous of these, land cover types well-known as training sites.

2.5.1 Object-based Classification

The object-based classification method could be an alternative method that has been used and suitable for medium spatial resolution to high spatial resolution of satellite imagery (Blaschke, 2010). The object-based classification is tries to build the meaningful objects through the image segmentation, and similar characteristics based on spatial and spectral properties. For objects segmentation were become to be the unit of analysis from spectral statistics such as standard deviation, spatial information such as image texture or spectral band means, that can be used for further analysis include satellite image classification.

2.5.2 Pixel-based Classification

The pixel-based classification method is the classification method that use only the spectral information available for individual pixels done on a per-pixel level (Sibaruddin, Shafri, Pradhan, & Haron, 2018). Hence, each pixel represents a training example for a classification algorithm, and this training example would be in the form of an n-dimensional vector, where n was the number of spectral bands in the image data. The train algorithm of classification would give output as a class prediction for each individual pixel in an image.

2.5.3 Easy Random Forest in Dzetsaka Plugin

Random Forest classification has become widely held used for real world in land cover mapping of Remote sensing field includes Mangrove forests mapping. Random Forest is assembling machine learning classification as well as Regression that handle in big data efficiently.

Random Forest algorithm is a good algorithm to solve the overfitting that it is one critical problem that can make the results worse. By the ways, the Random Forest algorithm is a classifier of Random Forest classify that provided a high classification accuracy, has the proficiency to determine the crucial variables and predict the

missing values during performing image classification, and modeled for categorical values. Random Forest is a combination of a number of non-parametric classification and Decision Tree/Classification and Regression Trees (CART). A Decision Tree is similar to a hierarchy composed of the root node, including all samples, node separator which has decision rules, and the end of the leaf node represents desired classes. Decision Trees are often handy tools to explain the intuition behind a prediction to people unfamiliar with Machine Learning. Decision tree is a simple, deterministic data structure for modelling decision rules for a specific classification problem

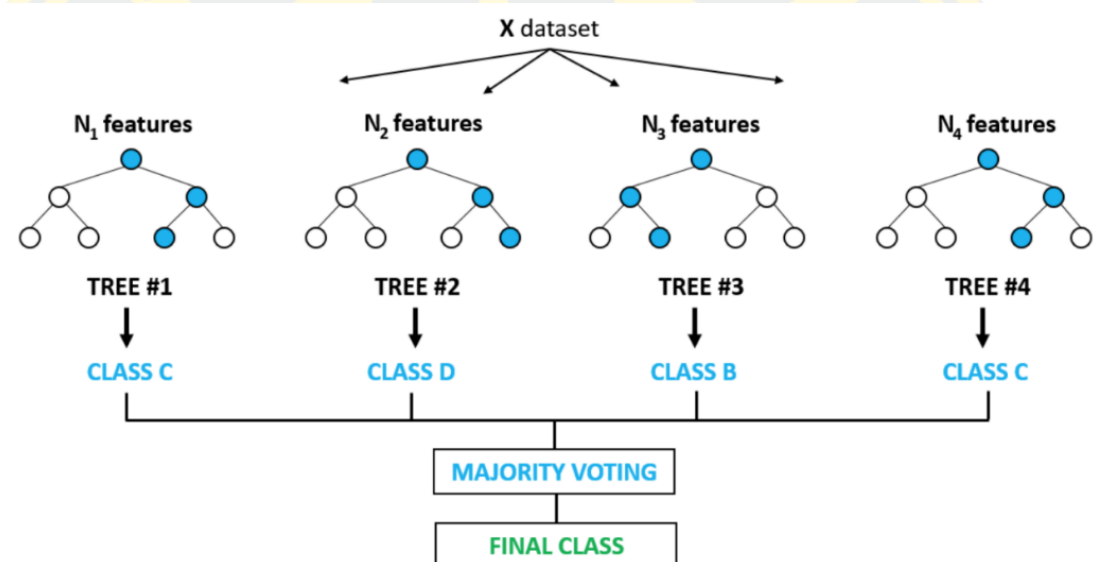
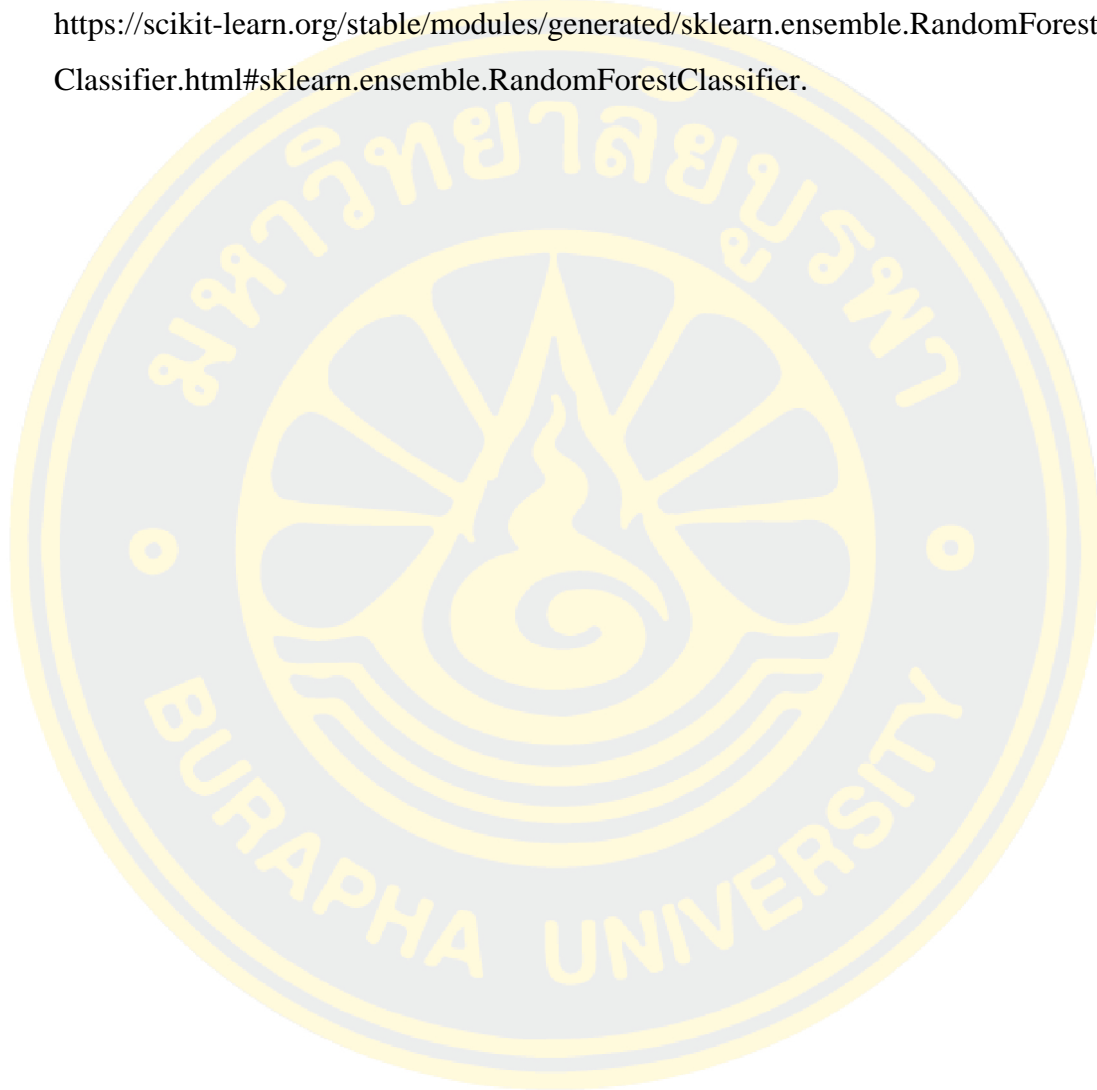


Figure 4. Ensemble of Decision Trees (Random Forest).

Initially based on Gaussian Mixture Model Classifier developed by Mathieu Fauvel. In present, Dzetsaka Plugin also supports the Random Forest (RF) classify, K-Nearest Neighbors (K-NN), and Support Vector Machine (SVM), this plugin is a more general tool than the Historical Map which was dedicated to classify the forests from old maps developed by Nicolas Karasiak, Random Forest often has better results, but it takes longer to perform the fit and the predicted process. To perform the Random Forest classifier in Dzetsaka Plugin, it needs to install of Scikit-learn python library because it supports working on Windows. Scikit-learn is probably the most useful library for machine learning in Python. To explore and understand about the

Scikit-learn library for machine learning python of this plugin including train algorithm, classification, and confusion matrix for accuracy calculation, just go directly to this website <https://github.com/nkarasiak/dzetsaka>. For understand more about progressing of Scikit-learn for Random Forest classifier:

<https://scikit-learn.org/stable/modules/generated/sklearn.ensemble.RandomForestClassifier.html#sklearn.ensemble.RandomForestClassifier>.



CHAPTER 3 METHODOLOGY

This chapter describes the methods were used to acquire data and process data. The main concept of this part is how to extract the mangrove forests and changing in mangrove forests areas from 2015 to 2020, and impacts of future Sea level rise on mangrove forests areas derived from Remote sensing (RS) imageries and Geographic Information System (GIS) tools. The methodology chapter includes data acquisition and data preprocessing, data processing. In this section, for performing classification to extract mangrove forests from 2015 to 2020 using Sentinel-2 imageries multi-temporal data based on the Random Forest algorithm of Random Forest (RF) Classification. Analysis of mangrove forests change during from 2015 to 2020 by land cover classes were conducted using Modules for Land Use Change Simulations (MOLUSCE) which is a plugin that allows performing convenient analysis of land-use changes evaluation. SRTM DEM with three different Sea level rise scenarios (SLR 40 cm, SLR 60 cm, and SLR 1 m) to create a geospatial model to identify the potential impacts of mangrove forests areas due to Sea level rise by overlap with mangrove forests map in 2020.

3.1 Study Area

Peam Krasop Wildlife Sanctuary (PKWS) is a large area located in 11°50'75" N & 103°06'77" E that located in Koh Kong Province in the Southwestern of Cambodia. Peam Krasop Wildlife Sanctuary (PKWS) is a coastal wildlife sanctuary established in 1993, and it is a protected area covering 25,897 ha. The part of PKWS lies inside the boundary of Koh Kapik and Islets Ramsar Site associated. Peam Krasop Wildlife Sanctuary (PKWS) is a unique supporting significant mangroves ecosystem that provides crucial benefits for fishery and other resources. This area provides various works for livelihoods who are living with its borders including charcoal production, aquaculture, and other reasons.

Particularly, Peam Krasop Wildlife Sanctuary (PKWS) is an area that worries about clearing of coastal swamp forest and the declining of mangrove forests to shrimp farming, that pushed a negative effect on wildlife habitat in this area. Thus, Peam Krasop Wildlife Sanctuary (PKWS) is a strong area affected by inter-tidal

levels and seasonally fluctuating freshwater inputs (Dara, 2009). The adjacent estuarine sea in Peam Krasop Wildlife Sanctuary (PKWS) is extremely vulnerable to rising sea levels that caused by climate change, it will cause increased salinity incursion and increases in sedimentation.

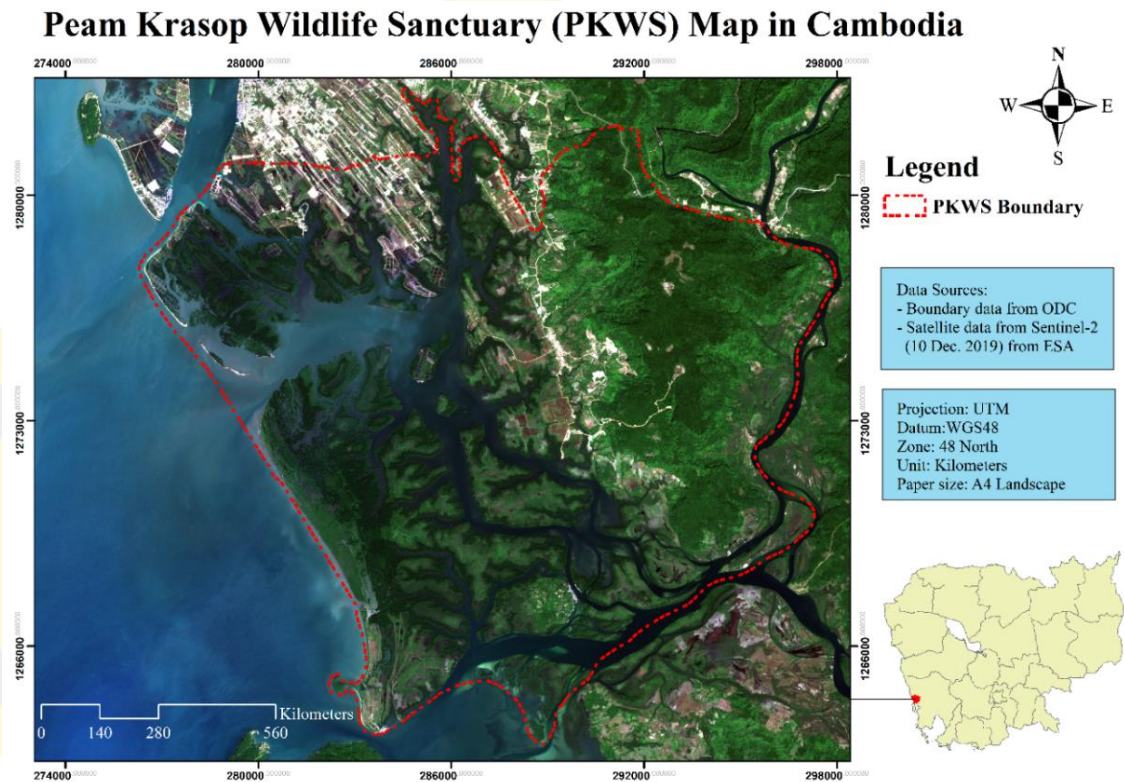


Figure 5. Map of Study area (Peam Krosop Wildlife Sanctuary).

3.2 Methodology Workflow

The methodology is divided into three parts, which can be broadly categorized as data acquisitions, image processing and image analysis. This chapter describes the workflows of the three methods (Figure 5) for (1) extracting the mangrove forests from 2015 to 2020, (2) analyze changing in mangrove forests areas during from 2015 to 2020, and (3) impacts of future Sea level rise on mangrove areas derived from Remote Sensing (RS) imageries and Geographic Information System (GIS) model.

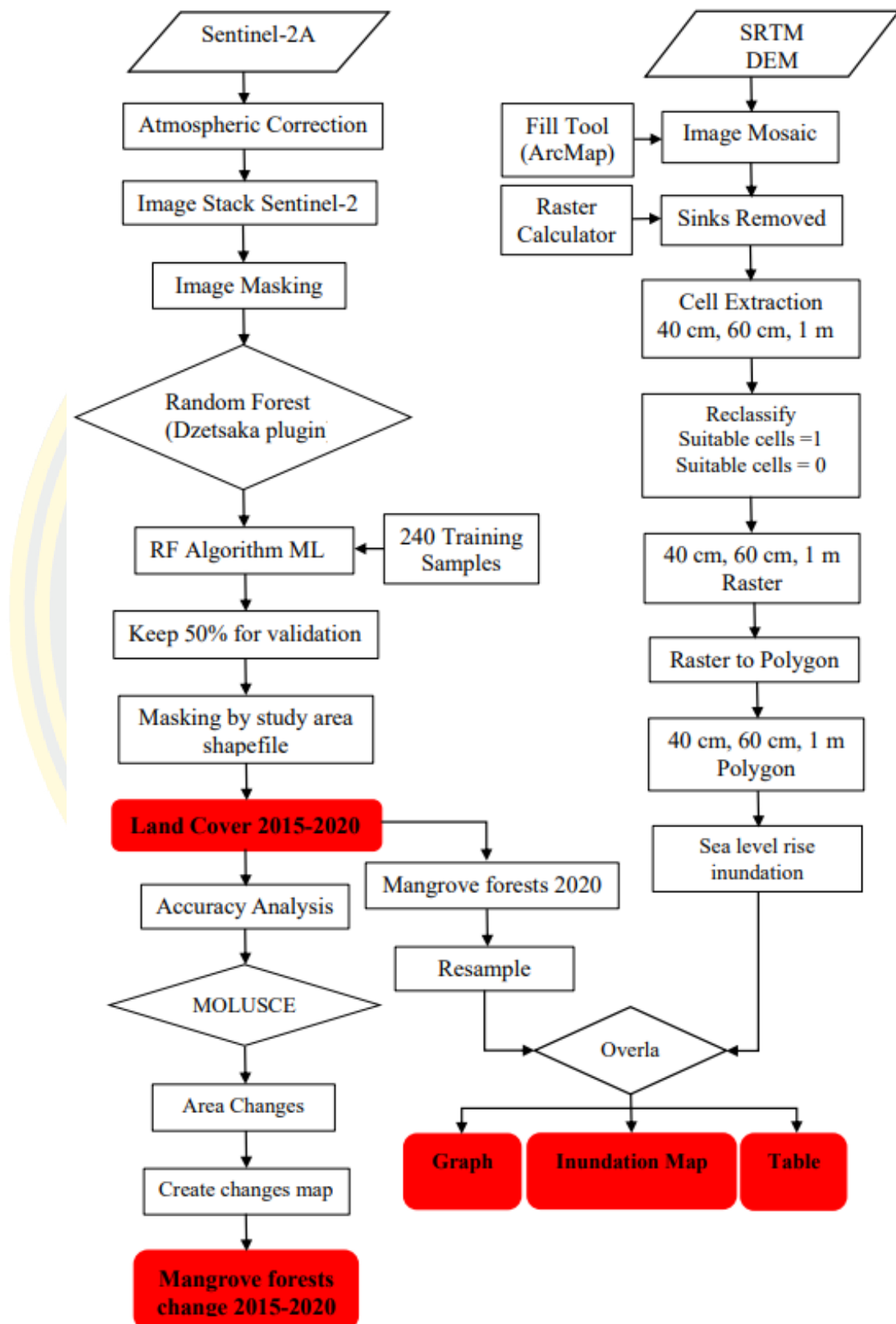


Figure 6. Potential inundation of SLR scenarios on mangroves forest areas by the end of this century workflow.

3.3 Data Acquisitions

3.3.1 Sentinel-2 Imagery

In this study, Sentinel-2 imageries have been selected to identify and study changes in mangrove forests and mangrove extraction. Sentinel-2 satellite image is an Earth observation mission from the European Space Agency (ESA) contains of a group of two satellites orbiting the poles, which are in orbit around the same sun, which are at 180 ° each other. There are two twin satellites, one is the Sentinel-2A sensor was launched in June 2015, and the Sentinel-2B sensor was launched in March 2017. This type of satellite has a full swath width at 290 km and a high return time for ten days at the equator of one Satellite. It supports the monitoring mission of Earth's surface changes and coverage limit from latitudes between 56 ° South and 84 ° North. This optical imagery includes 13 bands with high spatial resolution including 10 m, 20 m, and 60 m, over coastal waters and land. Sentinel-2A, only high spatial resolution 10m and 20 m were selected in this study.

Table 3. Description of spectral bands of Sentinel-2 (Hawryło & Wezyk, 2018)

Bands Spectral	Wavelength Range (nm)	Spatial Resolution (m)	Description
Band 1	32-453	60 m	Coastal aerosol
Band 2	458-523	10 m	Blue
Band 3	543-578	10 m	Green
Band 4	650-680	10 m	Red
Band 5	698-713	20 m	Red-edge 1
Band 6	733-748	20 m	Red-edge 2
Band 7	773-793	20 m	Red-edge
Band 8	785-900	10 m	Near Infrared (NIR)
Band 8A	855-875	20 m	Near Infrared narrow(NIRN)
Band 9	935-955	60 m	Water vapor
Band 10	1360-1390	60 m	Cirrus
Band 11	1565-1655	20 m	Shortwave Infrared (SWIR) 1
Band 12	2100-2280	20 m	Shortwave Infrared (SWIR) 2

Sentinel-2A, only high spatial resolution 10m and 20 m were selected in this study. Sentinel-2 imageries have been selected from 2015 to 2020. Sentinel-2 imageries were collected from the United State Geological Survey (USGS) and ESA Sentinels Scientific Data Hub.

Table 4. Data Acquisition for Sentinel-2 imagery

Sensor	Spatial Resolution (m)	Date	Path/row	Cloud Cover
Sentinel-2 L1C	10m, 20 m	2015-12-31	48/18	0.00
Sentinel-2 L1C	10m, 20 m	2016-02-31	48/18	38.84
Sentinel-2 L1C	10m, 20 m	2017-12-20	48/18	0.00
Sentinel-2 L1C	10m, 20 m	2018-11-25	48/18	1.93
Sentinel-2 L1C	10m, 20 m	2019-12-10	48/18	0.00
Sentinel-2 L1C	10m, 20 m	2020-12-29	48/18	32.80

Sentinel-2 L1C is Top Of Atmosphere (TOA) Orto-image products that need to applied atmospheric correction Orto-image products for more accurate and reliable data. To apply the atmospheric correction on Sentinel-2A L1C imageries, using the Semi-Automatic Classification Plugin (SCP), which this plugin provides tools for downloading, and preprocessing of Remote Sensing images.

3.3.2 Digital Elevation Model (DEM)

Digital Elevation Model (DEM) is a specialized database that represents the relief of a surface between points known as elevation. This elevation data can be derived from several sources such as photogrammetric data capture, ground surveys, and a rectangular DEM grid created. DEM provides multi-benefits, it serves to illustrate the appearance of the earth's surface (Octariady, Hikmat, Widyaningrum, Mayasari, & Fajari, 2017), GIS software can use DEM for some activities such as orthorectification image, creation of contour lines, erosion control, 3D surface visualization, flood simulation, and performing view-shed visibility analysis. DEM is really important as the main parameter to determine the impact of SLR on future mangrove forests area in PKWS. Therefore, in this section, SRTM DEM was

collected from United State Geological Survey (USGS) was used to remove regions of elevation of the ocean (elevation of zero), besides it was originally collected from the National Geospatial-Intelligence Agency (NGA) and National Aeronautics and Space Administration (NASA) by 11 February 2000. SRTM data were derived from C-band radar datasets which was distributed under the agreement of USGS, NGA, and NASA's Jet Propulsion Laboratory. SRTM product was utilized a C-band radar image to generate the elevation data over 80% of the land surface in the earth.

In this study, NASA SRTM DEM is including two images, which N11E102.SRTMGL1 with Center Latitude and Longitude 11°30'00"N, 102°30'00"E, and N11E103.SRTMGL1 with Center Latitude and Longitude 11°30'00"N, 103°30'00"E. NASA SRTM images were acquisition start date 2000-02-11 and acquisition end date 2000-02-21 with spatial resolution 30 meters (1 Arc-Second Global) covering most of the world with absolute vertical accuracy of less than 16m (RMSE of 9.73m). This SRTM DEM has to remove the sinks from the negative raster values into 0 values of mean sea level (MSL) defined the 'fill tool' in ArcMap software, this removing is for keeping the reliability in the generated results.

3.3.3 Sea Level Rise (SLR) Scenarios

Changing of sea-level has been measuring through the tide-gauge and satellite altimeter that related to changing of sea-level in global, regional, and local factors. Generally, tide-gauge is the tool that using for measurement and observation of the sea-level change rates. Mostly, tide-gauge data is used for the regional sea-level change of coastal wetlands (Gilman, Ellison, & Coleman, 2007) as well as mangrove dynamics. Even though, the regional sea-level change depends on various factors such as meteorological, and oceanographic factors where the coastal wetland is situated, coastal subsidence, sediment budget, and the distance of available tide-gauge data (Gilman et al., 2007).

In Cambodia is not available tide-gauge to observed the sea-level, hence the Sea level rise rates in this study area base on several sea-level observing sites are available in nearby countries such as Thailand, Vietnam, and Indonesia. The analysis includes data from these sites as well as from simulations of the 20th century and

21st-century Sea level rise predictions. The preliminary regional distribution of sea-level change for 2081-2100 compared with 1986-2005 for the RCP 8.5 scenario based on Atmosphere-Ocean General Circulation Models (AOGCMs) from CMIP5. Based on this RCP 8.5 emission scenario estimated that sea-level will rise from 40 to 60 cm by the end of the twenty-first century in Koh Kong province. These Sea level rise scenarios are essential as the raster cells data for processing with SRTM DEM data to create a Geospatial model of inundation level of Sea level rise impact on mangrove forests areas. There are three different Sea level rise scenarios were adopted such as SLR 40 cm, SLR 60 cm depended on Sea level rise projection for Koh Kong province, and SLR 1 m adopted in this study.

Table 5. Summarized data acquisition

Data	Spatial resolution	Temporal coverage	References
Sentinel-2 MS L1C	10m, 20m	2015-2020	United State Geological Survey ESA Sentinels Scientific Data Hub
SRTM DEM	30 m	11-21 02 2000	United State Geological Survey (USGS)
SLR Rates (40cm, 60cm,1m)		2081-2100	IPCC's SLR scenarios based on (1986-2005)

3.4 Data Processing

3.4.1 Mangrove Forests Extraction

Mangrove forest extraction has been classified using the easy machine learning Random Forest classified in Dzetsaka Plugin in QGIS. This plugin allows performing classifiers such as Gaussian Mixture Model Classifier developed by Mathieu Fauvel. In present, Dzetsaka Plugin also supports the Random Forest (RF) classify, K-Nearest Neighbors (K-NN), and Support Vector Machine (SVM), which developed by Nicolas Karasiak, (Pinasu D, 2020). Random Forest classification has been used to classified and extracted mangrove forests. Random Forest often has better results, but it takes longer to perform the fit and the predicted process. To

perform the Random Forest classifier in Dzetsaka Plugin, it needs to install of Scikit-learn python library because it supports working on Windows. Scikit-learn is probably the most useful library for machine learning in Python. To understand more about the library for machine learning python of this plugin including train algorithm, classification, and confusion matrix for accuracy calculation, just go directly to this website <https://github.com/nkarasiak/dzetsaka>.

This tool was developed to classify a different kind of vegetation while it is useful for mangrove forests study and research. There are two steps for procedures work are training data and perform the type of classification. For training Random Forest algorithm per every satellite image were 240 training data according to create a total of six classes. In Dzetsaka, Random Forest algorithm in the optional parameters flag save the error matrix that it was from specify split to 50%. So that 50% of the samples of the roi.shp file are used for training the algorithm and the rest for cross-validation. Random Forest algorithm works with two stages, first stage is pseudocode random forest creation, another stage is to make the random forest prediction pseudocode from the RF classifier created in the first stage. The process of the Random Forest algorithm is seeming easy to understand, but somehow it is really efficient.

Table 6. Number of samples selected for training classification

Year	Water	Mangroves	Saltmarsh	Forest Lands	Settlements	Other Lands
2015	40	40	40	40	40	40
2016	40	40	40	40	40	40
2017	40	40	40	40	40	40
2018	40	40	40	40	40	40
2019	40	40	40	40	40	40
2020	40	40	40	40	40	40

Land cover's mangroves class were classified into three level. The first level of land cover demarcated of land cover types' six classes includes water body,

mangrove forests, saltmarsh, forest lands, settlements, and other lands. The second level is reclassified into three classes namely water body, mangroves, non-mangroves (combination of saltmarsh, forest land, settlements, and other lands) using Reclassify tool in ArcMap. The third level demarcated of mangrove forests areas extraction by reclassified water body class and non-mangroves class into NoData, and keep only mangrove forests class in by using Reclassify tool in ArcMap.

Table 7. Mangrove forests classification levels

Land Cover classes	Level I	Level II	Level III
1	Water body	Water body	Mangrove forests
2	Mangrove forests	Mangrove forests	
3	Saltmarsh	Non-mangrove forests	
4	Forest lands		
5	Settlements		
6	Other lands		

3.4.2 Analysis Changes of Mangrove Forests

After land cover classification at level I has completed, Mangrove forests result in 2015 to 2020 were generated changing in mangrove forests of 5 years' mangrove forests. Mangrove forests have been analyzed change from mangrove forests class to other land cover classes between period times (2015, 2016, 2017, 2018, 2019, 2020). These changes were analyzed using QGIS plugin, Modules for Land Use Change Simulations (MOLUSCE) which this MOLUSCE allows performing the convenient analysis of land-use changes evaluation and quickly. This plugin consists of several parts: one part is Area Analysis, which provides procedures to calculate the amount change between the state of land cover classes and allows creating of change maps of the land cover classes. The Modeling provides submodules for modeling relations between input-output data.

The main purpose of area analysis module is to create and calculate change map. The area analysis module uses the next scheme of transition encoding. For 6 classes ($N=6$), there are $6*6= 36$ possible transitions:

Table 8. The transition encoding of classes

Classes	Water	Mangroves	Saltmarsh	Forest Lands	Settlements	Other Lands
Water	0	1	2	3	4	5
Mangroves	6	7	8	9	10	11
Saltmarsh	12	13	14	15	16	17
Forest Lands	18	19	20	21	22	23
Settlements	24	25	26	27	28	29
Other Lands	30	31	32	33	34	35

3.4.3 Analysis Potential Impacts of SLR on Mangrove Forests

Mangrove forest areas in 2020 will be used as the main data for predict the inundation level of mangrove forests impact due to Sea level rise scenarios. The potential impacts of Sea level rise inundated on mangrove forest areas in Peam Krasop Wildlife Sanctuary (PKWS) were analyzed spatial analysis using Sea level rise scenarios RCP 8.5 from IPCC. Sea level rise rates were generated to overlay mangrove forests map in 2020. Then, the inundated mangrove forest areas were analyzed and identified under Sea level rise scenarios. In this part, ArcMap will be an important tool to analyze the impact area. The raster Calculator tool in ArcMap was used to create the raster values of 40 cm, 60 cm, and 1 m.

3.5 Accuracy Assessments

For accuracy assessment of easy Random Forest classification were assessed using confusion matrix from the performing of 240 training sample polygons in Dzetsaka plugin. Thus, confusion matrix was created and presented overall accuracy and kappa statistics in Random Forest algorithm training from 50% split of total training samples for cross-validation, it means 50% of the pixels are randomly selected to training and 50% for validation. For accuracy assessment of the Random Forest Classification were calculated in several ways, include Overall Accuracy (OA), Kappa statistic, User's Accuracy (UA), and Producer's Accuracy (PA) were calculated using Confusion matrix online calculator based on Marco Vanetti, 2007 (Landis & Koch, 1977).

CHAPTER 4 EXPERIMENT RESULT

4.1 Land Cover of Mangrove Forests Extraction from 2015 to 2020

4.1.1 Land Cover Classes Level I

PKWS's land cover has been classified into six classes in level I included water, mangroves, saltmarsh, forest lands, settlements, and other lands between 2015 to 2020 derived from Sentinel-2 images based on Random Forest Classification (Figure 7 and Table 9).

In 2015 was predominantly covered with forest lands 9058.33 ha (35.04%) followed by mangrove forests 7157.90 ha (27.69%), water body 5240.86 ha (20.27%), saltmarsh 2362.72 (9.13%), other lands 1287.64 ha (4.98%) and settlements 746.57 ha (2.89%).

For land cover in 2016, was maximum covered of forest lands 9183.64 ha (35.52%), mangrove forests 7495.21 ha (28.99%), and water body 5526.56 ha (21.38%), followed by other lands 1819.45 ha (7.04%), saltmarsh 1415.94 ha (5.48%) and settlements 413.22 ha (1.59%).

For land cover in 2017, was maximum covered of forest lands 9491.25 ha (36.71%), mangrove forests 7337.47 (28.38%), and water body 5506.50 ha (21.30%), followed by other lands 1679.88 (6.50%), saltmarsh 1603.62 (6.20%) and settlements 299.77 (1.16%).

For land cover in 2018, was maximum covered of forest lands 9954.95 (38.50%), mangrove forests 6436.26 (24.90%) and water body 5201.85 (20.12%), followed by saltmarsh 2356.06 (9.11%), other lands 1605.13 (6.21%) and settlements 1605.13 (6.21%).

For land cover in 2019, was maximum covered of forest lands 10223.60 (39.54%), mangrove forests 6761.66 (26.15%) and water body 4915.04 (19.01%), followed by another area such saltmarsh 2095.10 (8.10%), other lands 1242.12 (4.81%) and settlements 616.50 (2.39%).

For land cover in 2020, it also showed that forest lands, mangrove forests, and water body were the three maximum areas covered 9629.52 ha (37.24%), 7045.64 ha (27.25%), and 5425.51 ha (20.99%), followed by other lands 1568.62 ha (6.07%), saltmarsh 1545.56 ha (5.98%), and settlements 639.17 ha (2.47%).

The overall accuracy of the Random Forest algorithm of Random Forest classification was well classified. The overall accuracy estimated to achieved 99.979% with Kappa statistic 100% in 2015, 99.975% with Kappa statistic 100% (2016), 99.981% with Kappa statistic 100% (2017), 99.961% with Kappa statistic 99% (2018), 99.754% with Kappa statistic 99%, and 99.96% with Kappa statistic 99%.

Table 9. Land cover classes Level I of PKWS from 2015 to 2020

Land cover Level I		Area (Hectare) and Percentage (%)				
Classes/Year	2015	2016	2017	2018	2019	2020
Water body	5240.86 (20.27)	5526.56 (21.38)	5506.50 (21.30)	5201.85 (20.12)	4915.04 (19.01)	5425.51 (20.99)
Mangroves	7157.90 (27.69)	7495.21 (28.99)	7337.47 (28.38)	6436.26 (24.90)	6761.66 (26.15)	7045.64 (27.25)
Saltmarsh	2362.72 (9.13)	1415.94 (5.48)	1603.62 (6.20)	2356.06 (9.11)	2095.10 (8.10)	1545.56 (5.98)
Forest lands	9058.33 (35.04)	9183.64 (35.52)	9491.25 (36.71)	9954.95 (38.50)	10223.60 (39.54)	9629.52 (37.24)
Settlements	746.57 (2.89)	413.22 (1.6)	235.30 (0.91)	299.77 (1.16)	616.50 (2.39)	639.17 (2.47)
Other lands	1287.64 (4.98)	1819.45 (7.04)	1679.88 (6.50)	1605.13 (6.21)	1242.12 (4.81)	1568.62 (6.07)
Total Area	25854.02	25854.02	25854.02	25854.02	25854.02	25854.02
OA (%)	99.979	99.975	99.981	99.961	99.754	99.96
Kappa	100	100	100	99	99	99

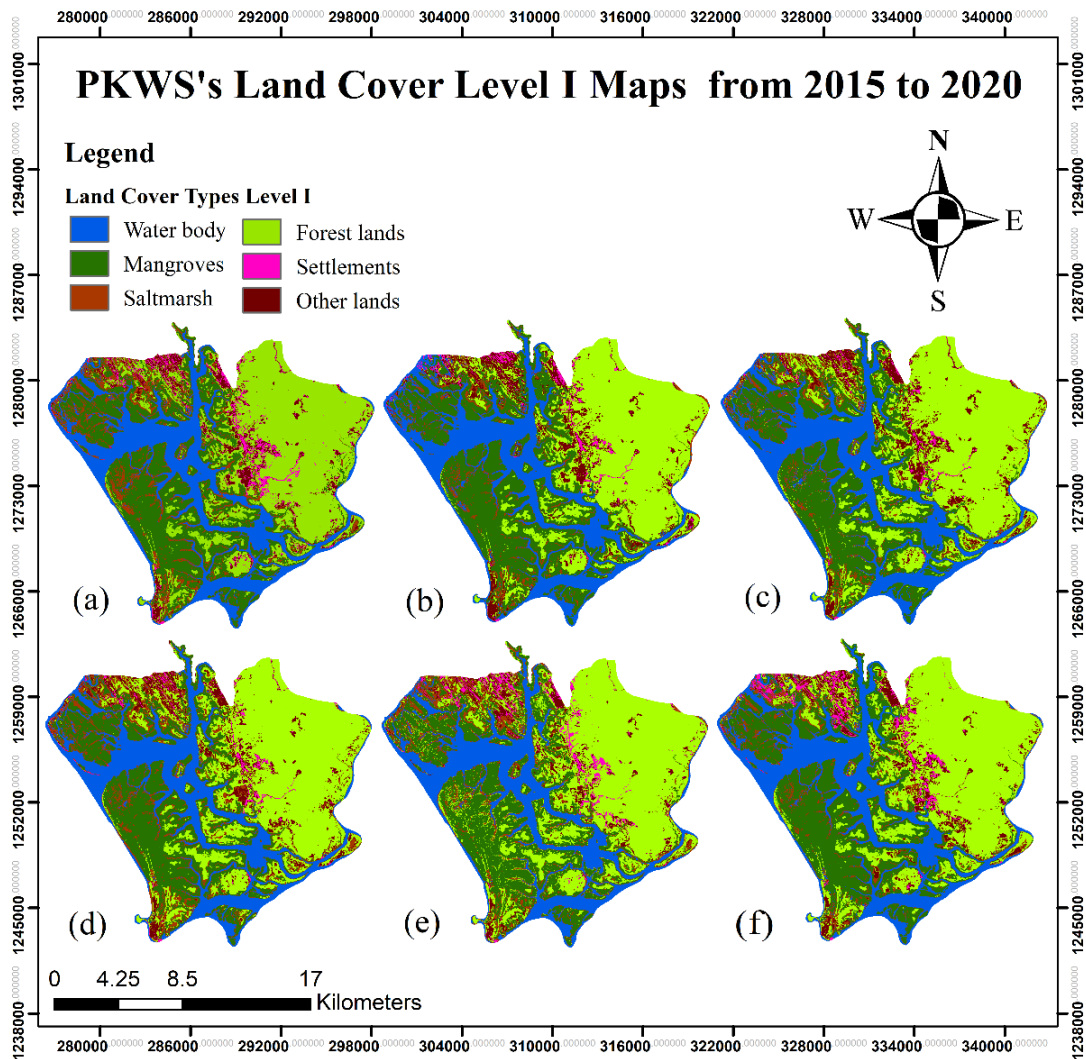


Figure 7. Land Cover Map level I of PWKS from 2015 to 2020. (a) Classify 2015, (b) Classify 2016, (c) Classify 2017, (d) Classify 2018, (e) Classify 2019, (f) Classify 2020.

4.1.2 Land Cover Classes Level II

Land cover on PKWS area have reclassified into three classes in level II such water, mangroves, non-mangroves (included saltmarsh, forest lands, settlements, and other lands) between 2015 to 2020 (Figure 8 and Table 10).

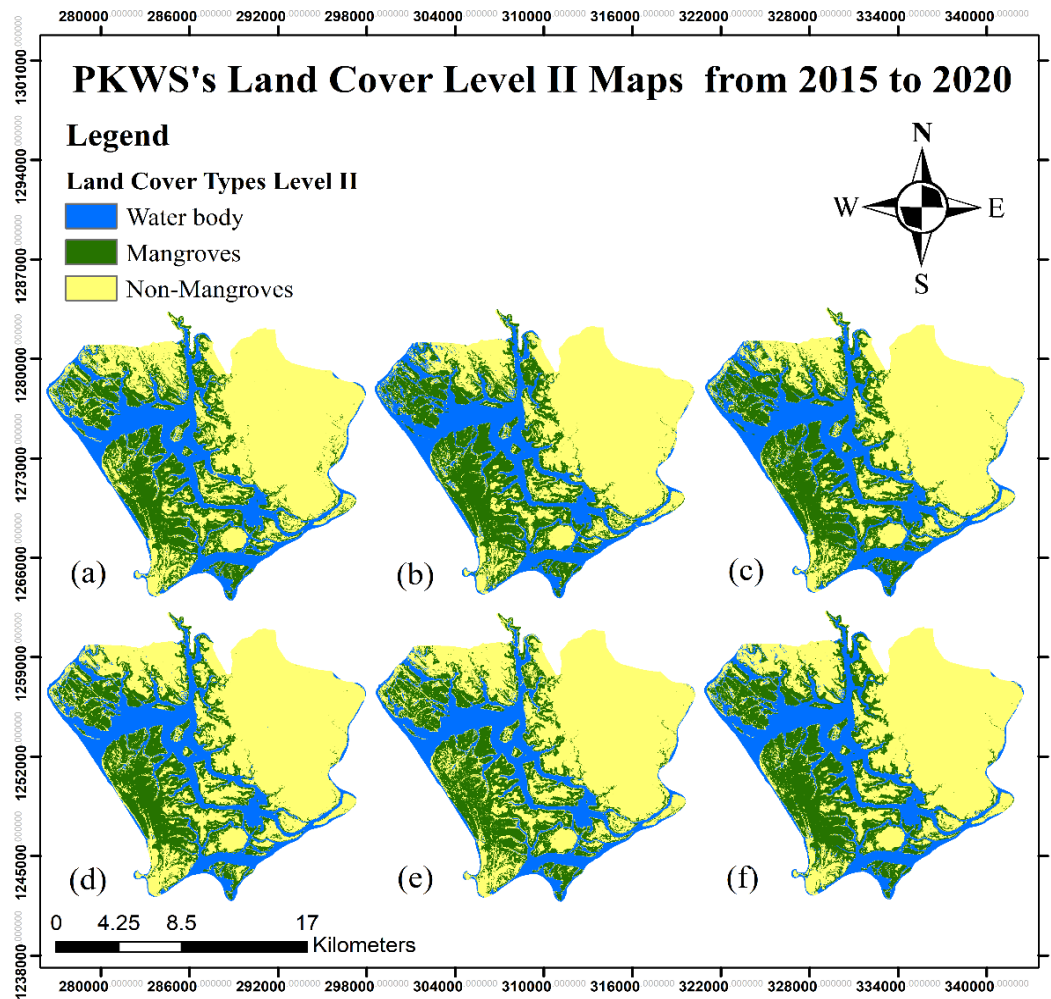


Figure 8. Land Cover Map Level II of PWKS from 2015 to 2020. (a) Classify 2015, (b) Classify 2016, (c) Classify 2017, (d) Classify 2018, (e) Classify 2019, (f) Classify 2020.

In 2015, was mainly covered with non-mangroves, mangrove forests, and water body, were about 13455.26 ha, 7157.90 ha, 5240.86 ha, which represented about 52.04%, 27.69%, 20.27%. In 2016, was mainly covered with non-mangroves, mangrove forests, and water body, were about 12832.25 ha, 7495.21 ha, 5526.56 ha, which represented about 49.63%, 28.99%, 21.38%. In 2017, was mainly covered with non-mangroves, mangrove forests, and water body, were about 13010.05 ha, 7337.47 ha, 5506.50 ha, which represented about 50.32%, 28.38%, 21.30%. In 2018, was mainly covered with non-mangroves, mangrove forests, and water body, were about 14215.91 ha, 6436.26 ha, 5201.85 ha, which represented about 54.98%, 24.90%, 20.12%. In 2019, was mainly covered with non-mangroves, mangrove forests, and

water body, were 14177.32 ha, 6761.66 ha, 4915.04 ha, which represented about 54.84%, 26.15%, 19.01%. In 2020, mostly covered by non-mangroves around 13382.87 ha, presenting 51.76%, followed by mangrove forests 7045.64 ha, presenting 27.25%, and water body 5425.51 ha, presenting 20.99%.

Table 10. Land cover classes Level II of PKWS from 2015 to 2020

Land cover		Area (Hectare) and Percentage (%)				
Level-II						
Classes/Year	2015	2016	2017	2018	2019	2020
Water body	5240.86 (20.27)	5526.56 (21.38)	5506.50 (21.30)	5201.85 (20.12)	4915.04 (19.01)	5425.51 (20.99)
Mangroves	7157.90 (27.69)	7495.21 (28.99)	7337.47 (28.38)	6436.26 (24.90)	6761.66 (26.15)	7045.64 (27.25)
Non-mangroves	13455.26 (52.04)	12832.25 (49.63)	13010.05 (50.32)	14215.91 (54.98)	14177.32 (54.84)	13382.87 (51.76)
Total Area (Ha)	25854.02	25854.02	25854.02	25854.02	25854.02	25854.02

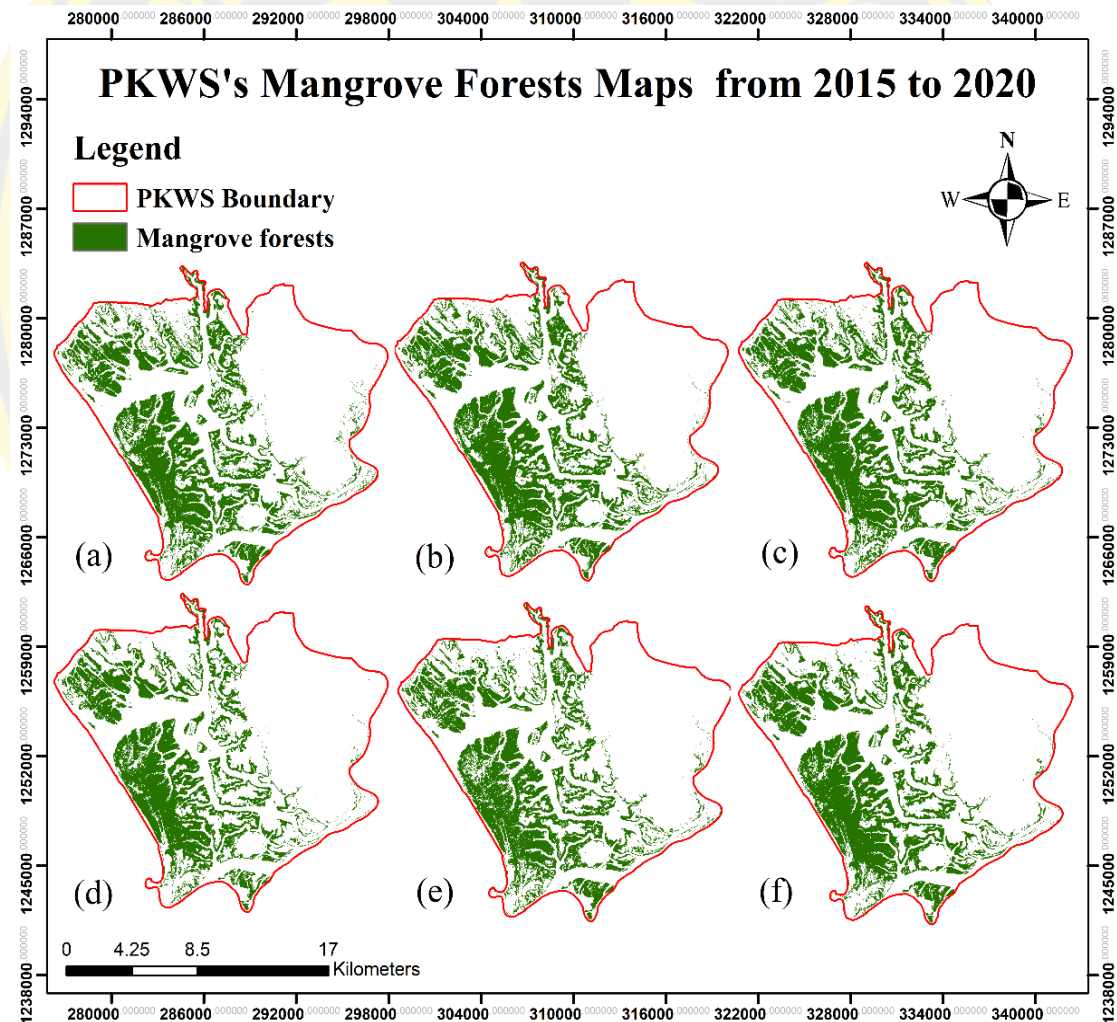
4.1.3 Land Cover Level III

The result of mangrove forests maps in PKWS are shown in green polygon (Figure 9, Table 11). Mangrove forests area in PKWS were 7157.90 ha in 2015, 7495.21 ha (2016), 7337.47 ha (2017), 6436.26 ha (2018), 6761.66 ha (2019), and covered 7045.64 ha in 2020.

The confusion matrix of the Random Forest algorithm indicated the mangrove forests class with producer's accuracy around 99.962% in 2015, 99.996 in 2016, and 100% for 2017, 2018, 2019, and 2020. The user's accuracy, mangrove forests were estimated accuracy of 100% every year of the time period.

Table 11. Land cover classes Level II of PKWS from 2015 to 2020

Land cover Level-III	Area (Hectare)					
Class/Year	2015	2016	2017	2018	2019	2020
Mangrove forests	7157.90	7495.21	7337.47	6436.26	6761.66	7045.64
Produce's accuracy (%)	99.962	99.966	100	100	100	100
User's accuracy (%)	100	100	100	100	100	100

**Figure 9.** PWKS's mangrove forests from 2015 to 2020. (a) Classify 2015, (b) Classify 2016, (c) Classify 2017, (d) Classify 2018, (e) Classify 2019, (f) Classify 2020.

4.2 Mangrove Forests Change from 2015 to 2020 Using MOLUSCE

4.2.1 Mangrove Forests Change from 2015-2016

Mangrove forests have changed from 7150.90 ha in 2015 to 7495.21 ha in 2016. Between 2015 and 2016, mangroves forest were significantly increased by 337.31 ha (Table 12). The result shows mangrove forests were increased from converting saltmarsh by about 445.78 ha. However, mangrove forests were changed to other land cover classes include water, saltmarsh, settlements, and other lands, about -1.86, -6.38, -4.77, and -95.46 ha in 2016 (Table 12, Figure 10).

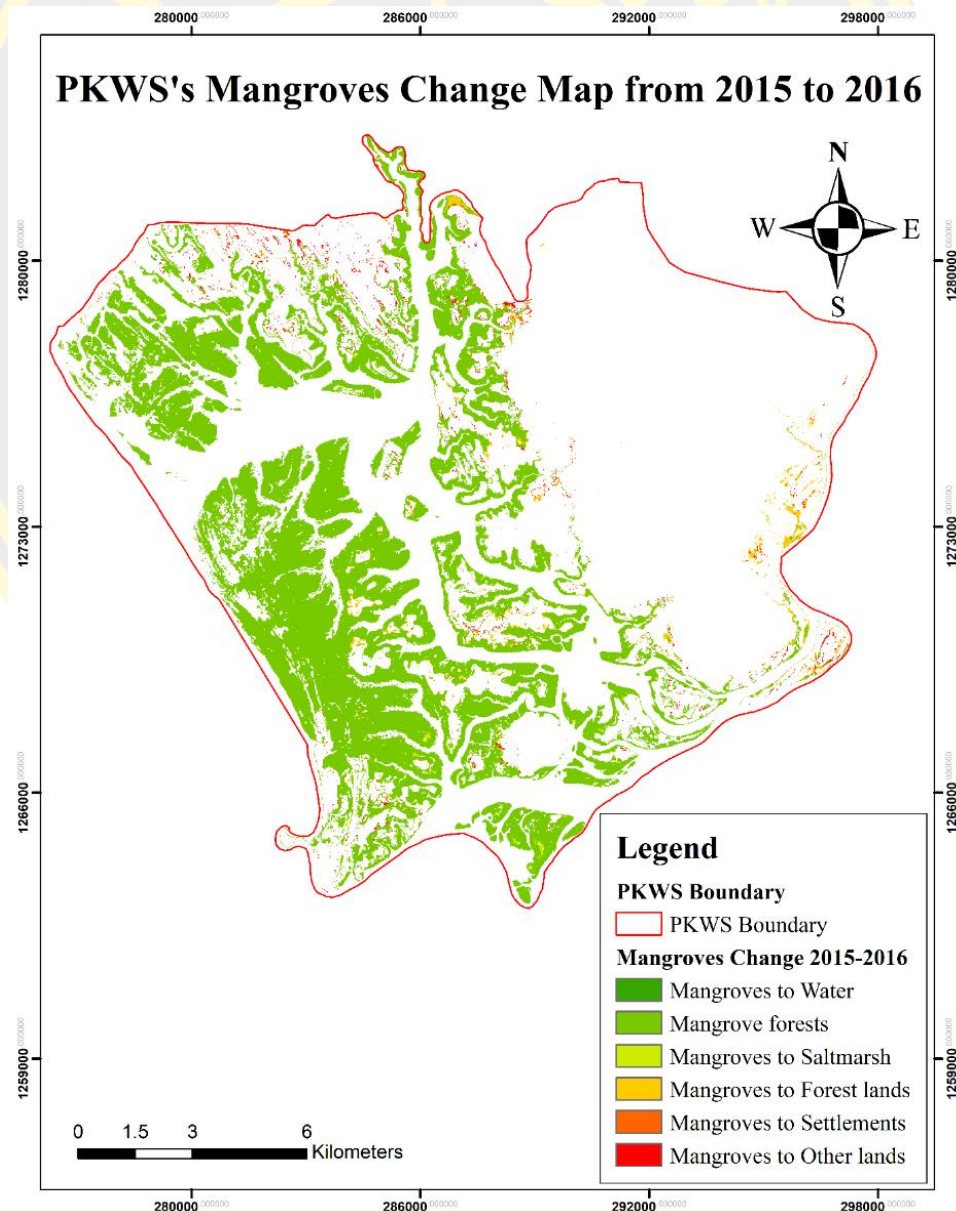


Figure 10. PKWS's Mangrove forests change between 2015 and 2016.

Table 12. Mangrove forests change (hectare) between 2015 to 2016

Classes/Year	2015	2016	Total (Hectares)
Mangrove to Water	3.24	1.38	-1.86
Mangrove forests	6762.06	6762.06	6762.06
Mangrove to Saltmarsh	56.28	502.06	445.78
Mangrove to Forest lands	205.55	199.17	-6.38
Mangrove to Settlements	5.74	0.97	-4.77
Mangrove to Other Lands	125.03	29.57	-95.46
Total (Hectare)	7157.90	7495.21	337.31

4.2.2 Mangrove Forests Change from 2016-2017

Mangrove forests in PKWS have changed from 7495.21 ha in 2016 to 7337.47 ha in 2017. In these years, mangrove forests were extremely decreased by 157.74 ha (Table 13, Figure 11). Mangrove forests were significantly decreased to forest lands about 246.67 ha, while converted from water, saltmarsh, settlements, and other lands, about 6.42, 3.26, 10.50, and 68.75 ha, to mangrove forests area in 2017.

Table 13. Mangrove forests change (hectare) between 2016 to 2017

Classes/Year	2016	2017	Total (Hectare)
Mangrove to Water	4.39	10.81	6.42
Mangrove forests	6951.32	6951.32	6951.32
Mangrove to Saltmarsh	184.98	188.24	3.26
Mangrove to Forest lands	345.34	98.67	-246.67
Mangrove to Settlements	0.77	11.27	10.50
Mangrove to Other Lands	8.41	77.16	68.75
Total (Hectare)	7495.21	7337.47	-157.74

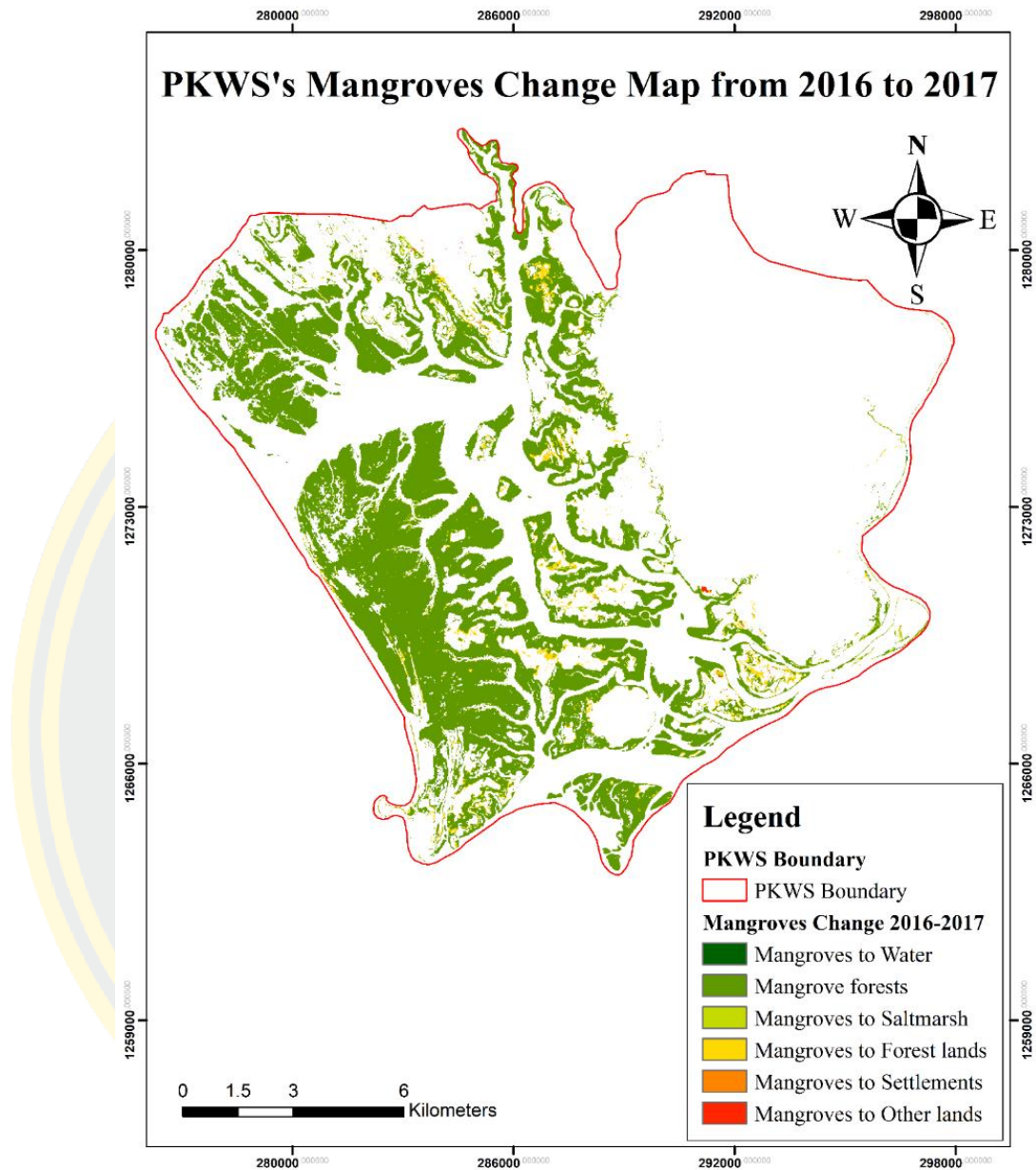


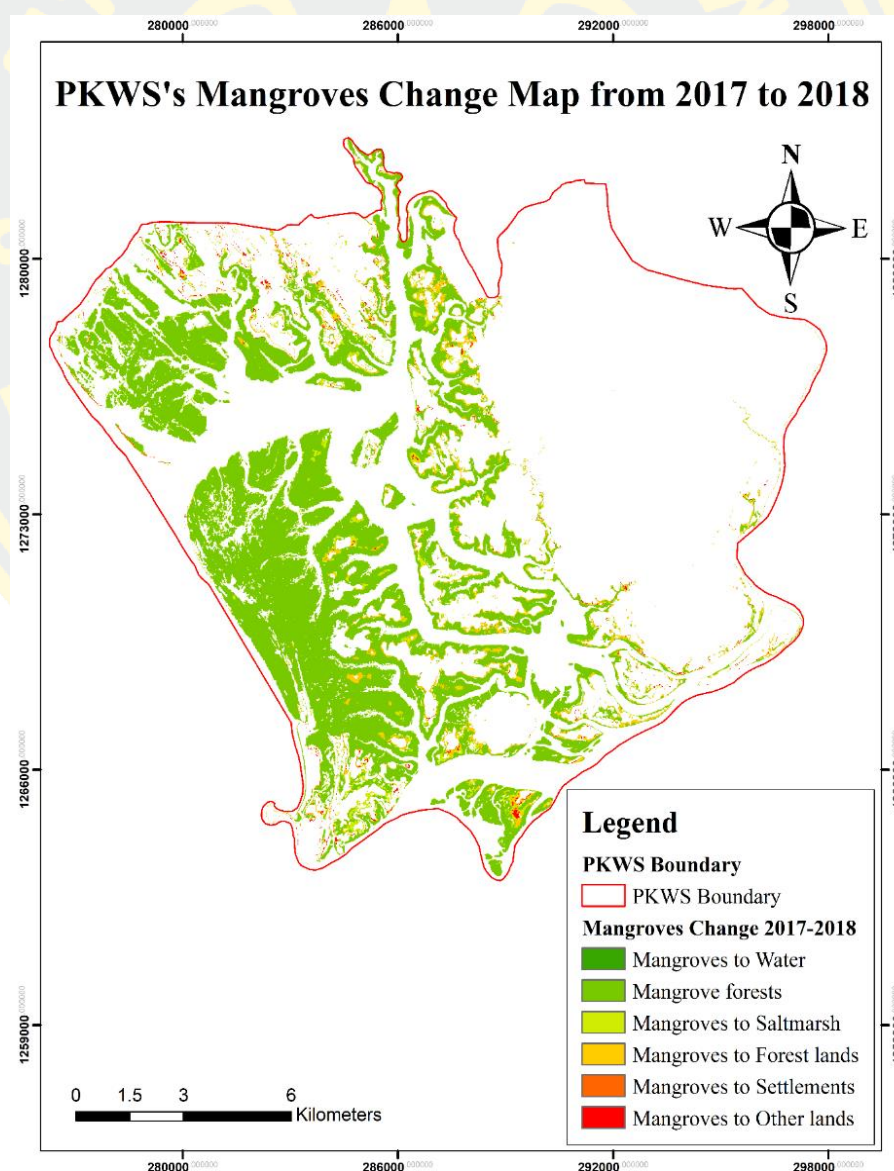
Figure 11. PKWS's Mangrove forests change between 2016 and 2017.

4.2.3 Mangrove Forests Change from 2017-2018

Similarly, mangrove forests have continued to decrease in 2018. In 2018, a decrease of mangrove forests about 901.21 ha was decline to forest lands, saltmarsh, other lands and settlements, represented about -442.91, -383.78, -76.13, and -5.35. This was extremely decreased from 7337.47 ha in 2017 to 6436.26 ha in 2018 (Table 14, Figure 12).

Table 14. Mangrove forests change (hectare) between 2017 to 2018

Classes/Year	2017	2018	Total (Hectare)
Mangrove to Water	0.54	7.50	6.96
Mangrove forests	6211.57	6211.57	6211.57
Mangrove to Saltmarsh	523.90	140.12	-383.78
Mangrove to Forest lands	519.65	76.74	-442.91
Mangrove to Settlements	5.36	0.01	-5.35
Mangrove to Other Lands	76.45	0.32	-76.13
Total (Hectare)	7337.47	6436.26	-901.21

**Figure 12.** PKWS's Mangrove forests change between 2017 and 2018.

4.2.4 Mangrove Forests Change from 2018-2019

Furthermore, mangrove forests have started to increase in PKWS in 2019. An increase of 325.40 ha were mangrove forests changed from 6436.26 ha in 2018 to 6761.66 ha in 2019. These significant changes from different classes such as saltmarsh, forest lands, other lands and settlements, represented about 270.46, 35.17, 19.90, and 0.46 ha (Table 15, Figure 13).

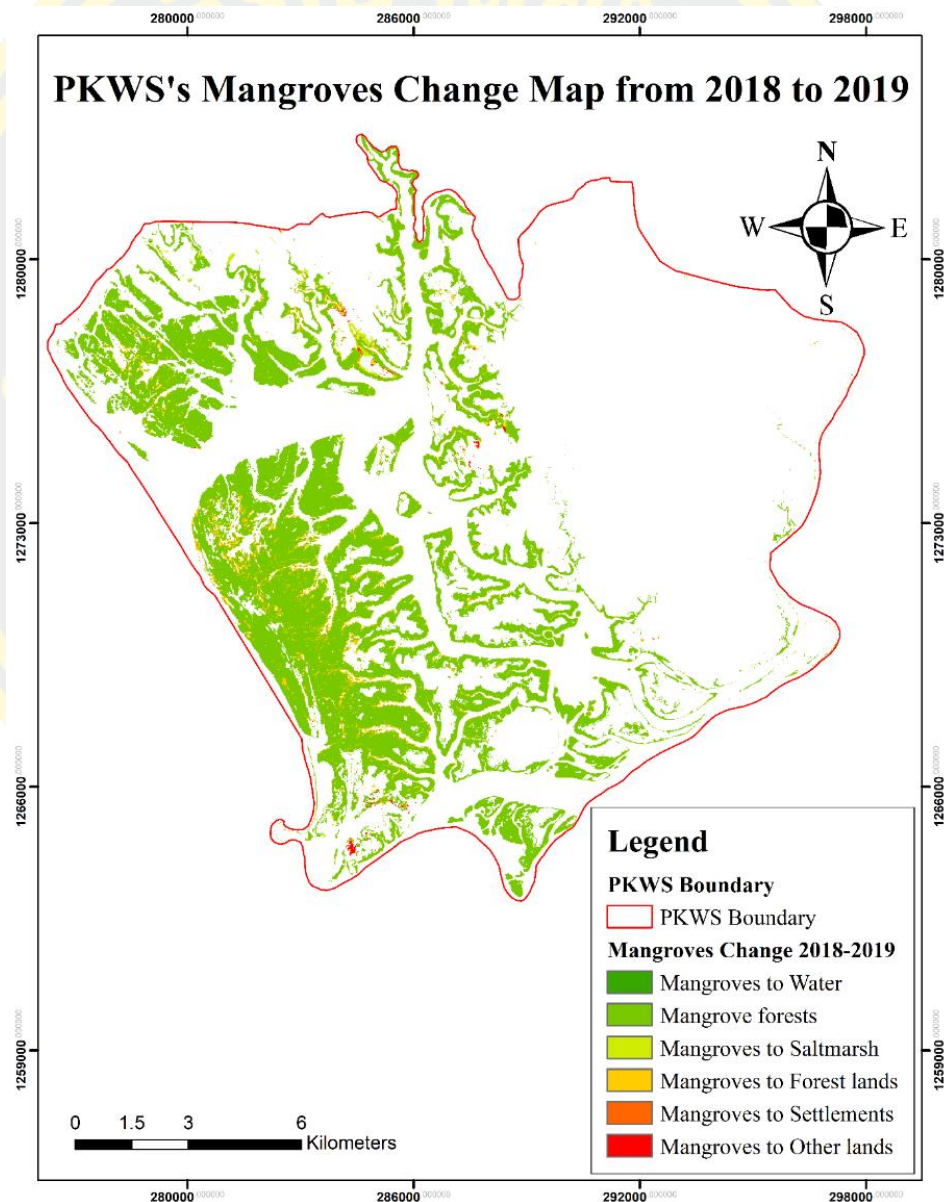


Figure 13. PKWS's Mangrove forests change between 2018 and 2019.

Table 15. Mangrove forests change (hectare) between 2018 to 2019

Classes/Year	2018	2019	Total (Hectare)
Mangrove to Water	0.82	0.23	-0.59
Mangrove forests	5825.80	5825.80	5825.80
Mangrove to Saltmarsh	128.70	399.16	270.46
Mangrove to Forest lands	457.16	492.33	35.17
Mangrove to Settlements	1.17	1.63	0.46
Mangrove to Other Lands	22.61	42.51	19.90
Total (Hectare)	6436.26	6761.66	325.40

4.2.5 Mangrove Forests Change from 2019-2020

Besides, between 2019 and 2020, mangrove forests have increased by approximately 283.98 ha. In detail, mangrove forests have changed from 6761.66 ha to 7045.64 ha between 2019-2020. An increase of these mangrove forests were converted from forest lands about 348.81 ha (Table 16, Figure 14).

Table 16. Mangrove forests change (hectare) between 2019 to 2020

Classes/Year	2019	2020	Total (Hectare)
Mangrove to Water	8.59	0.75	-7.84
Mangrove forests	6272.19	6272.19	6272.19
Mangrove to Saltmarsh	165.37	161.17	-4.20
Mangrove to Forest lands	248.17	596.98	348.81
Mangrove to Settlements	14.41	0.03	-14.38
Mangrove to Other Lands	52.93	14.52	-38.41
Total (Hectare)	6761.66	7045.64	283.98

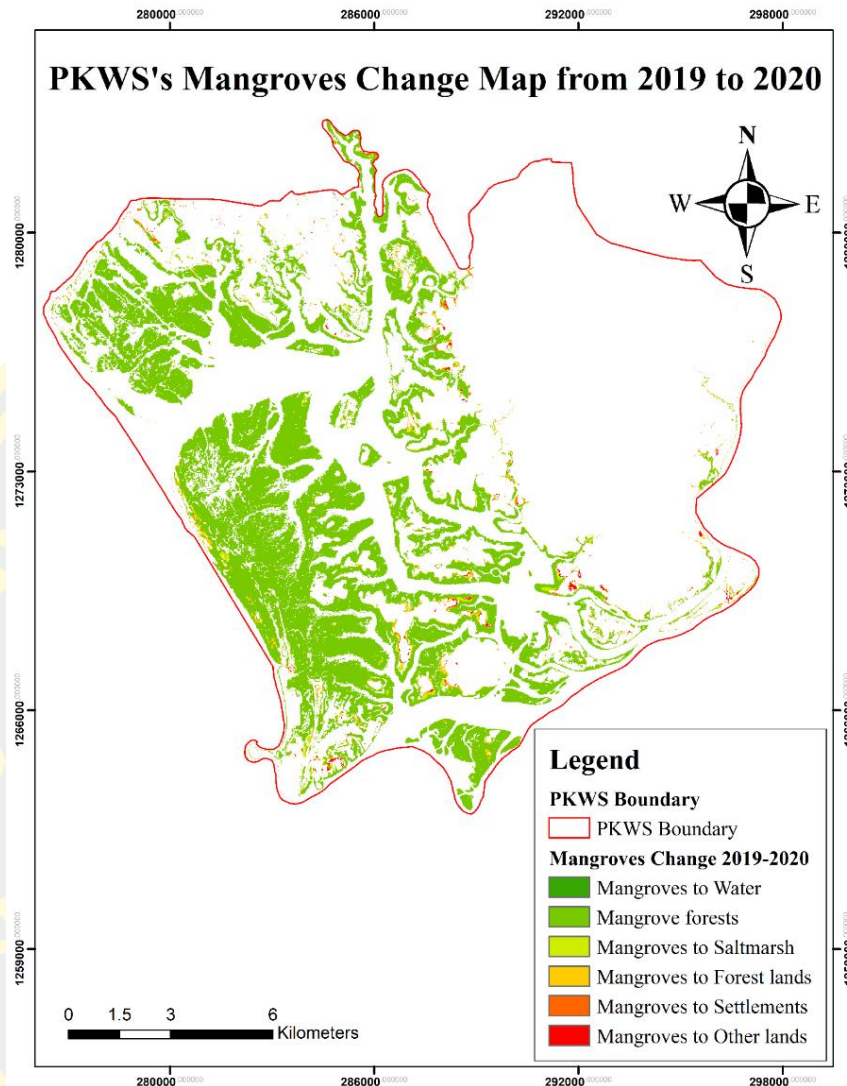


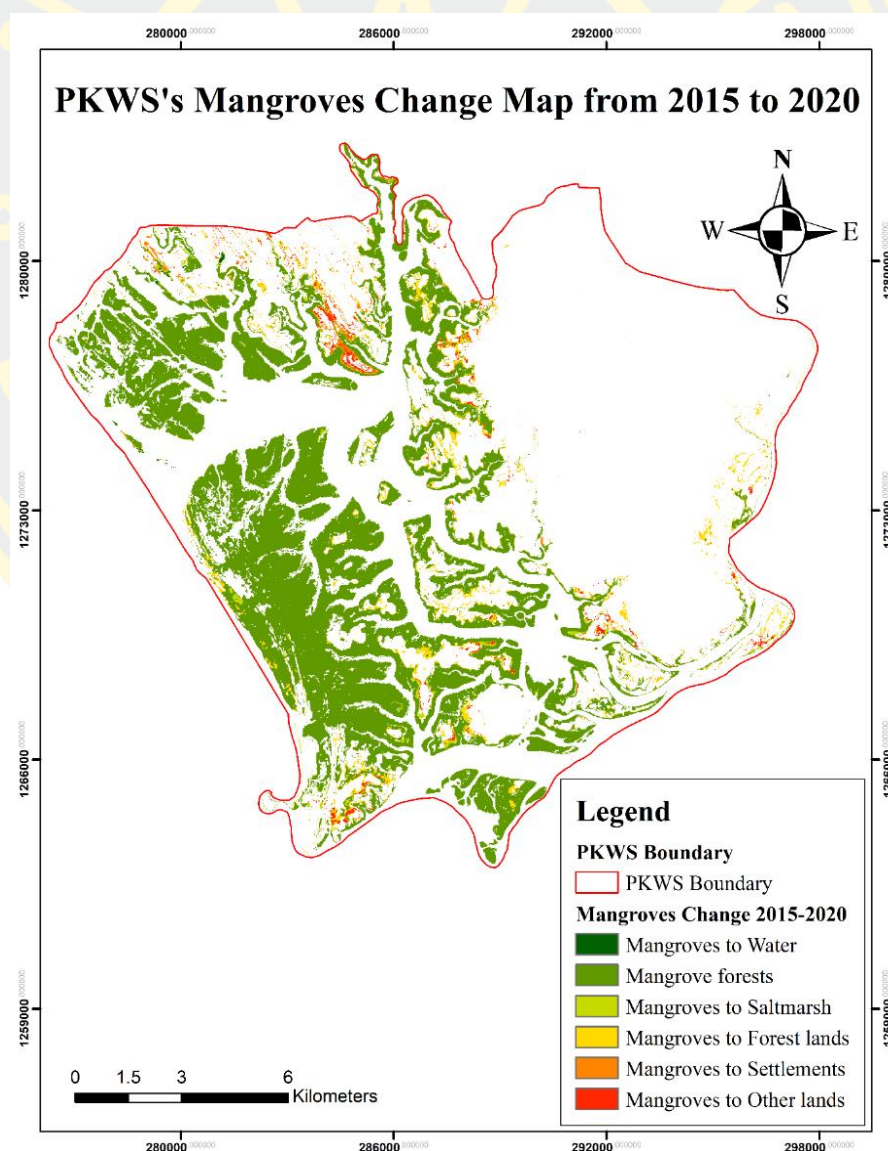
Figure 14. PKWS's Mangrove forests change between 2019 and 2020.

4.2.6 Mangrove Forests Change from 2015-2020

The long-term changing in mangrove forest areas during 2015 to 2020, mangrove forests were changed from 7157.90 ha to 7045.64 ha. Additionally, unchanged mangrove forests estimated about 6281.89 ha. During 5 years (2015-2020), mangrove forests decreased 561.59 ha, however the mangrove forests areas has regrowth about 451.91 ha. Totally, mangrove forests areas estimated to loss about 112.26 ha occurred in PKWS from 2015 to 2020 due to mangrove forests were transferred to other land cover classes. Mangrove forests are estimated converting to forest lands, other lands, settlements, and water, which were about -387.53, 115.78, 59.57, and -1.29 ha (Table 17, Figure 15 and 16).

Table 17. Mangrove forests change (hectare) between 2015 to 2020

Classes/Year	2015	2020	Total (Hectare)
Mangrove to Water	15.62	14.33	-1.29
Mangrove forests	6281.89	6281.89	6281.89
Mangrove to Saltmarsh	167.05	618.96	451.91
Mangrove to Forest lands	505.22	117.69	-387.53
Mangrove to Settlements	60.27	0.7	-59.57
Mangrove to Other Lands	127.85	12.07	-115.78
Total (Hectare)	7157.9	7045.64	-112.26

**Figure 15.** PKWS's Mangrove forests change between 2015 and 2020.

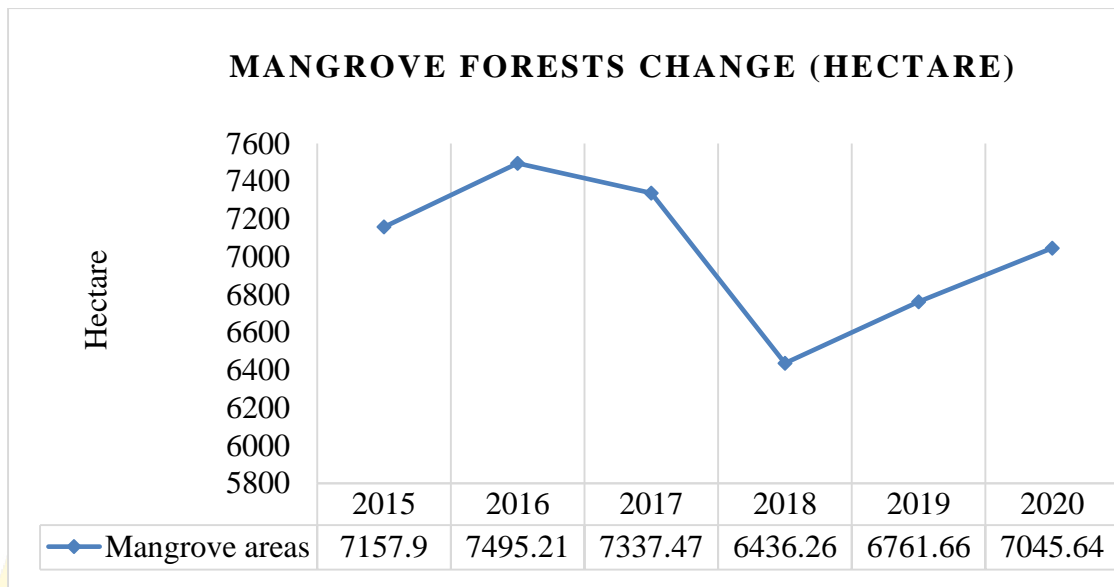


Figure 16. Diagram of mangrove forests change during from 2015 to 2020.

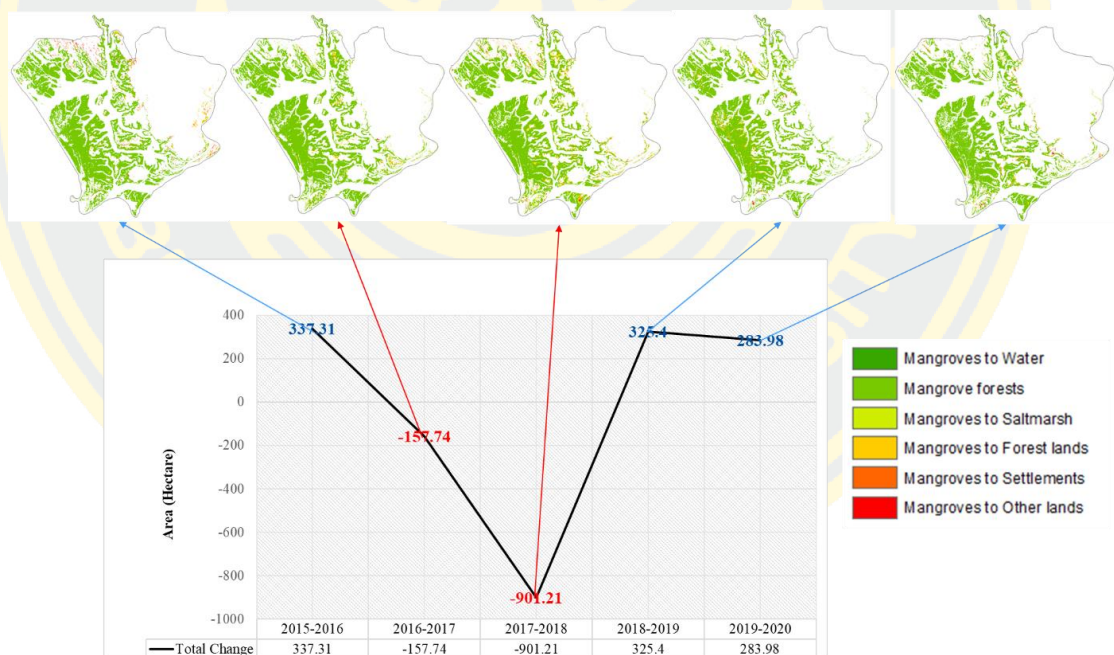


Figure 17. Increased and Decreased of Mangrove forests area from 2015-2020.

4.3 Potential Inundation of SLR on Mangrove Forests Area

In this part, mangrove forests extraction in 2020 was used to analyze the vulnerable mangrove forests areas in Peam Krasop Wildlife Sanctuary response to the impact of Sea level rise based on Sea level rise scenarios year 1986-2005. The results specify that the potential inundated mangrove area will submerge by Sea level rise

with the different Sea level rise scenarios. Mangrove forest areas are projected to be inundated by 40.44 ha by increasing SLR 40 and 60 cm by the end of the year 2100. Moreover, mangrove forest area is predicted to be inundated by 53.14 ha besides increasing 1 m for high Sea level rise scenarios respectively.

Table 18. The inundation of different SLR scenarios vulnerable to mangrove forests areas

Mangrove forest areas	Sea Level Rise Scenarios		
	40 cm	60 cm	1m
Vulnerable area (hectare)	40.44	40.44	53.14

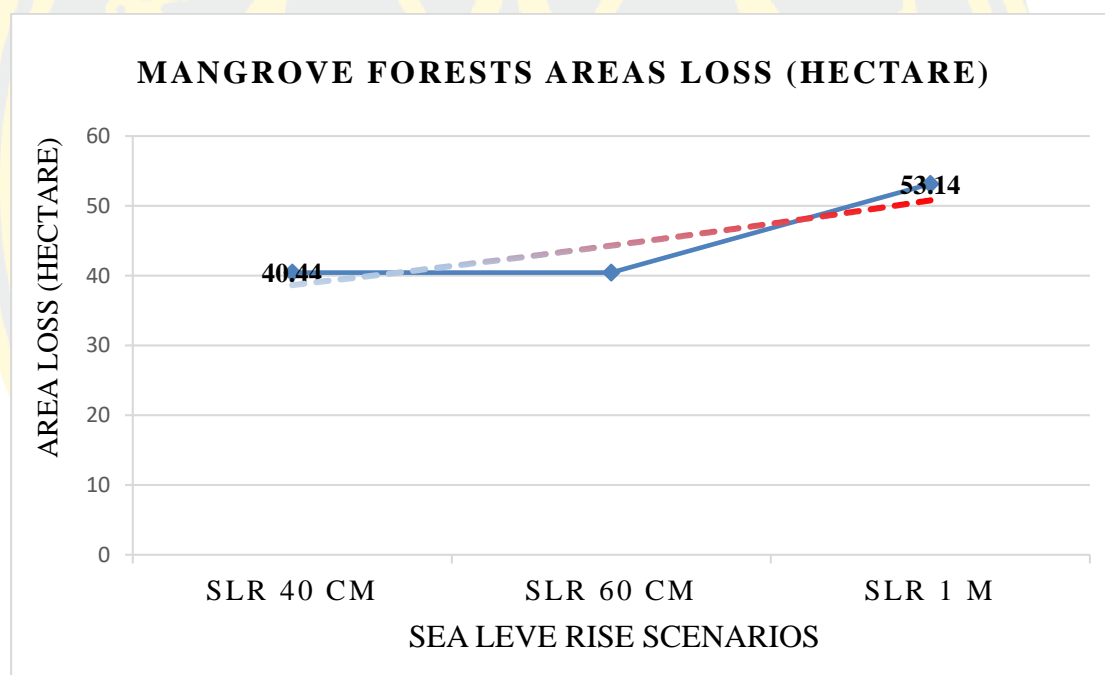


Figure 18. Total mangrove forests area loss under three different SLR scenarios in Peam Krasop Wildlife Sanctuary by the end of the twenty-first century.

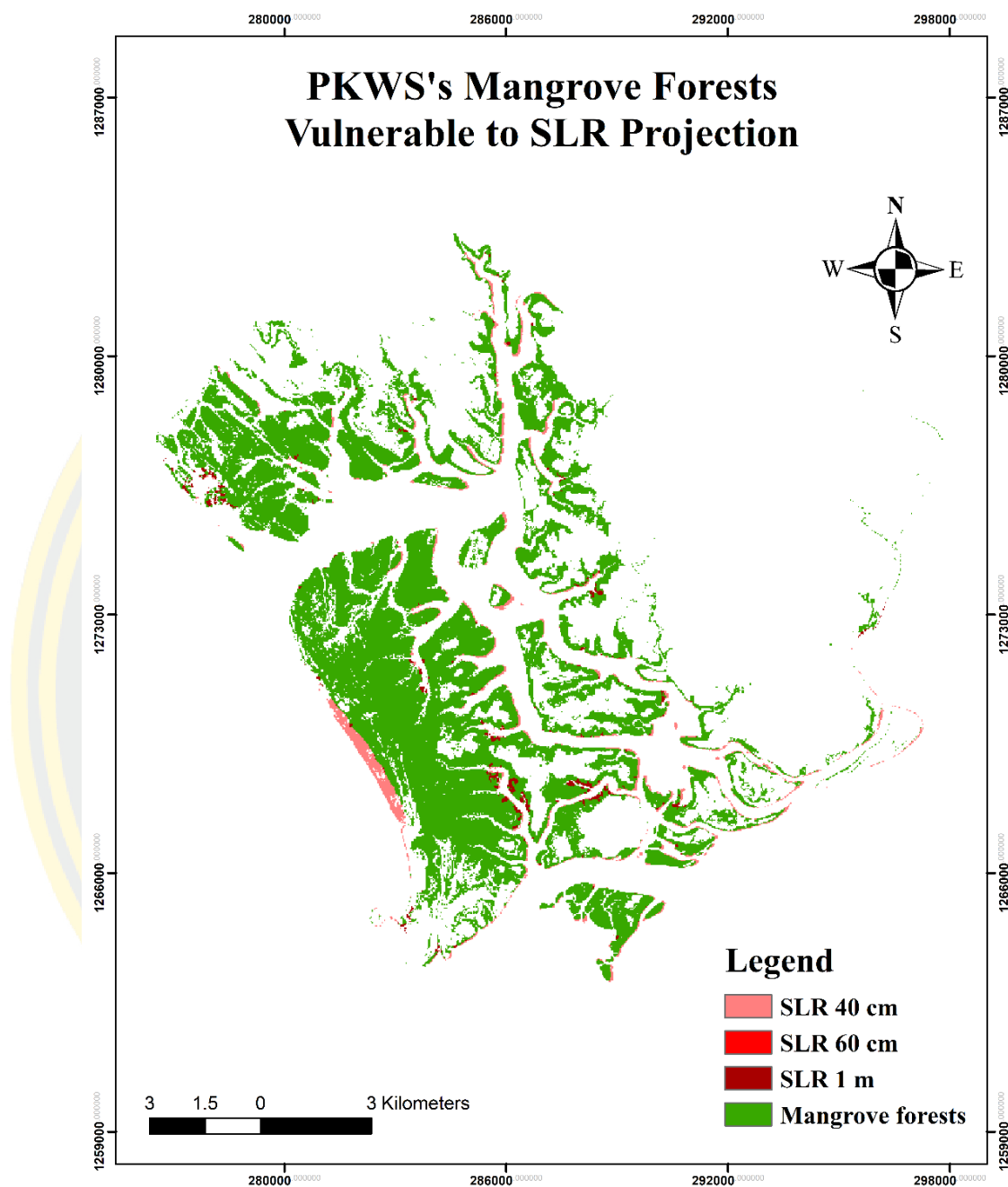


Figure 19. Analysis of the inundation of mangrove areas in Peam Krasop Wildlife Sanctuary due to three different SLR scenarios

CHAPTER 5 DISCUSSION, FUTURE WORK, AND CONCLUSION

5.1 Discussion

In this study, the numerous mangrove forests maps of Peam Krasop Wildlife Sanctuary in Cambodia from 2015 to 2020 were produced. To the best of our knowledge, this is the first interesting topic conducted in Cambodia about vulnerable mangrove forests area due to the potential impact of Sea level rise in Cambodia based on Remote Sensing (RS) and GIS techniques. For conducted these mangroves maps from 2015 to 2020 defined from classification employed time-series data of multi-temporal Sentinel-2 L1C optical imageries with easy machine learning Random Forest based on Sci-kit learn python library that can be achieved an overall accuracy reach to 99.97% for 2015, 99.97 for 2016, 99.98 for 2017, 99.96 for 2018, 99.754 for 2019, 99.96 for 2020. The accuracy checking was based on the Random Forest algorithm training with 240 samples per satellite imageries. For land cover changes were used MOLUSCE in SCP plugin in QGIS.

According to (Potic & Potic, 2017) the result of accuracy assessment results demonstrate how Machine Learning algorithms execute the classification in Dzetsaka including Gaussian Mixture Model (GMM), K-Neighbors Classifier, and Random Forest. The best result is given by the Random Forest algorithm with perfect accuracy of 100% for 2016 and 96.35% for 2017 that the creation of land cover map from BOA processed of Sentinel 2 data required a ground training samples. To obtain such areas and create necessary vector file as training material, historical google maps were employed using different sources and the accuracy assessment was performed using training sample polygons in Dzetsaka machine learning plugin and the land cover change was performed using SCP plugin in QGIS. Seven different classes recognized for both 2016 and 2017 and consist of 175 and 164 polygons respectively. The Confusion matrix was created and presents overall accuracy and kappa hat.

In this research developed Geospatial model base on Digital elevation model and Sea Level Rise scenarios 40-60 cm in Koh Kong province and will add one more Sea Level Rise scenarios 1 m to visualize the potential inundation of Sea level rise on

mangrove forests in Peam Krasop Wildlife Sanctuary in Cambodia. For creating this Geospatial model used the available Digital Elevation Model that derived from USGS. This elevation was SRTM DEM with spatial resolution 30 meters (1 Arc-Second Global) covering most of the world with absolute vertical accuracy of less than 16m (RMSE of 9.73m).

Based on a research (Pramanik, 2016), assess the impacts of Sea Level Rise on mangrove dynamics in the Indian part of Sundarbans based on Geospatial techniques using ASTER DEM data (2014) that collected from the USGS website. For collecting data about sea level of nearest tidal gauge station Haldia (2.59 ± 1.0 mm/year) and Diamond Harbor (4.67 ± 0.68 mm/year). Moreover, the study indicates that the low-level mangrove islands would threaten with the rates of increasing sea level under present climate change. However, the amount of net loss is about 10009 ha at the rate of 164.08 ha per year of the four more vulnerable islands. According to another research, to assess the potential impacts of sea level rise (SLR) on the spatial distribution of mangrove species and estimate the potential inundation and subsequent mangrove area loss, a Geospatial model of potentially inundated areas was developed using the high resolution (<1 m vertical error) DEM data was obtained from Water Resources Planning Organization (WRPO), Bangladesh. The Landsat Operational Land Imager (OLI) data, obtained from the Center for Earth Resources Observation and Science (EROS) website (www.glovis.usgs.gov), was also used to map the mangrove species composition of the Bangladesh Sundarbans to overlay with the DEM data to see how mangrove species face to three different SLR scenarios of 0.46 m (low), 0.75 m (medium) and 1.48 m based on the mean and peak projections under the RCP 4.5 scenario for West Bengal, India (Payo et al., 2016), and the extreme case scenario resembles the H_{pp} scenario range which considers the 95% value for RCP 8.5 (0.98 m) plus 0.5 m associated with Ice Sheet melting (Levermann et al., 2014). The extreme case scenario is considered plausible but unlikely (Allen et al., 2014). The mangrove areas of 2646 ha, 9599 ha and 74,720 ha are projected to be inundated and subsequently lost by the end of the twenty first century for the low, medium and high SLR scenarios respectively under the net subsidence rate ± 2.4 mm/ year relative to the baseline year 2000.

5.2 Future Work

For future work suggest to focus on developing a geospatial model of a combination DEM with high spatial resolution and Sea level rise data observing by tide gauge or altimeter satellite. This could be assessing the accuracy of this model in the future. This future work should be considering and research in more detail in Cambodia, while our research was the first knowledge about the vulnerable area of mangrove forests that affected by future Sea level rise using advanced technology of Remote Sensing (RS) and GIS model. Our research result might be accurate or not accurate depended on developing a geospatial model using the medium spatial resolution of DEM overlap with land cover's mangrove forests. The main reason to research as a study about the potential impacts of Sea level rise to mangrove forests. In the previous research studies, mostly used the lower accuracy DEM to create a Geospatial model to measure the effect of Sea level rise on land cover and mangrove forests. Although this study is really important to enhance the mangrove forests changes and show resilience to future Sea level rise.

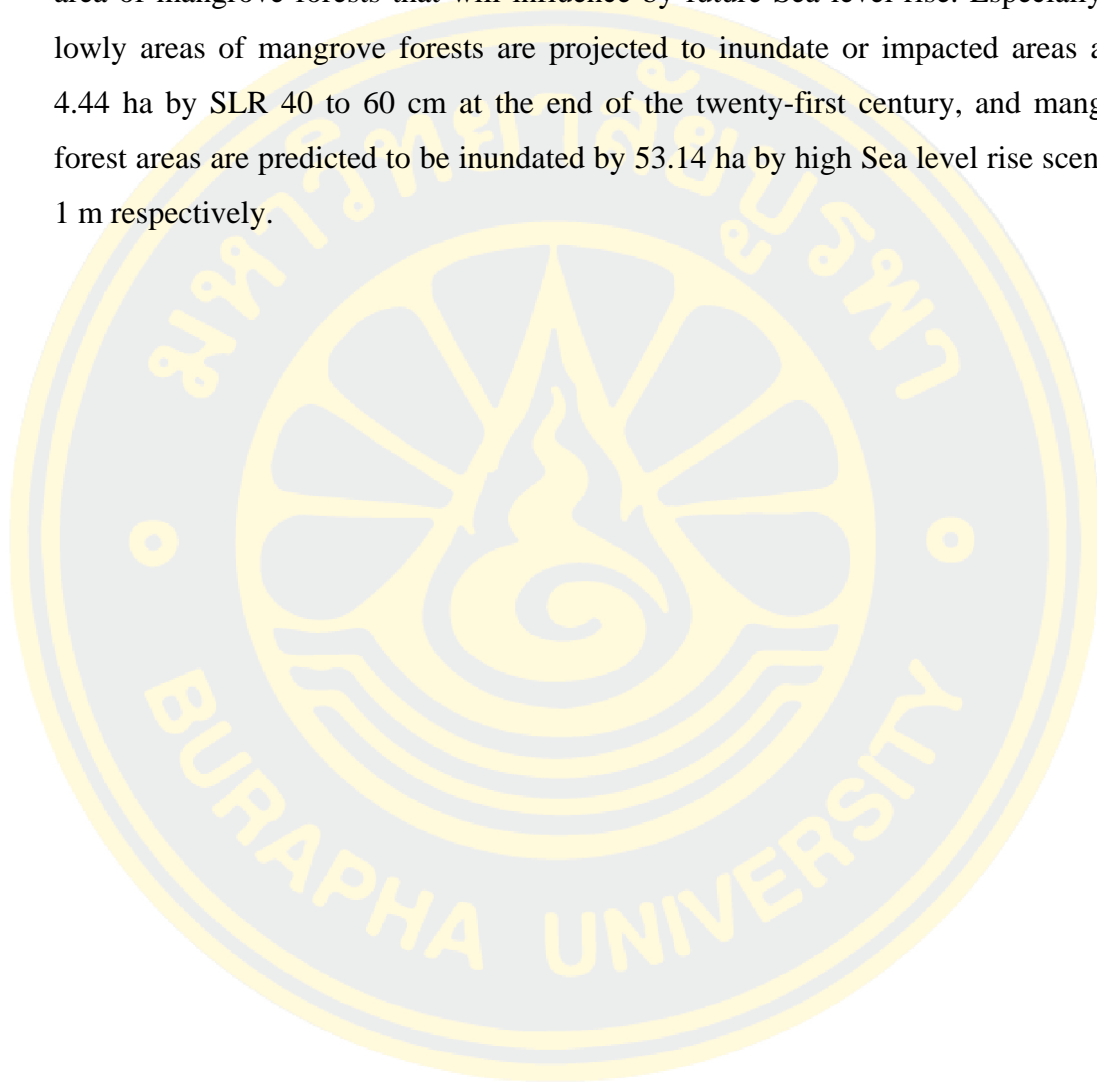
5.3 Conclusion

A quantitative of mangrove forests maps in Peam Krasop Wildlife Sanctuary between 2015 and 2020, the results show that mangrove forests areas in 2015, 2016, 2017, 2018, 2019, and 2020, were estimated at 7157.90 ha, 7495.21 ha, 7337.47 ha, 6436.26 ha, 6761.66 ha, and 7045.64 ha.

Either, mangrove forest areas in PKWS in this study were analyzed changed from 2015 until 2020 based on MOLUSCE. Our contribution to mangrove forest areas changes in this period time. Mangrove forests were significantly increased by about 337.31 ha between 2015 and 2016. In contrast, mangrove forests in PKWS were decreased 157.74 ha in 2017. Similarly, mangrove forests have continued to lose 901.21 ha from 7337.47 ha to 6436.26 ha in 2018. However, mangrove forests have started to increase 325.40 ha in PKWS in 2019, were increased from 6436.26 ha to 6761.66 ha. Mangrove forests have continued to increase by approximately 283.98 ha in 2020 as well. The total long-term changes of mangrove forests in Peam Krasop

Wildlife Sanctuary from 2015 to 2020, mangrove forests were lost about 112.26 ha from 7157.90 ha to 7045.64 ha.

Therefore, based on the results provide a new knowledge about the vulnerable area of mangrove forests that will influence by future Sea level rise. Especially, the lowly areas of mangrove forests are projected to inundate or impacted areas about 4.44 ha by SLR 40 to 60 cm at the end of the twenty-first century, and mangrove forest areas are predicted to be inundated by 53.14 ha by high Sea level rise scenarios 1 m respectively.



REFERENCES

- Aggarwal, N., Srivastava, M., & Dutta, M. (2016). Comparative Analysis of Pixel-Based and Object-Based Classification of High Resolution Remote Sensing Images – A Review. *International Journal of Engineering Trends and Technology*, 38, 5-11. doi:10.14445/22315381/IJETT-V38P202
- Al-Jeneid S, B. M., Nasr S, Raey M (2008). Vulnerability assessment and adaptation to the impacts of sea level rise on the Kingdom of Bahrain. *Mitig Adapt Strat Glob Change*, 13, 87–104.
- Allen, Barros, V., Broome, J., Cramer, W., Christ, R., Church, J., . . . Urge-Vorsatz, D. (2014). *Climate Change 2014: Synthesis Report*.
- Bann, C. (1997). Alternative mangrove management strategies in Cambodia.
- BCC-PPCR, M. C. G. (2014). Climate Change Impact Modeling and Vulnerability Assessments for Koh Kong and Mondulakiri Provinces in Cambodia.
- Bk, V., & Quang, N. (2019). Mangrove forests of Cambodia: Recent changes and future threats. *Ocean & Coastal Management*, 181. doi:10.1016/j.ocecoaman.2019.104895
- Blaschke, T. (2010). Object based image analysis for remote sensing. *ISPRS Journal of Photogrammetry and Remote Sensing*, 65(1), 2-16. doi:<https://doi.org/10.1016/j.isprsjprs.2009.06.004>
- Blasco, F., Aizpuru, M., & Gers, C. (2001). Depletion of the mangroves of Continental Asia. *Wetlands Ecology and Management*, 9(3), 255-266. doi:10.1023/A:1011169025815
- Bosire, J. O., Dahdouh-Guebas, F., Walton, M., Crona, B. I., Lewis, R. R., Field, C., . . . Koedam, N. (2008). Functionality of restored mangroves: A review. *Aquatic Botany*, 89(2), 251-259. doi:<https://doi.org/10.1016/j.aquabot.2008.03.010>
- Brinkman RM, M. S., Ridd PV, Furukawa K (1997). Surface wave attenuation in mangrove forests.
- Church, J. A., & White, N. J. (2011). Sea-Level Rise from the Late 19th to the Early 21st Century. *Surveys in Geophysics*, 32(4-5), 585-602. doi:10.1007/s10712-011-9119-1

- Dahdouh-Guebas, F., Jayatissa, L. P., Di Nitto, D., Bosire, J. O., Lo Seen, D., & Koedam, N. (2005). How effective were mangroves as a defence against the recent tsunami? *Current Biology*, 15(12), R443-R447. doi:10.1016/j.cub.2005.06.008
- Dara, A., Piseth, H., Mather, R., & Kim Sreng, K. . (2009). Integrated assessment for identification of a preliminary zoning scheme for Peam Krasob Wildlife Sanctuary in southwest Cambodia.
- FAO. (2010). *Global forest resources assessment, 2010 :main report* (Vol. no. 163). Rome :: Food and Agriculture Organization of the United Nations.
- Ghosh, M. K., Kumar, L., & Kibet Langat, P. (2019). Geospatial modelling of the inundation levels in the Sundarbans mangrove forests due to the impact of sea level rise and identification of affected species and regions. *Geomatics, Natural Hazards and Risk*, 10(1), 1028-1046. doi:10.1080/19475705.2018.1564373
- Gilman, E., Ellison, J., & Coleman, R. (2007). Assessment of mangrove response to projected relative sea-level rise and recent historical reconstruction of shoreline position. *Environ Monit Assess*, 124(1-3), 105-130. doi:10.1007/s10661-006-9212-y
- Giri, C., Long, J., Abbas, S., Murali, R. M., Qamer, F. M., Pengra, B., & Thau, D. (2015). Distribution and dynamics of mangrove forests of South Asia. *Journal of Environmental Management*, 148, 101-111. doi:https://doi.org/10.1016/j.jenvman.2014.01.020
- Giri, C., Ochieng, E., Tieszen, L. L., Zhu, Z., Singh, A., Loveland, T., . . . Duke, N. (2011). Status and distribution of mangrove forests of the world using earth observation satellite data. *Global Ecology and Biogeography*, 20(1), 154-159. doi:10.1111/j.1466-8238.2010.00584.x
- Gravelle G, Mimura N (2008) Vulnerability assessment of sea-level rise in Viti Levu, Fiji Islands. *Sustain Sci* 3:171–180.
- Green, E. P., Clark, C. D., Mumby, P. J., Edwards, A. J., & Ellis, A. C. (1998). Remote sensing techniques for mangrove mapping. *International Journal of Remote Sensing*, 19(5), 935-956. doi:10.1080/014311698215801
- Hamilton, L. S., & Snedaker, S. C. (1984). Handbook for mangrove area management.

123.

- Hawryło, P., & Wezyk, P. (2018). Predicting Growing Stock Volume of Scots Pine Stands Using Sentinel-2 Satellite Imagery and Airborne Image-Derived Point Clouds. *Forests*, 9, 274. doi:10.3390/f9050274
- Hunter, J. (2011). A simple technique for estimating an allowance for uncertain sea-level rise. *Climatic Change*, 113(2), 239-252. doi:10.1007/s10584-011-0332-1
- IPCC. (2013). Summary for Policymakers. In: Climate Change 2013: The Physical Science Basis.
- Kuleli, T. (2010). City-Based Risk Assessment of Sea Level Rise Using Topographic and Census Data for the Turkish Coastal Zone. *Estuaries and Coasts*, 33(3), 640-651. doi:10.1007/s12237-009-9248-7
- Kumar, M. (2015). Remote sensing and GIS based sea level rise inundation assessment of Bhitarkanika forest and adjacent eco-fragile area, Odisha. *International Journal of Geomatics and geosciences*, 5, 684-696.
- Kumar, T., Panigrahy, S., Kumar, P., & Parihar, J. S. (2012). Classification of floristic composition of mangrove forests using hyperspectral data: case study of Bhitarkanika National Park, India. *Journal of Coastal Conservation*, 17(1), 121-132. doi:10.1007/s11852-012-0223-2
- Landis, J. R., & Koch, G. G. (1977). The Measurement of Observer Agreement for Categorical Data. *Biometrics*, 33(1), 159-174. doi:10.2307/2529310
- Levermann, A., Winkelmann, R., Nowicki, S., Fastook, J., Frieler, K., Greve, R., . . . Bindschadler, R. (2014). Projecting antarctic ice discharge using response functions from SeaRISE ice-sheet models.
- Li, S., Meng, X., Ge, Z., & Zhang, L. (2014). Vulnerability assessment of the coastal mangrove ecosystems in Guangxi, China, to sea-level rise. *Regional Environmental Change*, 15(2), 265-275. doi:10.1007/s10113-014-0639-3
- Li, X., Rowley, R., Kostelnick, J., Braaten, D., Meisel, J., & Hulbutta, K. (2009). GIS Analysis of Global Impacts from Sea Level Rise. *Photogrammetric Engineering & Remote Sensing*, 75, 807-818. doi:10.14358/PERS.75.7.807
- Lu, J., Chen, X., Tian, L., & Zhang, W. (2014). Numerical simulation-aided MODIS capture of sediment transport for the Bohai Sea in China. *International Journal of*

- Remote Sensing, 35(11-12), 4225-4238. doi:10.1080/01431161.2014.916045
- Lu, J., Chen, X., Zhang, P., & Huang, J. (2017). Evaluation of spatiotemporal differences in suspended sediment concentration derived from remote sensing and numerical simulation for coastal waters. *Journal of Coastal Conservation*, 21(1), 197-207. doi:10.1007/s11852-016-0491-3
- Lu, J., Li, H., Chen, X., & Liang, D. (2019). Numerical Study of Remote Sensed Dredging Impacts on the Suspended Sediment Transport in China's Largest Freshwater Lake. *Water*, 11(12). doi:10.3390/w11122449
- Lu, J., Wai, O. W. H., Chen, X., & Zhang, P. (2014). Flow prediction using ENVISAT RA-2 sea surface height validated model: A case study for the effect of Hong Kong-Zhuhai-Macau Bridge in the Pearl River Estuary, China. *Aquatic Ecosystem Health & Management*, 17(3), 305-315. doi:10.1080/14634988.2014.944478
- Malik, A., & Abdalla, R. (2016). Geospatial modeling of the impact of sea level rise on coastal communities: application of Richmond, British Columbia, Canada. *Modeling Earth Systems and Environment*, 2, 146. doi:10.1007/s40808-016-0199-2
- Marfai, M. A., & King, L. (2007). Potential vulnerability implications of coastal inundation due to sea level rise for the coastal zone of Semarang city, Indonesia. *Environmental Geology*, 54(6), 1235-1245. doi:10.1007/s00254-007-0906-4
- McIvor, A. L., Möller, I., Spencer, T., & Spalding, M. (2012). Reduction of wind and swell waves by mangroves. Natural Coastal Protection Series: Report 1. Cambridge Coastal Research Unit Working. *Nature Conservancy and Wetlands International, Cambridge.*, 40.
- MoE. (2009). Cambodia Environment Outlook. Ministry of Environment, Phnom Penh, Cambodia.
- Natesan, U., & Parthasarathy, A. (2010). The potential impacts of sea level rise along the coastal zone of Kanyakumari District in Tamilnadu, India. *Journal of Coastal Conservation*, 14(3), 207-214. doi:10.1007/s11852-010-0103-6
- Nop, S., DasGupta, R., Shaw, R. (2017). *Opportunities and challenges for participatory management of mangroves resource (PMMR) in Cambodia. In: DasGupta, R.,*

Shaw, R. (Eds.), *Participatory Mangrove Management in a Changing Climate, Disaster and Risk Reduction*.

- Octariady, J., Hikmat, A., Widyaningrum, E., Mayasari, R., & Fajari, M. (2017). *VERTICAL ACCURACY COMPARISON OF DIGITAL ELEVATION MODEL FROM LIDAR AND MULTITEMPORAL SATELLITE IMAGERY* (Vol. XLII-1/W1).
- Payo, A., Mukhopadhyay, A., Hazra, S., Ghosh, T., Ghosh, S., Brown, S., . . . Haque, A. (2016). Projected changes in area of the Sundarban mangrove forest in Bangladesh due to SLR by 2100. *Climatic Change*, 139. doi:10.1007/s10584-016-1769-z
- Potic, I., & Potic, M. (2017). Remote sensing machine learning algorithms in environmental stress detection: Case study of Pan-European south section of Corridor 10 in Serbia. *The University Thought - Publication in Natural Sciences*, 7(2), 41-46. doi:10.5937/univtho7-14957
- Pramanik, M. K. (2014). Assessment the Impact of Sea Level Rise on Mangrove Dynamics of Ganges Delta in India using Remote Sensing and GIS. *Journal of Environment and Earth Science*.
- Pramanik, M. K. (2016). Assessment of the Impacts of Sea Level Rise on Mangrove Dynamics in the Indian Part of Sundarbans Using Geospatial Techniques. *Journal of Biodiversity, Bioprospecting and Development*, 03(01). doi:10.4172/2376-0214.1000155
- Quartel, S., Kroon, A., Augustinus, P. G. E. F., Van Santen, P., & Tri, N. H. (2007). Wave attenuation in coastal mangroves in the Red River Delta, Vietnam. *Journal of Asian Earth Sciences*, 29(4), 576-584. doi:<https://doi.org/10.1016/j.jseaes.2006.05.008>
- Radić, V., & Hock, R. (2011). Radic V, Hock R. Regionally differentiated contribution of mountain glaciers and ice caps to future sea-level rise. *Nature Geoscience* 4:–. <<http://dx.doi.org/10.1038/ngeo1052>. *Nature Geoscience - NAT GEOSCI*, 4. doi:10.1038/ngeo1052
- Rizvi, A. R., Singer, U., . (2011). Cambodia Coastal Situation Analysis. International Union for Conservation of Nature and Natural Resources (IUCN), Gland. 58.

- Sibaruddin, H. I., Shafri, H. Z. M., Pradhan, B., & Haron, N. A. (2018). Comparison of pixel-based and object-based image classification techniques in extracting information from UAV imagery data. *IOP Conference Series: Earth and Environmental Science*, 169, 012098. doi:10.1088/1755-1315/169/1/012098
- Slangen, A. B. A., Katsman, C. A., van de Wal, R. S. W., Vermeersen, L. L. A., & Riva, R. E. M. (2011). Towards regional projections of twenty-first century sea-level change based on IPCC SRES scenarios. *Climate Dynamics*, 38(5-6), 1191-1209. doi:10.1007/s00382-011-1057-6
- Vaiphasa, C. (2006). Consideration of smoothing techniques for hyperspectral remote sensing. *ISPRS Journal of Photogrammetry and Remote Sensing*, 60, 91-99. doi:10.1016/j.isprsjprs.2005.11.002
- Valiela, I., Bowen, J. L., & York, J. K. (2001). Mangrove Forests: One of the World's Threatened Major Tropical Environments. *Bioscience*, 51(10). doi:10.1641/0006-3568(2001)051[0807:Mfootw]2.0.Co;2
- Veettil, B. K., Ward, R.D., Quang, N.X., Trang, N.T.T., Giang, T.H. (2019). Mangroves of Vietnam: historical development, current state of research and future threats.
- Wang, L., Jia, M., Yin, D., & Tian, J. (2019). A review of remote sensing for mangrove forests: 1956–2018. *Remote Sensing of Environment*, 231, 111223. doi:<https://doi.org/10.1016/j.rse.2019.111223>
- Ward, R. D., Friess, D. A., Day, R. H., & Mackenzie, R. A. (2017). Impacts of climate change on mangrove ecosystems: a region by region overview. *Ecosystem Health and Sustainability*, 2(4). doi:10.1002/ehs2.1211
- Wulder, M.A.; White, J.C.; Hay, G.J.; Castilla, G. Towards automated segmentation of forest inventory polygons on high spatial resolution satellite imagery. *Forest. Chron.* 2008, 84, 221-230.
- Xu, Y., Feng, L., Zhao, D., & Lu, J. (2020). Assessment of Landsat atmospheric correction methods for water color applications using global AERONET-OC data. *International Journal of Applied Earth Observation and Geoinformation*, 93. doi:10.1016/j.jag.2020.102192
- Yang, S., Chen, X., Lu, J., Hou, X., Li, W., & Xu, Q. (2021). Impacts of agricultural topdressing practices on cyanobacterial bloom phenology in an early eutrophic

plateau Lake, China. Journal of Hydrology, 594.
doi:10.1016/j.jhydrol.2020.125952



BIOGRAPHY

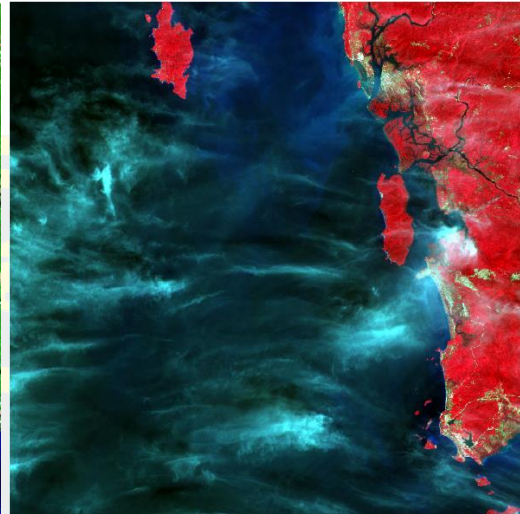
NAME	PHORN NAYELIN
DATE OF BIRTH	27 April 1997
PLACE OF BIRTH	Kiri Sakor district, Koh Kong province, Cambodia
PRESENT ADDRESS	Sangkat Tek Thla, Khan Sensok, Phnom Penh, Cambodia
POSITION HELD	Officer in National Committee for Disaster Management
EDUCATION	2015-2019 Bachelor Degree on Geography and Land management 2019-Now Master Program in Geoinformatics
AWARDS OR GRANTS	Awarded a scholarship to Master of Science in Geoinformatics at Burapha University (Thailand) and Wuhan University (China) from Geo-Informatics and Space Technology Development Agency (Public Organization): GISTDA



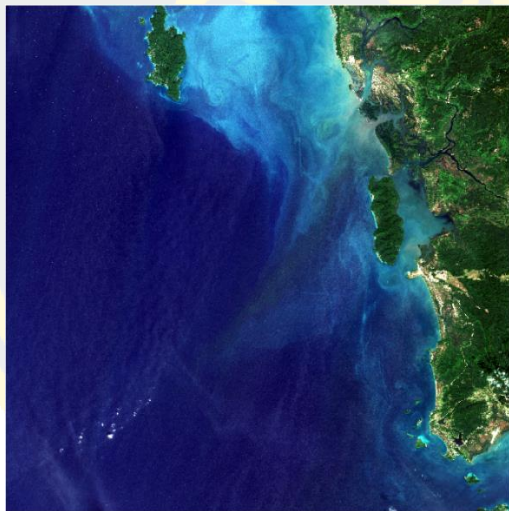
Appendix 1: Remote sensing data (Sentinel-2 imageries with Band composite from 2015 to 2020)



Date: 31 12 2015



Date: 09 02 2016



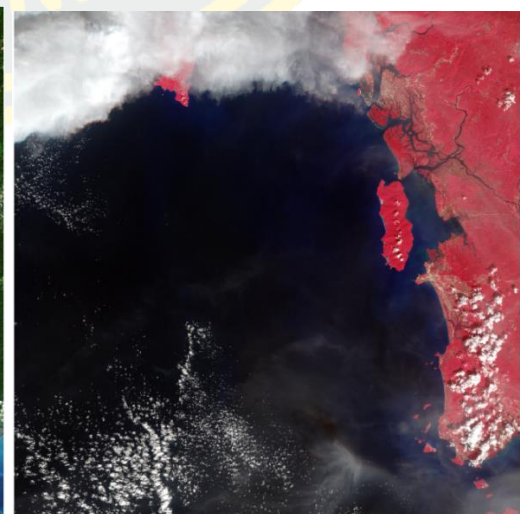
Date: 20 12 2017



Date: 25 12 2018

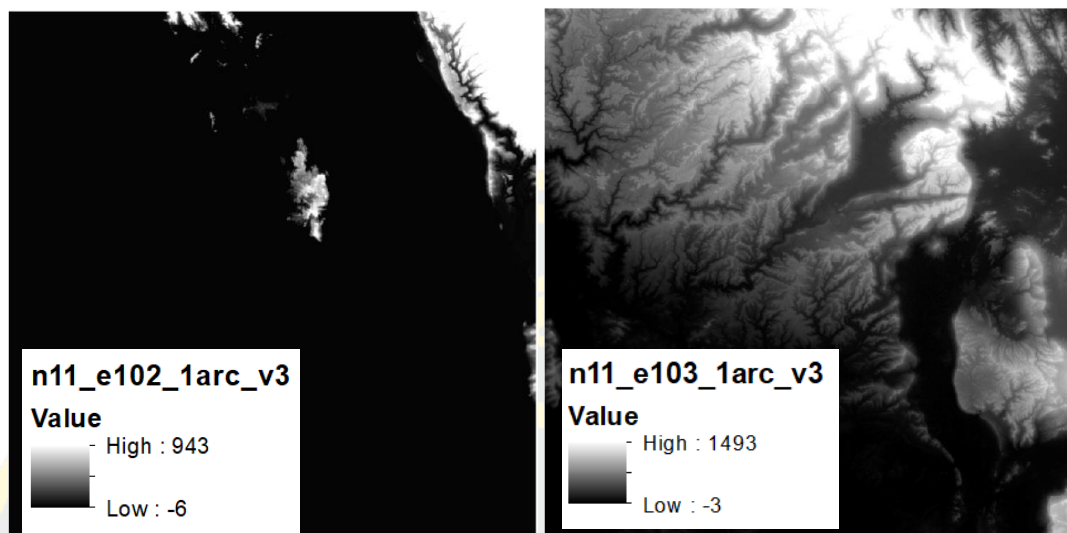


Date: 10 12 2019

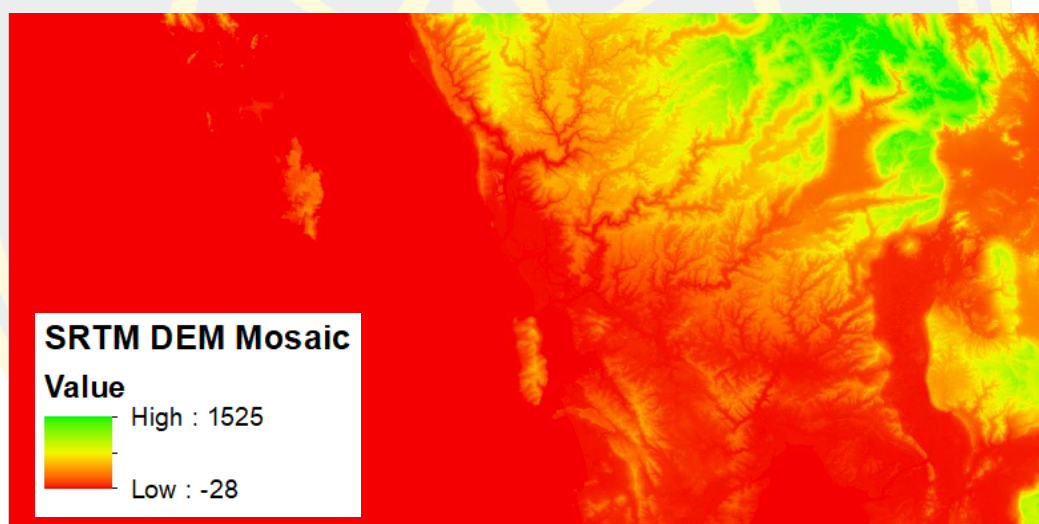


Date: 29 12 2020

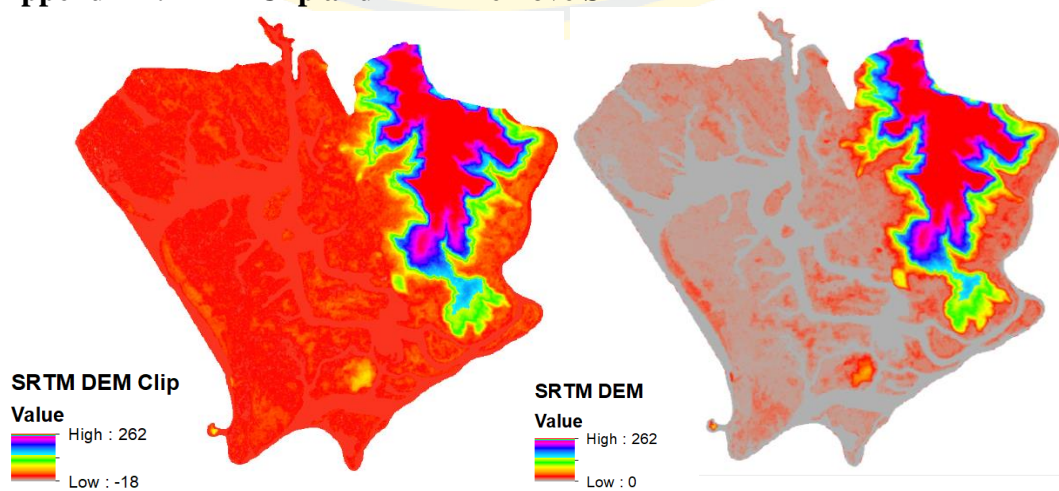
Appendix 2: Remote sensing data (SRTM DEM, 2014)



Appendix 3: DEM Mosaic



Appendix 4: DEM Clip and DEM Remove Sink



Appendix 5: Images subset



Date: 31 12 2015



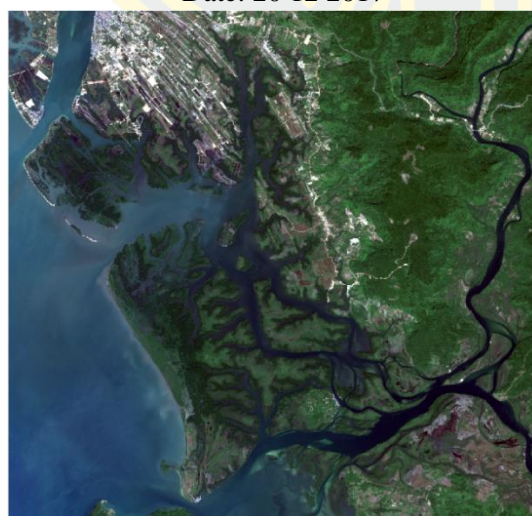
Date: 09 02 2016



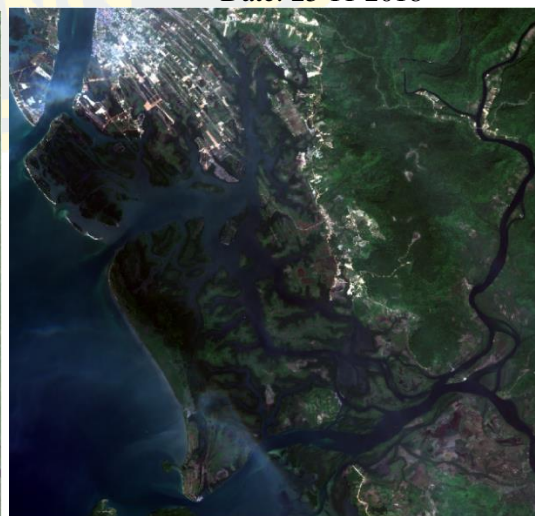
Date: 20 12 2017



Date: 25 11 2018



Date: 10 12 2019

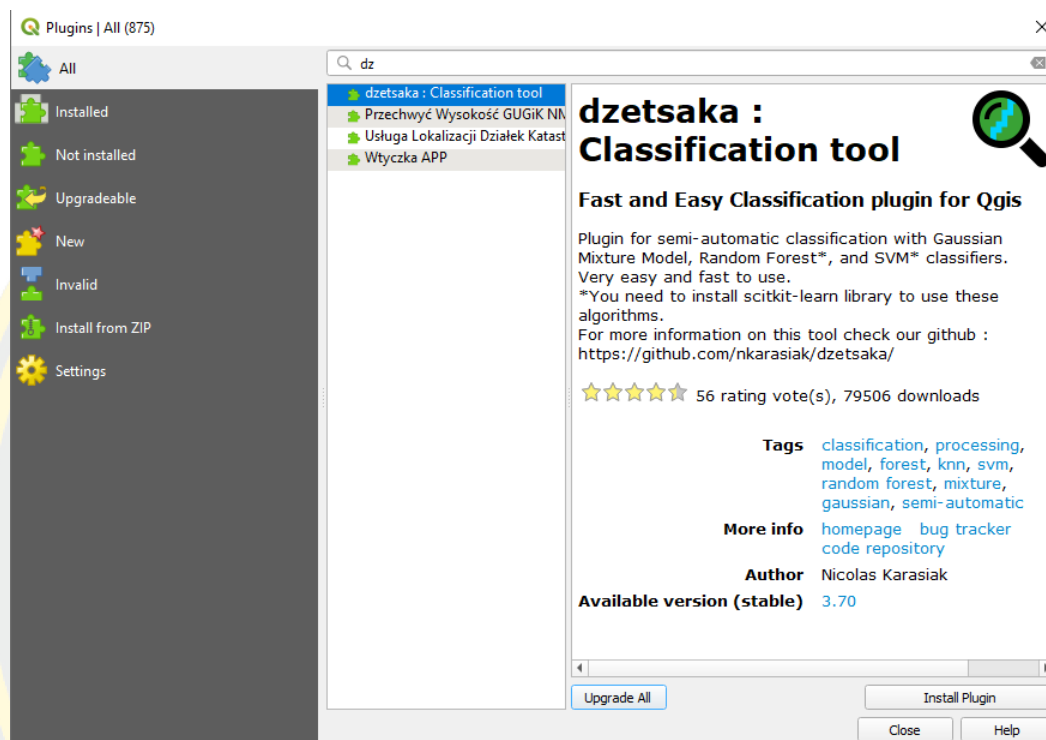


Date: 29 12 2020

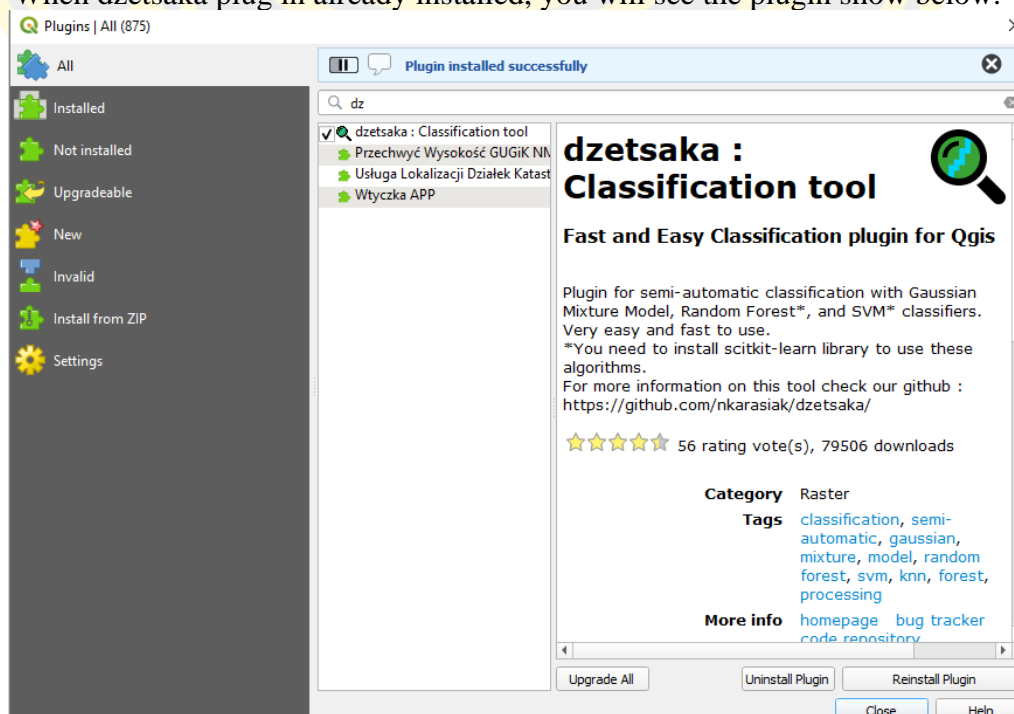
Appendix 6: dzetsaka plug in

Step 1: Dzetsaka install

1. First, need to install the dzetsaka plugin in QGIS software by go to Plugins > Manage and Install Plugins. Then search the dzetsaka plugin in the search box.

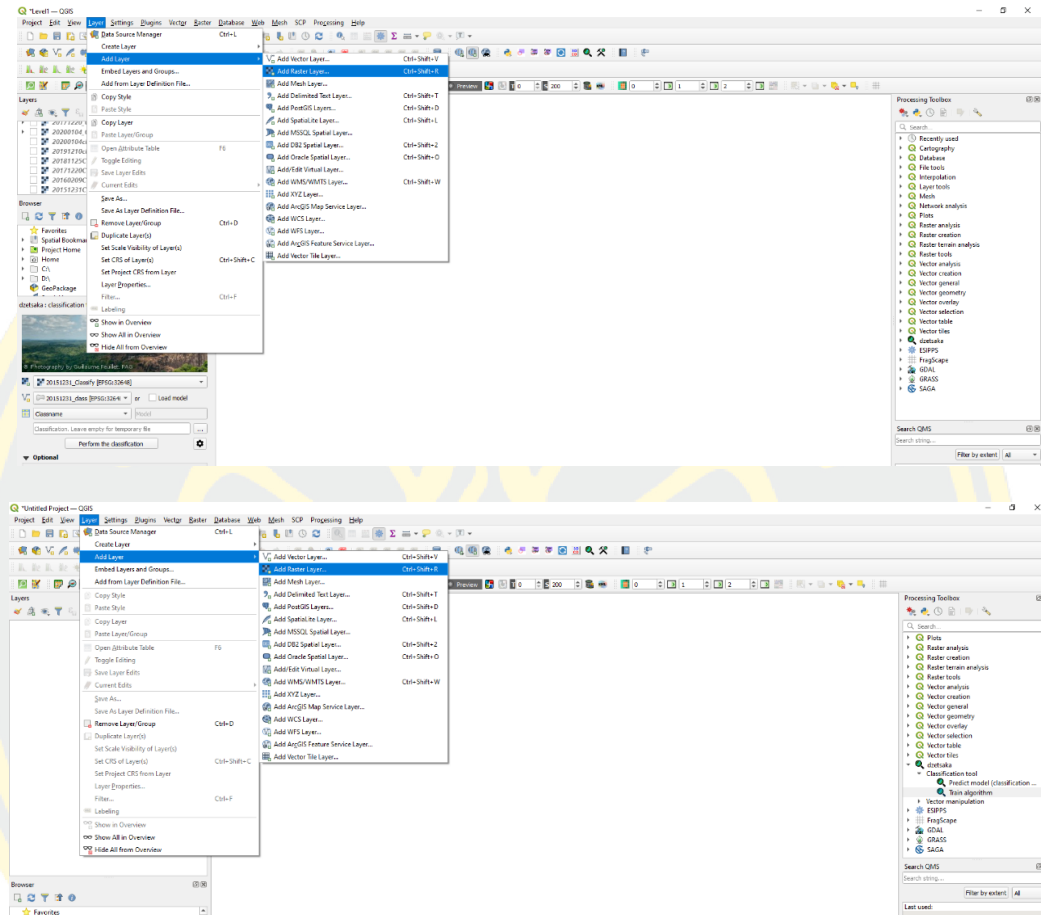


2. When dzetsaka plug in already installed, you will see the plugin show below.

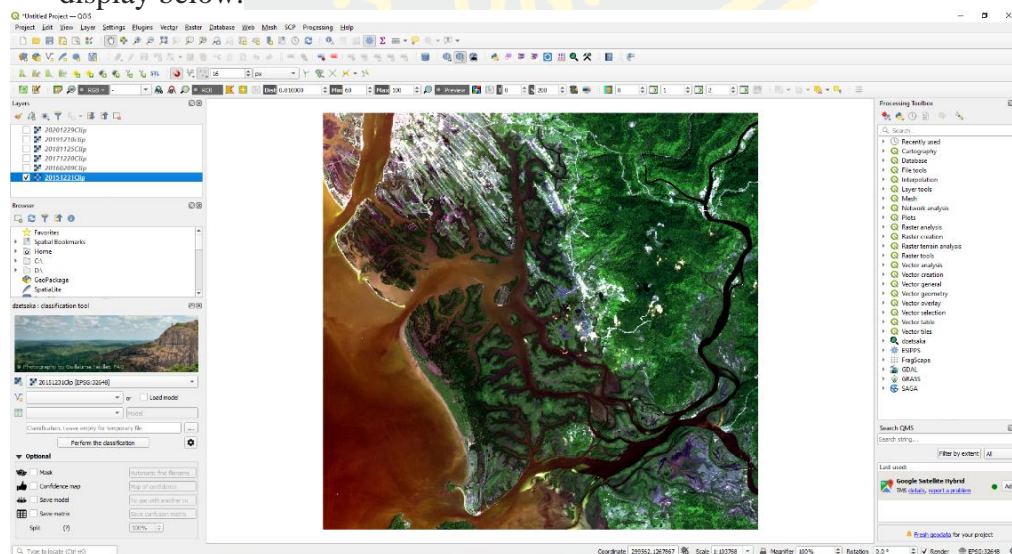


Step 2: Import raster data into QGIS

1. Import raster data (the specify the file path of the satellite image from 2015 to 2020) into QGIS by go to Layer > Add Layer > Add Raster Layer.



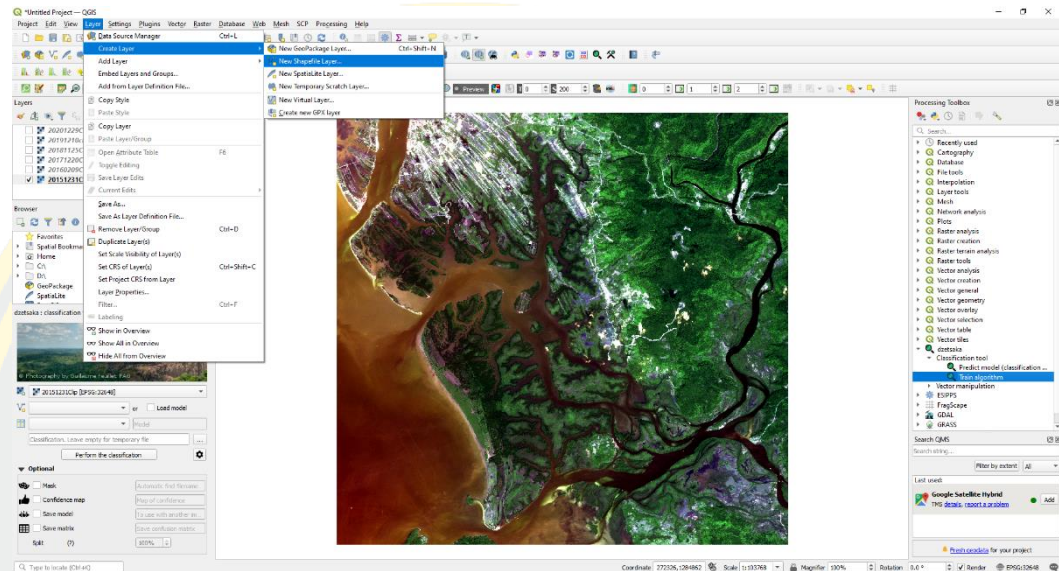
2. After add raster data of the satellite image from 2015 to 2020, the screen will display below.



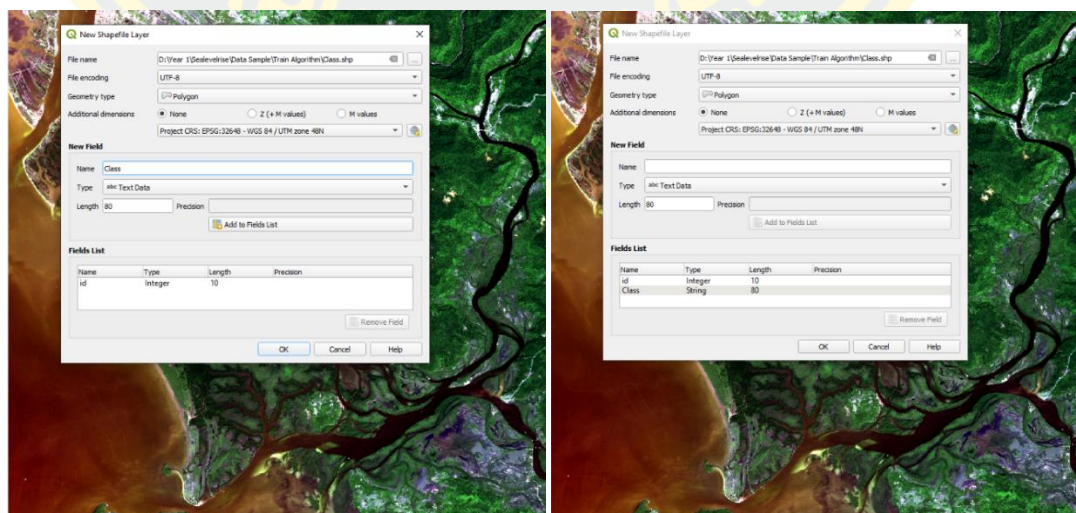
Step 3: Create training data

When the raster data were added, we need to create the training data.

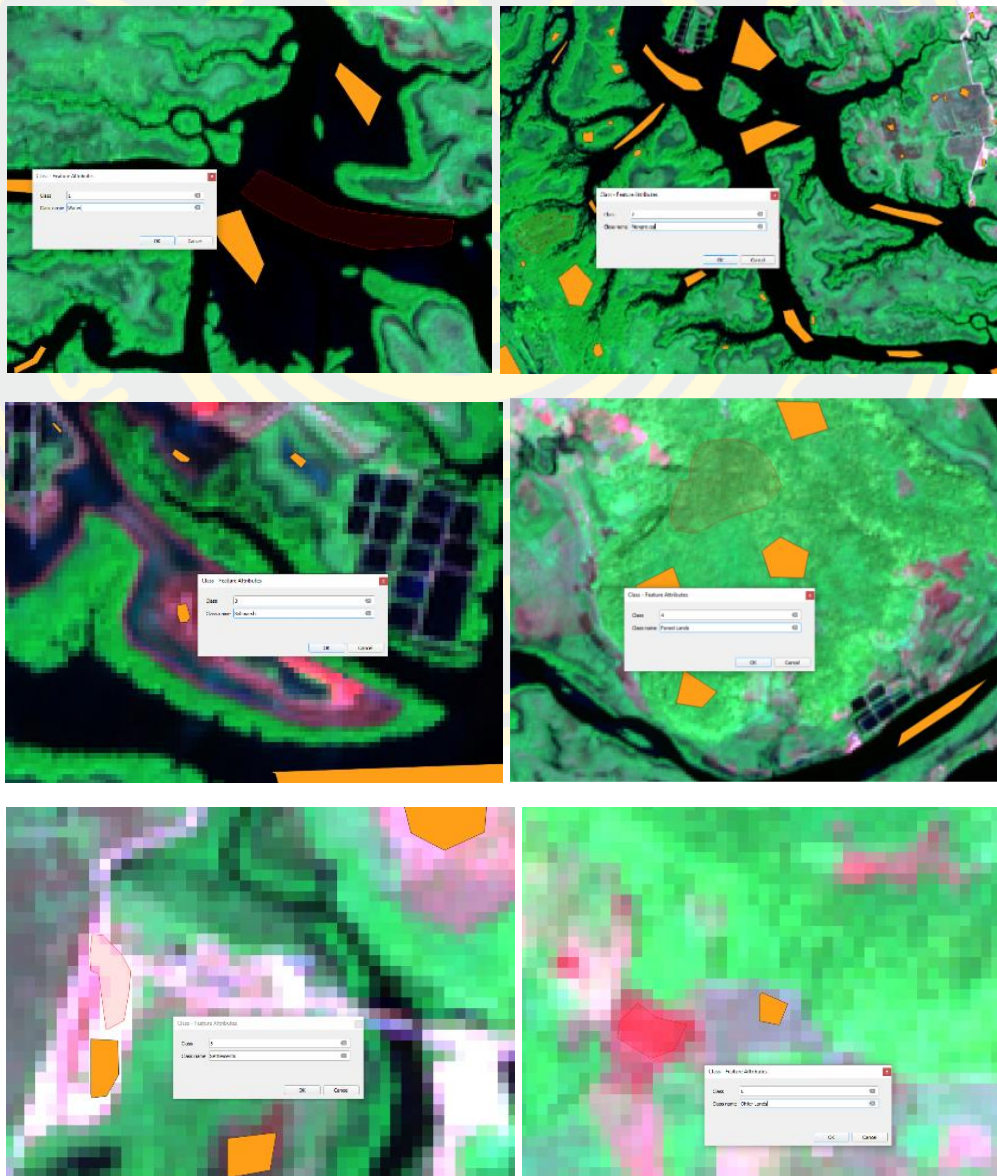
1. We go to Layer > Create Layer > New Shapefile layer. After that we will fill the detail of creating training data.



2. There are four steps of creating training data: (1) specify the name output of shapefile, (2) select the geometry type as Polygon, (3) select the coordinate system as (Project CRS: EPSG:32648-WGS/UTM zone 48N), (4) create a new field for specifying class of the area as TextData type and click Add to Fields List, and there are two fields show on the field list. Then, click OK to start.



3. When the New shapefile were created, it was the time to draw the 240 samples data of 6 classes include Water (id 1), Mangroves (id 2), Saltmarsh (id 3), Forest Lands (id 4), Settlements (id 5), and Other Lands (id 6). For drawing these kinds of classes, we need to go to digitize toolbar, and then click on toggle editing (yellow pencil) to the active tool. Then click on the add polygon tool (green icon), and started to draw the shapes on the area of satellite images. When you draw finished of a class, just right-click and specify the id and class name. Afterward, just click save on the digitizing tool.



After saving the creating training samples data, we can check the training data in attribute data of shapefile shown as below.

The figure consists of three screenshots of the QGIS attribute table window, each showing a different class of training data. Each window has a title bar indicating 'Class -- Features Total: 298, Filtered: 240, Selected: 0'.

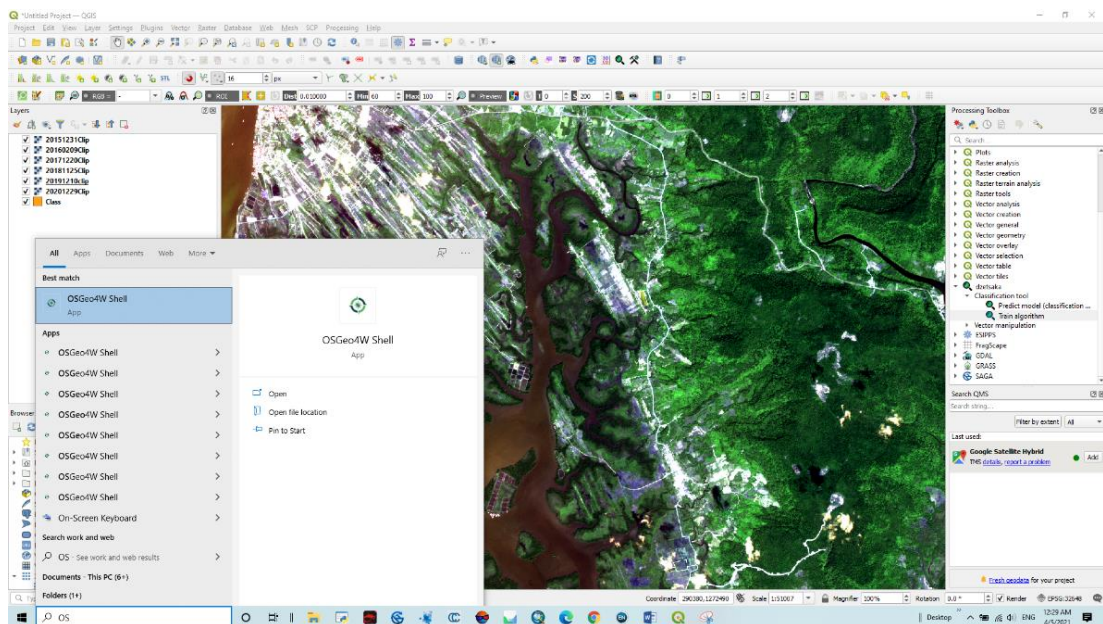
Left Screenshot (Class 1): Shows features for 'Water' (Class 1) and 'Mangroves' (Class 2). The 'Class' column contains values 1 and 2, and the 'Class name' column contains 'Water' and 'Mangroves' respectively.

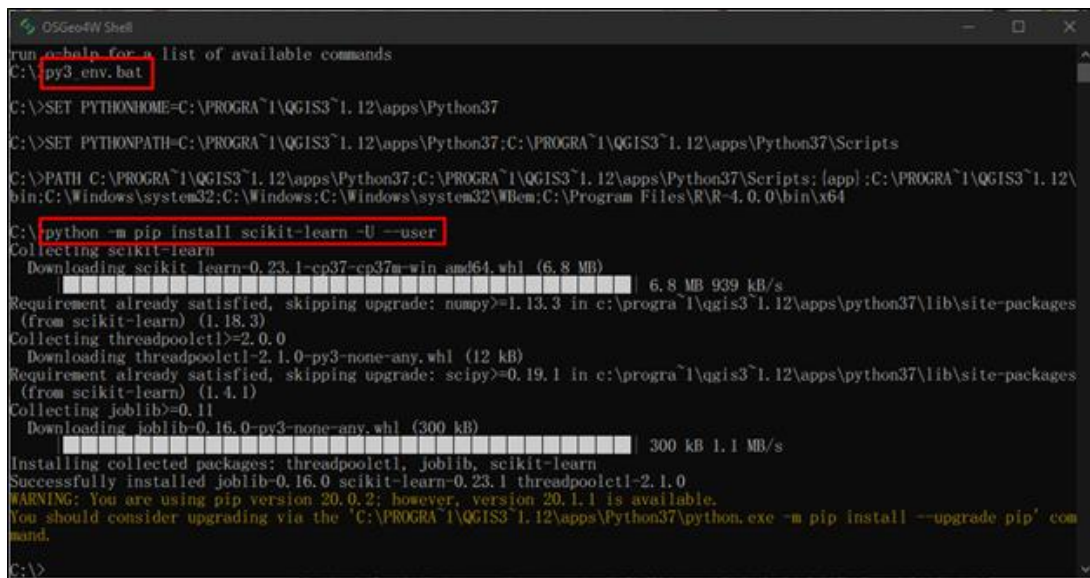
Middle Screenshot (Class 3): Shows features for 'Saltmarsh' (Class 3) and 'Forest Lands' (Class 4). The 'Class' column contains values 3 and 4, and the 'Class name' column contains 'Saltmarsh' and 'Forest Lands' respectively.

Right Screenshot (Class 5): Shows features for 'Settlements' (Class 5) and 'Other Lands' (Class 6). The 'Class' column contains values 5 and 6, and the 'Class name' column contains 'Settlements' and 'Other Lands' respectively.

Step 4: Installation of scikit-learn

If we want to use the Random Forest classifier in dzetsaka plug in, we have to install of scikit-learn because it can support to work on Windows. For understand more about scikit-lit python library, you can go direct to website: <https://github.com/nkarasiak/dzetsaka/find/master>. For install the scikit-learn in QGIS, Open OsGeo shall on our laptop by searching it in the search box on laptop. For Qgis3, just open the OsGeo shell, then: `py3_env.bat`, and `python3 -m pip install scikit-learn`



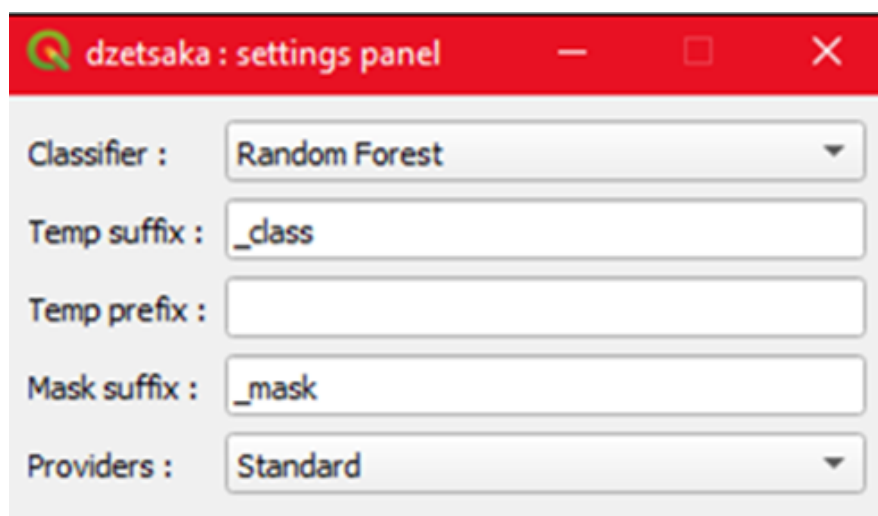


```

QGIS Shell
run -h for a list of available commands
C:\>py3_env.bat
C:\>SET PYTHONHOME=C:\PROGRA~1\QGIS3~1.12\apps\Python37
C:\>SET PYTHONPATH=C:\PROGRA~1\QGIS3~1.12\apps\Python37;C:\PROGRA~1\QGIS3~1.12\apps\Python37\Scripts
C:\>PATH C:\PROGRA~1\QGIS3~1.12\apps\Python37;C:\PROGRA~1\QGIS3~1.12\apps\Python37\Scripts;[app]:C:\PROGRA~1\QGIS3~1.12\
bin;C:\Windows\system32;C:\Windows;C:\Windows\system32\Wbem;C:\Program Files\R~4.0.0\bin\x64
C:\>python -m pip install scikit-learn -U --user
Collecting scikit-learn
  Downloading scikit-learn-0.23.1-cp37-cp37m-win_amd64.whl (6.8 MB)
    |#####| 6.8 MB 939 kB/s
Requirement already satisfied, skipping upgrade: numpy>=1.13.3 in c:\progra~1\qgis3~1.12\apps\python37\lib\site-packages
(from scikit-learn) (1.18.3)
Collecting threadpoolctl>=2.0.0
  Downloading threadpoolctl-2.1.0-py3-none-any.whl (12 kB)
Requirement already satisfied, skipping upgrade: scipy>=0.19.1 in c:\progra~1\qgis3~1.12\apps\python37\lib\site-packages
(from scikit-learn) (1.4.1)
Collecting joblib>=0.11
  Downloading joblib-0.16.0-py3-none-any.whl (300 kB)
    |#####| 300 kB 1.1 MB/s
Installing collected packages: threadpoolctl, joblib, scikit-learn
Successfully installed joblib-0.16.0 scikit-learn-0.23.1 threadpoolctl-2.1.0
WARNING: You are using pip version 20.0.2; however, version 20.1.1 is available.
You should consider upgrading via the 'C:\PROGRA~1\QGIS3~1.12\apps\Python37\python.exe -m pip install --upgrade pip' com
mand.
C:\>

```

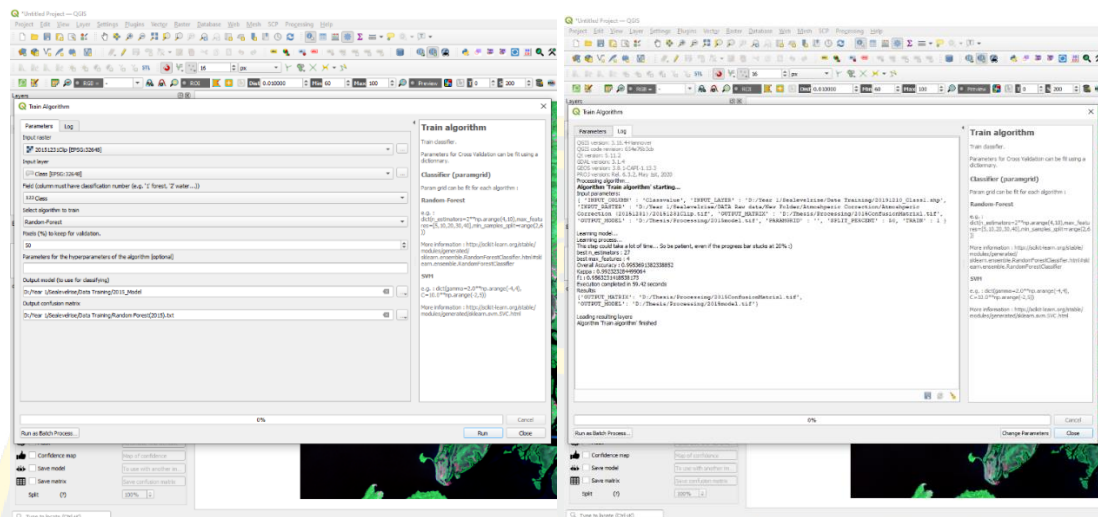
After running the pip install scikit-learn, now we can use K-Nearest Neighbors (KNN), Random Forest (RF), and Support Vector Machine (SVM). In our study, we selected the Random Forest classification.



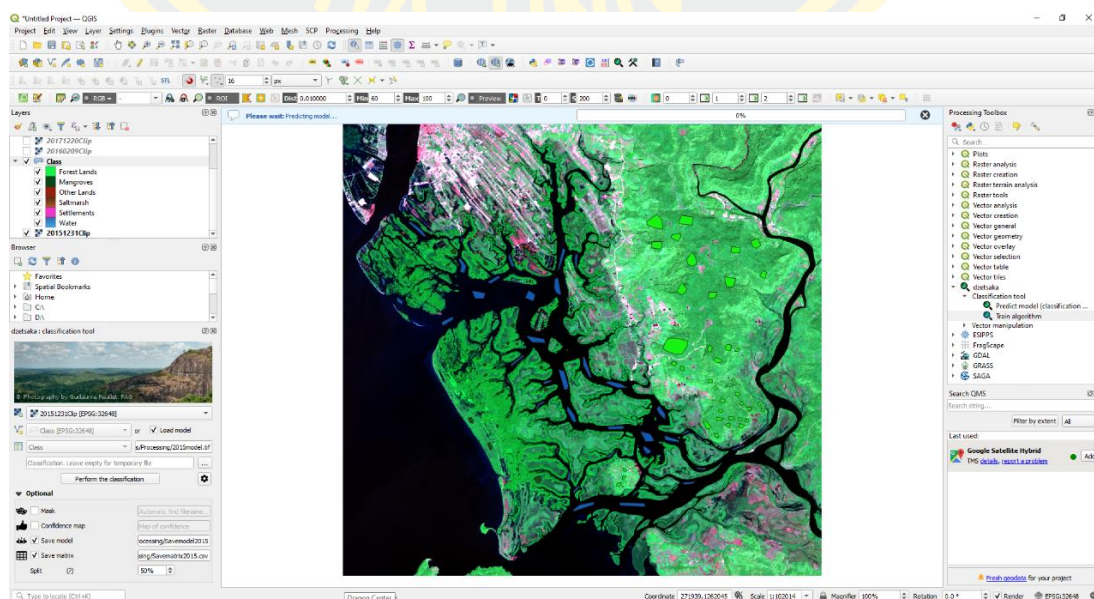
Step 5: Classification of the satellite image:

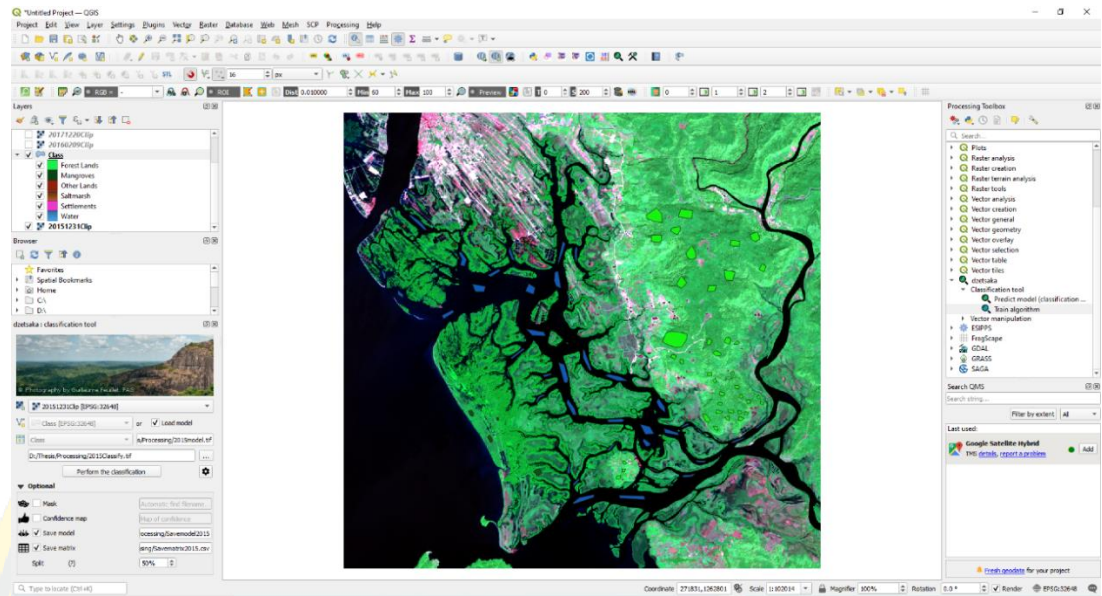
After we installed the scikit-learn, we can perform the classification. Go to dzetsaka plug in, and select Classification tool > Train Algorithm. For train algorithm parameters, we have 6 steps inside, (1) Input the raster file that we want to classify, (2) Input the training class into Input Layer, (3) Select the field as a class, (4) Select the algorithm to train as Random Forest, (5) for Pixel (%) keep for validation by 50%, (6)

we can save the output or training algorithm use for classification and save the output of confusion matrix for calculate the accuracy error.

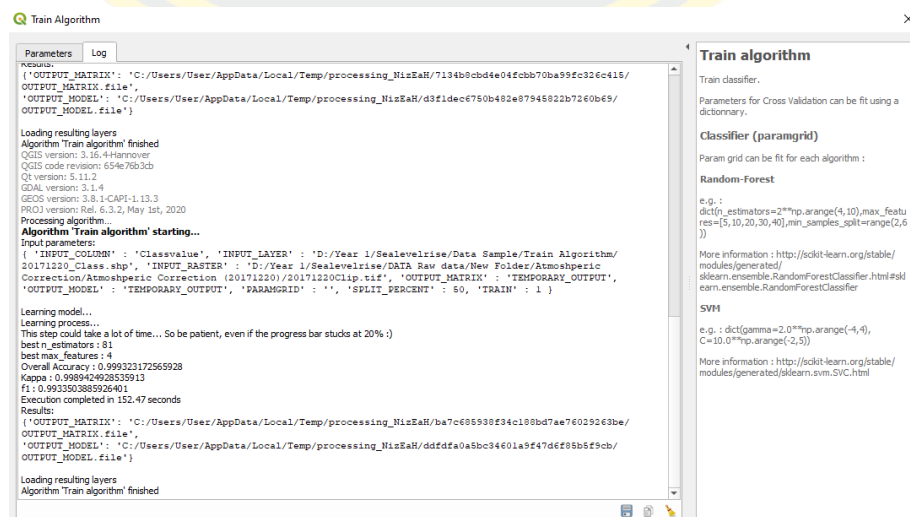
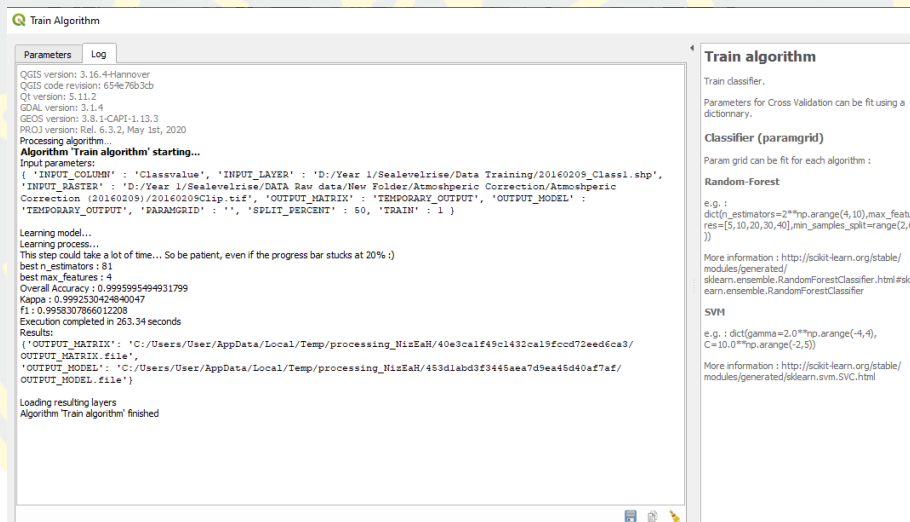
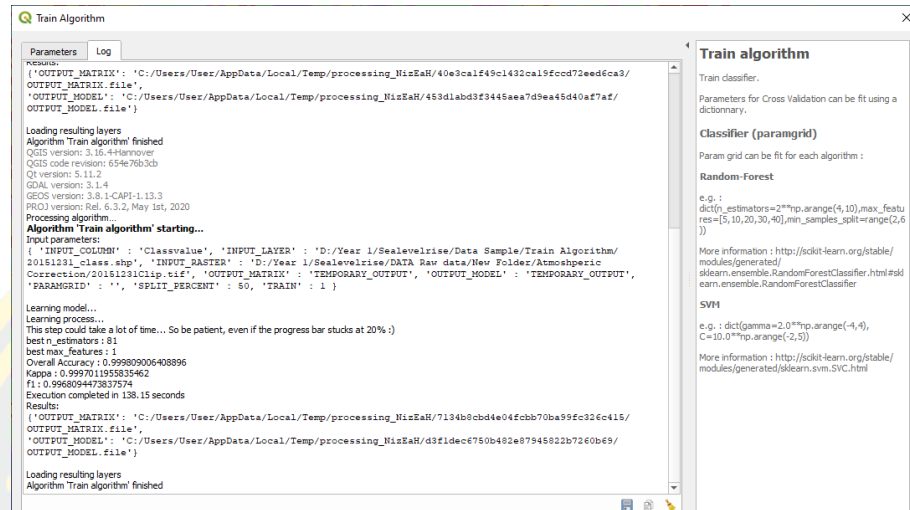


We need to open the dzetsaka plugin again. In the classification tool, we just specify the raster data to classify and specify ROI as “training data” by Load Model from our output model saving or select the column name as “class”. Then, click to specify area to save the output of classification. In this part, we can save models and saves matrix after classification if we don’t save the models and confusion matrix from the Train Algorithm part. After that, we can click on this button to perform the classification of the satellite image. When the processing is finished, you will see the output displayed on our screen, and we can customize the output by changing color and specifying the name of land cover classes.





Appendix 7: Training Algorithm of Random Forest classify for land cover from 2015 to 2020



Train Algorithm

Parameters Log

```

Results:
{'OUTPUT_MATRIX': 'C:/Users/User/AppData/Local/Temp/processing_NizSaH/ba7c685938f34c188bd7ae76029263be/OUTPUT_MATRIX.file',
'OUTPUT_MODEL': 'C:/Users/User/AppData/Local/Temp/processing_NizSaH/d4dfda0a5bc34601a9f47d6f05b5f5cb/OUTPUT_MODEL.file'}

Loading resulting layers
Algorithm 'Train algorithm' finished
QGIS version: 3.16.4-Hannover
QGIS code revision: 654e76b3cb
Qt version: 5.11.2
GDAL version: 3.1.4
GEOS version: 3.8.1-CAPI-1.13.3
PROJ version: Rel. 6.3.2, May 1st, 2020
Processing algorithm...
Algorithm 'Train algorithm' starting...
Input parameters:
{'INPUT_COLUMN': 'Classvalue', 'INPUT_LAYER': 'D:/Year 1/Sealevelrise/Data Sample/Train Algorithms/20181125_Class.shp', 'INPUT_RASTER': 'D:/Year 1/Sealevelrise/DATA Raw data/New Folder/Atmospheric Correction/Atmospheric Correction (20181125)/20181125clip.tif', 'OUTPUT_MATRIX': 'TEMPORARY_OUTPUT', 'OUTPUT_MODEL': 'TEMPORARY_OUTPUT', 'PARAMGRID': '', 'SPLIT_PERCENT': 50, 'TRAIN': 1 }

Learning model...
Learning process...
This step could take a lot of time... So be patient, even if the progress bar sticks at 20% :)
best n_estimators: 81
best max_features: 4
Overall Accuracy: 0.999428630791606
Kappa: 0.9990855251552577
f1: 0.992236491082252
Execution completed in 141.73 seconds
Results:
{'OUTPUT_MATRIX': 'C:/Users/User/AppData/Local/Temp/processing_NizSaH/f6921ffd22a5400fa56d6a863ad5d42b/OUTPUT_MATRIX.file',
'OUTPUT_MODEL': 'C:/Users/User/AppData/Local/Temp/processing_NizSaH/d0820a44fd5042249d63c1c0c0e5c24/OUTPUT_MODEL.file'}

Loading resulting layers
Algorithm 'Train algorithm' finished

```

Train algorithm

Train classifier.

Parameters for Cross Validation can be fit using a dictionary.

Classifier (paramgrid)

Param grid can be fit for each algorithm :

Random-Forest

e.g. :

```
dict(n_estimators=2**np.arange(4,10),max_features=[5,10,20,30,40],min_samples_split=range(2,6))
```

More information : <http://scikit-learn.org/stable/modules/generated/sklearn.ensemble.RandomForestClassifier.html#sklearn.ensemble.RandomForestClassifier>

SVH

e.g. : dict(gamma=2.0**np.arange(-4,4), C=10.0**np.arange(-2,5))

More information : <http://scikit-learn.org/stable/modules/generated/sklearn.svm.SVC.html>

Train Algorithm

Parameters Log

```

Results:
{'OUTPUT_MATRIX': 'C:/Users/User/AppData/Local/Temp/processing_NizSaH/f6921ffd22a5400fa56d6a863ad5d42b/OUTPUT_MATRIX.file',
'OUTPUT_MODEL': 'C:/Users/User/AppData/Local/Temp/processing_NizSaH/d0820a44fd5042249d63c1c0c0e5c24/OUTPUT_MODEL.file'}

Loading resulting layers
Algorithm 'Train algorithm' finished
QGIS version: 3.16.4-Hannover
QGIS code revision: 654e76b3cb
Qt version: 5.11.2
GDAL version: 3.1.4
GEOS version: 3.8.1-CAPI-1.13.3
PROJ version: Rel. 6.3.2, May 1st, 2020
Processing algorithm...
Algorithm 'Train algorithm' starting...
Input parameters:
{'INPUT_COLUMN': 'Classvalue', 'INPUT_LAYER': 'D:/Year 1/Sealevelrise/Data Training/20191210_Class1.shp', 'INPUT_RASTER': 'D:/Year 1/Sealevelrise/DATA Raw data/New Folder/Atmospheric Correction/Atmospheric Correction (20191210)/20191210clip.tif', 'OUTPUT_MATRIX': 'TEMPORARY_OUTPUT', 'OUTPUT_MODEL': 'TEMPORARY_OUTPUT', 'PARAMGRID': '', 'SPLIT_PERCENT': 50, 'TRAIN': 1 }

Learning model...
Learning process...
This step could take a lot of time... So be patient, even if the progress bar sticks at 20% :)
best n_estimators: 81
best max_features: 1
Overall Accuracy: 0.999547559482621
Kappa: 0.999207962572537
f1: 0.993927171478951
Execution completed in 167.09 seconds
Results:
{'OUTPUT_MATRIX': 'C:/Users/User/AppData/Local/Temp/processing_NizSaH/956bb12228634321ac17d862276c4e8c/OUTPUT_MATRIX.file',
'OUTPUT_MODEL': 'C:/Users/User/AppData/Local/Temp/processing_NizSaH/22589ae8a5d349d8ba14f9e1144c2405/OUTPUT_MODEL.file'}

Loading resulting layers
Algorithm 'Train algorithm' finished

```

Train algorithm

Train classifier.

Parameters for Cross Validation can be fit using a dictionary.

Classifier (paramgrid)

Param grid can be fit for each algorithm :

Random-Forest

e.g. :

```
dict(n_estimators=2**np.arange(4,10),max_features=[5,10,20,30,40],min_samples_split=range(2,6))
```

More information : <http://scikit-learn.org/stable/modules/generated/sklearn.ensemble.RandomForestClassifier.html#sklearn.ensemble.RandomForestClassifier>

SVH

e.g. : dict(gamma=2.0**np.arange(-4,4), C=10.0**np.arange(-2,5))

More information : <http://scikit-learn.org/stable/modules/generated/sklearn.svm.SVC.html>

Train Algorithm

Parameters Log

```

QGIS version: 3.16.4-Hannover
QGIS code revision: 654e76b3cb
Qt version: 5.11.2
GDAL version: 3.1.4
GEOS version: 3.8.1-CAPI-1.13.3
PROJ version: Rel. 6.3.2, May 1st, 2020
Processing algorithm...
Algorithm 'Train algorithm' starting...
Input parameters:
{'INPUT_COLUMN': 'Classvalue', 'INPUT_LAYER': 'D:/Year 1/Sealevelrise/Data Training/20201229_Class.shp', 'INPUT_RASTER': 'D:/Year 1/Sealevelrise/DATA Raw data/New Folder/Atmospheric Correction/Atmospheric Correction (20201229)/20201229clip.tif', 'OUTPUT_MATRIX': 'TEMPORARY_OUTPUT', 'OUTPUT_MODEL': 'TEMPORARY_OUTPUT', 'PARAMGRID': '', 'SPLIT_PERCENT': 50, 'TRAIN': 1 }

Learning model...
Learning process...
This step could take a lot of time... So be patient, even if the progress bar sticks at 20% :)
best n_estimators: 81
best max_features: 1
Overall Accuracy: 0.9996138173489226
Kappa: 0.9992436186746432
f1: 0.9928001707218931
Execution completed in 116.57 seconds
Results:
{'OUTPUT_MATRIX': 'C:/Users/User/AppData/Local/Temp/processing_dPEjpr/fd6f5c29453540008ce1e0c2a53265cc/OUTPUT_MATRIX.file',
'OUTPUT_MODEL': 'C:/Users/User/AppData/Local/Temp/processing_dPEjpr/8aa4f74023ec4e908396ae531d7ad85d/OUTPUT_MODEL.file'}

Loading resulting layers
Algorithm 'Train algorithm' finished

```

Train algorithm

Train classifier.

Parameters for Cross Validation can be fit using a dictionary.

Classifier (paramgrid)

Param grid can be fit for each algorithm :

Random-Forest

e.g. :

```
dict(n_estimators=2**np.arange(4,10),max_features=[5,10,20,30,40],min_samples_split=range(2,6))
```

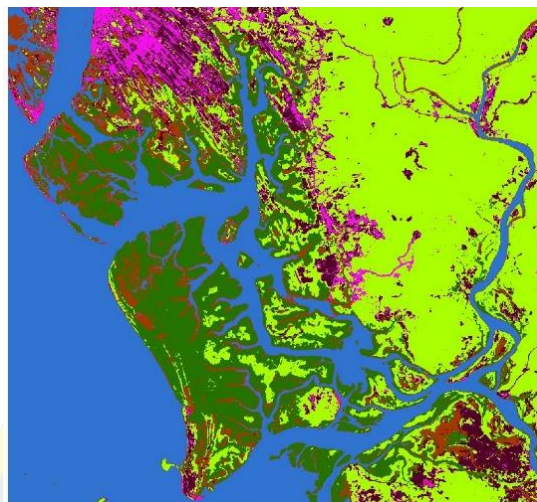
More information : <http://scikit-learn.org/stable/modules/generated/sklearn.ensemble.RandomForestClassifier.html#sklearn.ensemble.RandomForestClassifier>

SVH

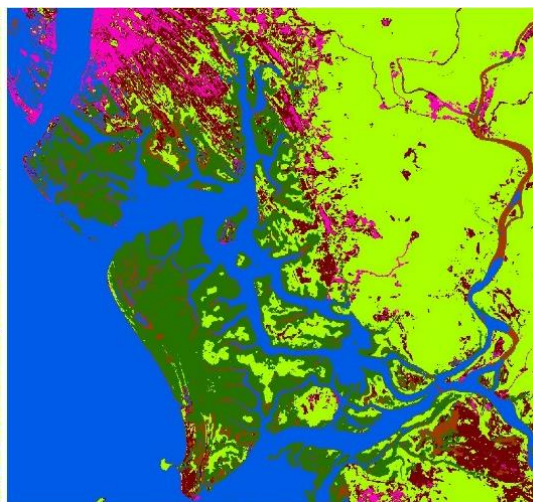
e.g. : dict(gamma=2.0**np.arange(-4,4), C=10.0**np.arange(-2,5))

More information : <http://scikit-learn.org/stable/modules/generated/sklearn.svm.SVC.html>

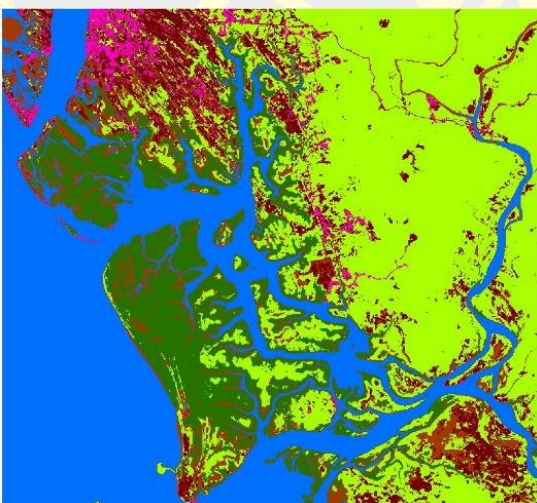
**Appendix 8: Image classification: Land cover classification level 1 using
Random Forest Classification in QGIS (2015-2020)**



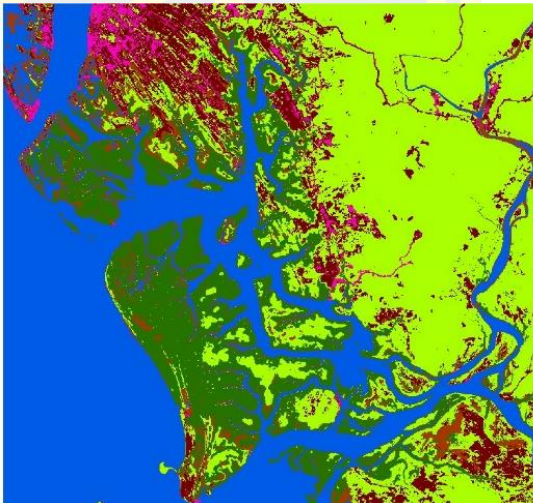
Date: 31 12 2015



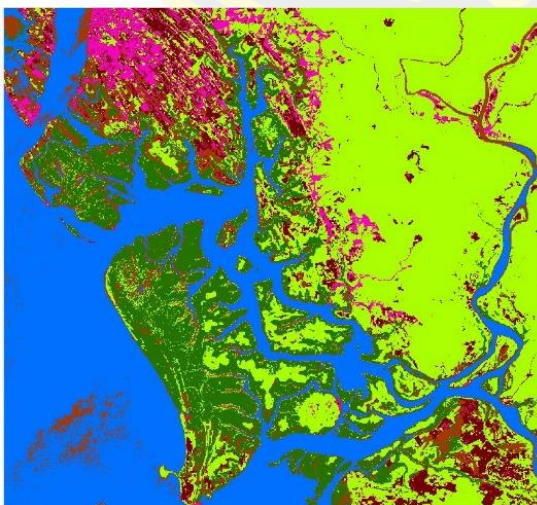
Date: 09 02 2016



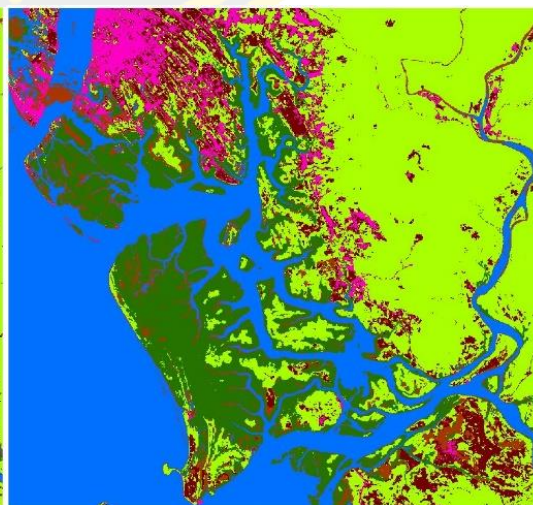
Date: 20 12 2017



Date: 25 11 2018



Date: 10 12 2019

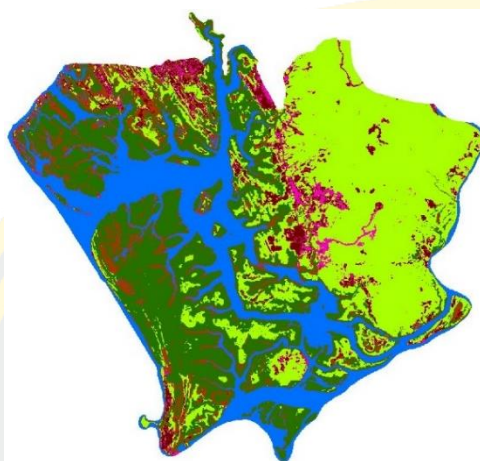


Date: 29 12 2020

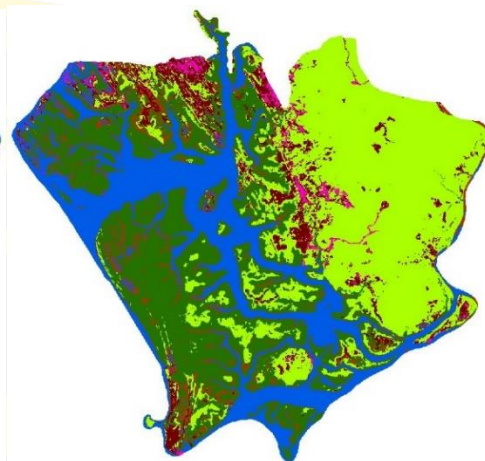
Appendix 9: Land cover level I clip using Clip in Raster processing in ArcMap

Land Cover Types

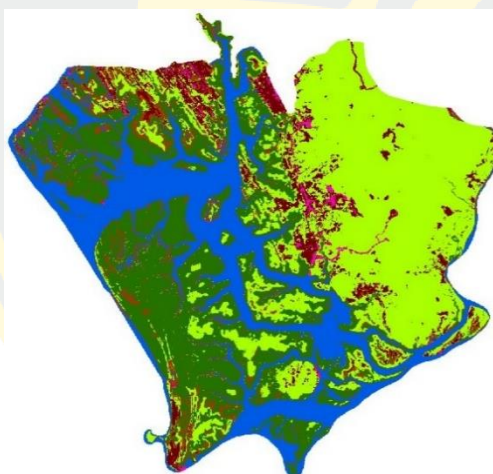
	Water		Forest Lands
	Mangroves		Settlements
	Saltmarsh		Other Lands



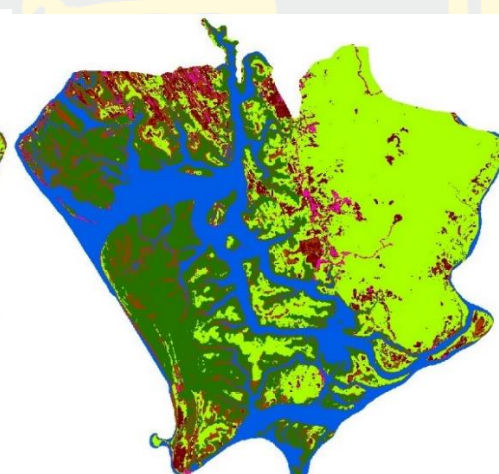
Date: 31 12 2015



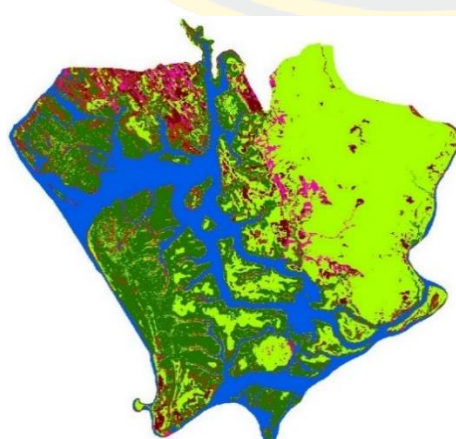
Date: 09 02 2016



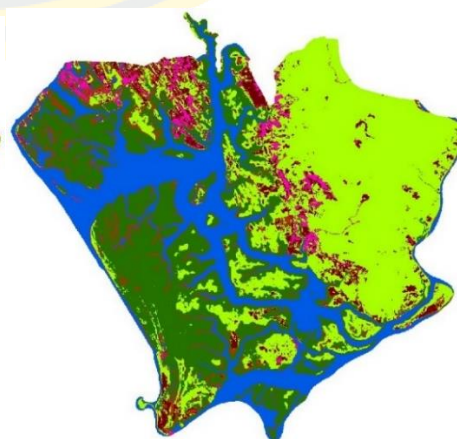
Date: 20 12 2017



Date: 25 11 2018



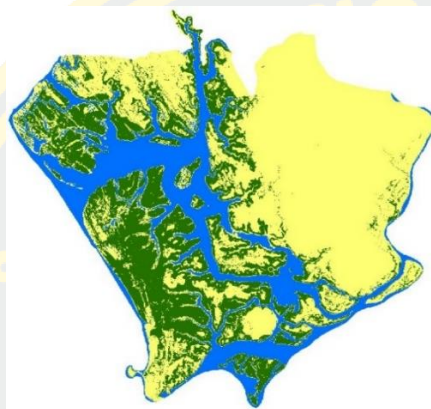
Date: 10 12 2019



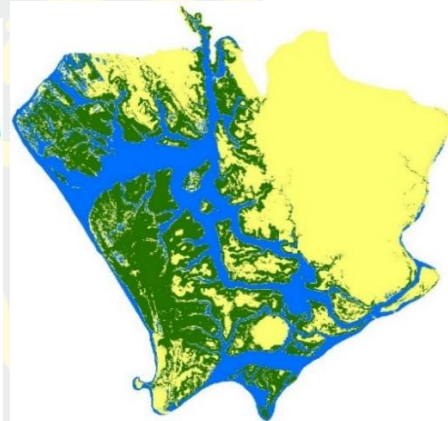
Date: 29 12 2020

Appendix 10: Land cover level II clip using Reclassify in Spatial Analyst Tools (ArcMap)

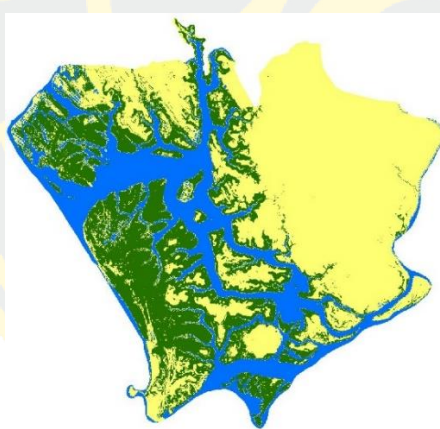
Legend



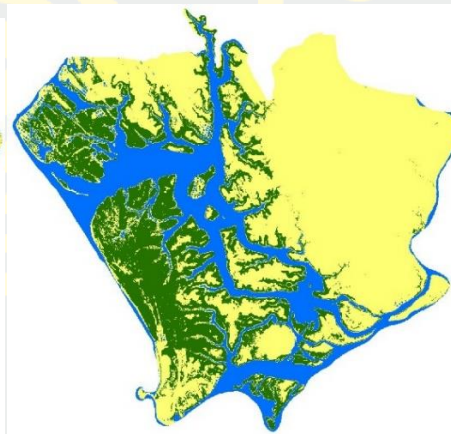
Date: 31 12 2015



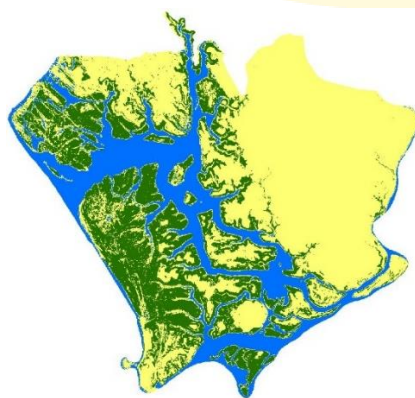
Date: 09 02 2016



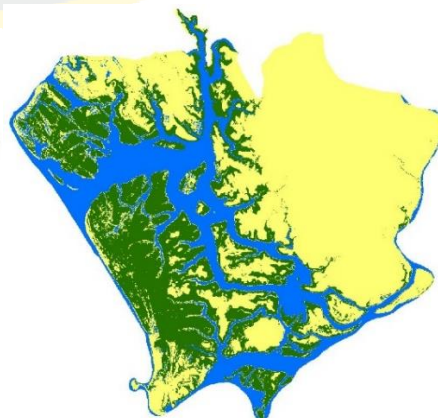
Date: 20 12 2017



Date: 25 11 2018



Date: 10 12 2019

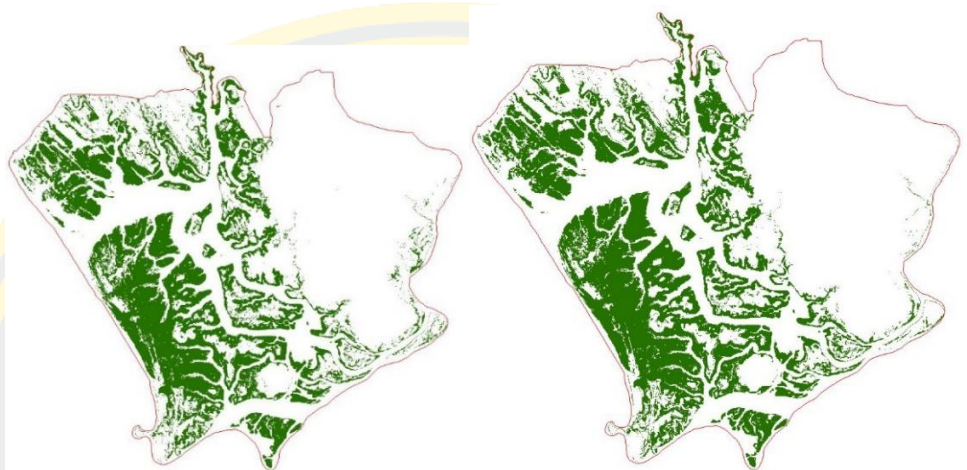


Date: 29 12 2020

Appendix 11: Mangrove forests clips using Reclassify in Spatial Analyst Tools (ArcMap)

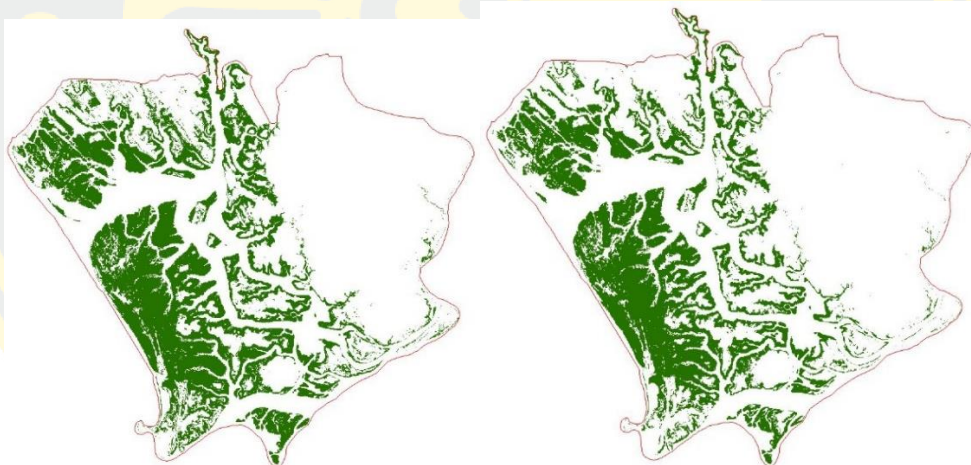
Legend

 Mangrove Forests



Date: 31 12 2015

Date: 09 02 2016



Date: 20 12 2017

Date: 25 11 2018



Date: 10 12 2019

Date: 29 12 2020

Appendix 12: Area Change Analysis using MOLUSCE in Hectare from 2015 to 2020

MOLUSCE

Inputs Evaluating correlation **Area Changes** Transition Potential Modelling Cellular Automata Simulation Validation

Class statistics ha

	Class color	2015	2016	Δ	2015 %	2016 %	Δ %
1	Water body	5240.86 ha	5526.56 ha	285.70 ha	20.2709675323	21.3760181202	1.10505058788
2	Mangroves	7157.90 ha	7495.21 ha	337.31 ha	27.6858299019	28.9905012837	1.30467138186
3	Saltmarsh	2362.72 ha	1415.94 ha	-946.78 ha	9.13869487221	5.47667248652	-3.66202238569
4	Forest Lands	9058.33 ha	9183.64 ha	125.31 ha	35.0364469433	35.5211297895	0.484682846227
5	Settlements	746.57 ha	413.22 ha	-333.35 ha	2.88763604267	1.5982814278	-1.28935461487
6	Other Lands	1287.64 ha	1819.45 ha	531.81 ha	4.98042470765	7.03739689224	2.0569721846

Transition matrix from 2015 to 2016

MOLUSCE

Inputs Evaluating correlation **Area Changes** Transition Potential Modelling Cellular Automata Simulation Validation

Class statistics ha

	Class color	2016	2017	Δ	2016 %	2017 %	Δ %
1	Water body	5526.56 ha	5506.50 ha	-20.06 ha	21.3760181202	21.298428639	-0.0775894812489
2	Mangroves	7495.21 ha	7337.47 ha	-157.74 ha	28.9905012837	28.3803833988	-0.610117884956
3	Saltmarsh	1415.94 ha	1603.62 ha	187.68 ha	5.47667248652	6.20259441278	0.725921926261
4	Forest Lands	9183.64 ha	9491.25 ha	307.61 ha	35.5211297895	36.7109254189	1.18979562946
5	Settlements	413.22 ha	235.30 ha	-177.92 ha	1.5982814278	0.910109917142	-0.688171510659
6	Other Lands	1819.45 ha	1679.88 ha	-139.57 ha	7.03739689224	6.49755821338	-0.539838678859

Transition matrix from 2016 to 2017

MOLUSCE

Inputs Evaluating correlation **Area Changes** Transition Potential Modelling Cellular Automata Simulation Validation

Class statistics ha

	Class color	2017	2018	Δ	2017 %	2018 %	Δ %
1	Water body	5506.50 ha	5201.85 ha	-304.65 ha	21.298428639	20.120081906	-1.17834673293
2	Mangroves	7337.47 ha	6436.26 ha	-901.21 ha	28.3803833988	24.8946198696	-3.48576352923
3	Saltmarsh	1603.62 ha	2356.06 ha	752.44 ha	6.20259441278	9.11293485501	2.91034044222
4	Forest Lands	9491.25 ha	9954.95 ha	463.70 ha	36.7109254189	38.5044569471	1.79353152817
5	Settlements	235.30 ha	299.77 ha	64.47 ha	0.910109917142	1.15947152512	0.249361607982
6	Other Lands	1679.88 ha	1605.13 ha	-74.75 ha	6.49755821338	6.20843489716	-0.289123316219

Transition matrix from 2017 to 2018

MOLUSCE

Inputs Evaluating correlation Area Changes Transition Potential Modelling Cellular Automata Simulation Validation

Class statistics ha

	Class color	2018	2019	Δ	2018 %	2019 %	Δ %
1	Water body	5201.85 ha	4915.04 ha	-286.81 ha	20.120081906	19.0107379819	-1.10934392408
2	Mangroves	6436.26 ha	6761.66 ha	325.40 ha	24.8946198696	26.1532249143	1.25860504479
3	Saltmarsh	2356.06 ha	2095.10 ha	-260.96 ha	9.11293485501	8.10357538209	-1.00935947292
4	Forest Lands	9954.95 ha	10223.60 ha	268.65 ha	38.5044569471	39.5435603438	1.03910339669
5	Settlements	299.77 ha	616.50 ha	316.73 ha	1.15947152512	2.3845421331	1.22507060798
6	Other Lands	1605.13 ha	1242.12 ha	-363.01 ha	6.20843489716	4.80435924471	-1.40407565245

Transition matrix from 2018 to 2019

MOLUSCE

Inputs Evaluating correlation Area Changes Transition Potential Modelling Cellular Automata Simulation Validation

Class statistics ha

	Class color	2019	2020	Δ	2019 %	2020 %	Δ %
1	Water body	4915.04 ha	5425.51 ha	510.47 ha	19.0107379819	20.9851698111	1.97443182917
2	Mangroves	6761.66 ha	7045.64 ha	283.98 ha	26.1532249143	27.251622765	1.0983978507
3	Saltmarsh	2095.10 ha	1545.56 ha	-549.54 ha	8.10357538209	5.97802585439	-2.12554952769
4	Forest Lands	10223.60 ha	9629.52 ha	-594.08 ha	39.5435603438	37.2457358662	-2.29782447759
5	Settlements	616.50 ha	639.17 ha	22.67 ha	2.3845421331	2.47222675623	0.0876846231263
6	Other Lands	1242.12 ha	1568.62 ha	326.50 ha	4.80435924471	6.067218947	1.26285970228

Transition matrix from 2019 to 2020

MOLUSCE

Inputs Evaluating correlation Area Changes Transition Potential Modelling Cellular Automata Simulation Validation

Class statistics ha

	Class color	2015	2020	Δ	2015 %	2020 %	Δ %
1	Water body	5240.86 ha	5425.51 ha	184.65 ha	20.2709675323	20.9851698111	0.714202278795
2	Mangroves	7157.90 ha	7045.64 ha	-112.26 ha	27.6858299019	27.251622765	-0.43420713684
3	Saltmarsh	2362.72 ha	1545.56 ha	-817.16 ha	9.13869487221	5.97802585439	-3.16066901782
4	Forest Lands	9058.33 ha	9629.52 ha	571.19 ha	35.0364469433	37.2457358662	2.20928892296
5	Settlements	746.57 ha	639.17 ha	-107.40 ha	2.88763604267	2.47222675623	-0.415409286448
6	Other Lands	1287.64 ha	1568.62 ha	280.98 ha	4.98042470765	6.067218947	1.08679423935

Transition matrix from 2015 to 2020

Appendix 13: Accuracy Assessments using Calculate confusion matrix online

Draw confusion matrix for classes.

Classifier results	Truth data						Classification overall	User's accuracy (Precision)
	Class 1	Class 2	Class 3	Class 4	Class 5	Class 6		
	Class 1	8401	0	0	0	0	8401	100%
	Class 2	0	2650	0	0	0	2650	100%
	Class 3	0	0	0350	0	0	350	100%
	Class 4	0	0001	0	7100	0	7101	99.986%
	Class 5	0	0	0	0	0232	232	100%
	Class 6	0	0	0	0	0003	0115	97.458%
Truth overall	8401	2651	350	7100	235	115	18852	
Producer's accuracy (Recall)	100%	99.962%	100%	100%	98.723%	100%		

Overall accuracy (OA):

Kappa¹:

> Calculate confusion matrix <

2007 by Marco Vanetti

¹See: J. Richard Landis and Gary G. Koch - *The Measurement of Observer Agreement for Categorical Data*, Biometrics, Vol. 33, No. 1 (Mar., 1977), pp. 159-174.

Confusion Matrix calculation 2015

Draw confusion matrix for classes.

Classifier results	Truth data						Classification overall	User's accuracy (Precision)
	Class 1	Class 2	Class 3	Class 4	Class 5	Class 6		
	Class 1	8397	0	0	0	0	8397	100%
	Class 2	0	2967	0	0	0	2967	100%
	Class 3	0003	0	0348	0	0	351	99.145%
	Class 4	0	0001	0	19858	0001	19860	99.99%
	Class 5	0	0	0	0	0259	259	100%
	Class 6	0001	0	0002	0	0129	132	97.727%
Truth overall	8401	2968	350	19858	259	130	31966	
Producer's accuracy (Recall)	99.952%	99.966%	99.429%	100%	100%	99.231%		

Overall accuracy (OA):

Kappa¹:

> Calculate confusion matrix <

2007 by Marco Vanetti

¹See: J. Richard Landis and Gary G. Koch - *The Measurement of Observer Agreement for Categorical Data*, Biometrics, Vol. 33, No. 1 (Mar., 1977), pp. 159-174.

Confusion Matrix calculation 2016

Draw confusion matrix for classes.

Classifier results	Truth data						Classification overall	User's accuracy (Precision)
	Class 1	Class 2	Class 3	Class 4	Class 5	Class 6		
	Class 1	7353	0	0001	0	0	7354	99.986%
	Class 2	0	2425	0	0	0	2425	100%
	Class 3	0001	0	0298	0	0	299	99.666%
	Class 4	0	0	0	5620	0	5620	100%
	Class 5	0	0	0	0	0151	152	99.342%
	Class 6	0	0	0	0	0107	107	100%
Truth overall	7354	2425	299	5620	151	108	15957	
Producer's accuracy (Recall)	99.986%	100%	99.666%	100%	100%	99.074%		

Overall accuracy (OA):

Kappa¹:

[> Calculate confusion matrix <](#)

2007 by Marco Vanetti

¹See: J. Richard Landis and Gary G. Koch - *The Measurement of Observer Agreement for Categorical Data*, Biometrics, Vol. 33, No. 1 (Mar., 1977), pp. 159-174.

Confusion Matrix calculation 2017

Draw confusion matrix for classes.

Classifier results	Truth data						Classification overall	User's accuracy (Precision)
	Class 1	Class 2	Class 3	Class 4	Class 5	Class 6		
	Class 1	7353	0	0001	0	0	7354	99.986%
	Class 2	0	1902	0	0	0	1902	100%
	Class 3	0001	0	0299	0	0003	303	98.68%
	Class 4	0	0	0	5584	0	5584	100%
	Class 5	0	0	0	0	0145	145	100%
	Class 6	0	0	0	0	0001	0115	99.138%
Truth overall	7354	1902	300	5584	146	118	15404	
Producer's accuracy (Recall)	99.986%	100%	99.667%	100%	99.315%	97.458%		

Overall accuracy (OA):

Kappa¹:

[> Calculate confusion matrix <](#)

2007 by Marco Vanetti

¹See: J. Richard Landis and Gary G. Koch - *The Measurement of Observer Agreement for Categorical Data*, Biometrics, Vol. 33, No. 1 (Mar., 1977), pp. 159-174.

Confusion Matrix calculation 2018

Draw confusion matrix for classes.

	Truth data						Classification overall	User's accuracy (Precision)
	Class 1	Class 2	Class 3	Class 4	Class 5	Class 6		
Class 1	7997	0	0004	0	0	0	8001	99.95%
Class 2	0	1819	0	0	0	0	1819	100%
Class 3	0001	0	0242	0	0005	0	248	97.581%
Class 4	0	0	0	19335	0014	0026	19375	99.794%
Class 5	0	0	0005	0005	0470	0008	488	96.311%
Class 6	0	0	0001	0	0005	0099	105	94.286%
Truth overall	7998	1819	252	19340	494	133	30036	
Producer's accuracy (Recall)	99.987%	100%	96.032%	99.974%	95.142%	74.436%		

Overall accuracy (OA):

Kappa¹:

[> Calculate confusion matrix <](#)

2007 by Marco Vanetti

¹See: J. Richard Landis and Gary G. Koch - *The Measurement of Observer Agreement for Categorical Data*, Biometrics, Vol. 33, No. 1 (Mar., 1977), pp. 159-174.

Confusion Matrix calculation 2019

Draw confusion matrix for classes.

	Truth data						Classification overall	User's accuracy (Precision)
	Class 1	Class 2	Class 3	Class 4	Class 5	Class 6		
Class 1	7998	0	2	0	0	0	8000	99.975%
Class 2	0	1819	0	0	0	0	1819	100%
Class 3	0	0	248	0	0	0	248	100%
Class 4	0	0	0	19337	0	0	19337	100%
Class 5	0	0	2	0	492	3	497	98.994%
Class 6	0	0	0	3	2	133	138	96.377%
Truth overall	7998	1819	252	19340	494	136	30039	
Producer's accuracy (Recall)	100%	100%	98.413%	99.984%	99.595%	97.794%		

Overall accuracy (OA):

Kappa¹:

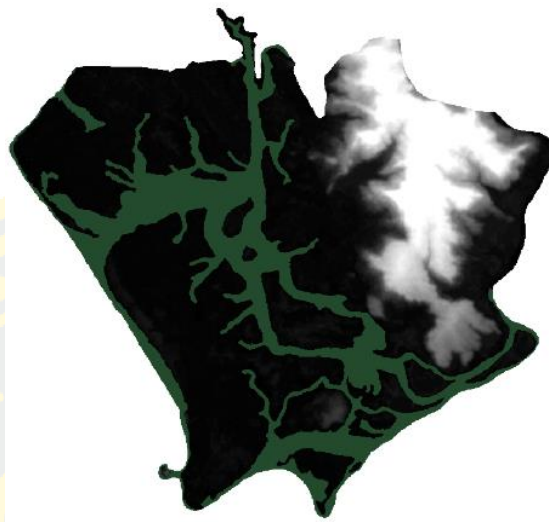
[> Calculate confusion matrix <](#)

2007 by Marco Vanetti

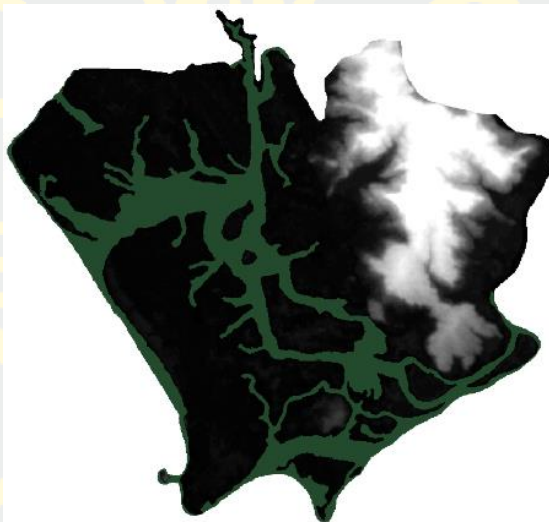
¹See: J. Richard Landis and Gary G. Koch - *The Measurement of Observer Agreement for Categorical Data*, Biometrics, Vol. 33, No. 1 (Mar., 1977), pp. 159-174.

Confusion Matrix calculation 2020

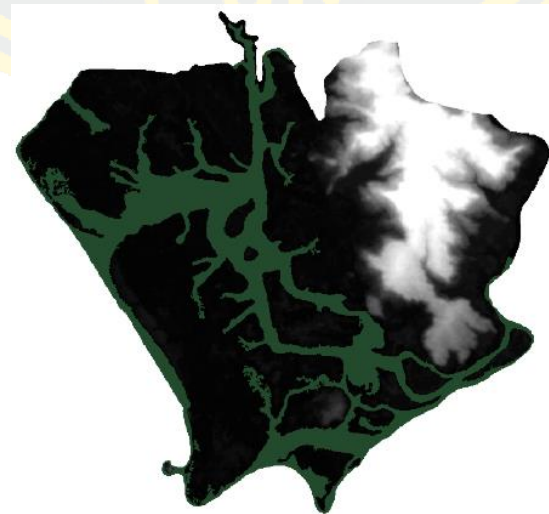
Appendix 14: SRTM DEM generated based on Sea level rise scenarios



Inundation 40 cm



Inundation 60 cm



Inundation 1 m